Lopingian brachiopods from the Abadeh section (Central Iran) and their biostratigraphic implications

MARCO VIARETTI, GAIA CRIPPA, RENATO POSENATO, SHUZHONG SHEN & LUCIA ANGIOLINI

M. Viaretti, Dipartimento di Scienze della Terra "A. Desio", Università degli Studi di Milano, Via Mangiagalli 34, I-20133 Milano; marco.viaretti@unimi.it
G. Crippa, Dipartimento di Scienze della Terra "A. Desio", Università degli Studi di Milano, Via Mangiagalli 34, I-20133 Milano; gaia.crippa@unimi.it
R. Posenato, Dipartimento di Fisica e Scienze della Terra, Università di Ferrara, Via Saragat 1, I-44121 Ferrara; psr@unife.it
S.Z. Shen, State Key Laboratory for Mineral Deposits Research, School of Earth Sciences and Engineering and Frontiers Science Center for Critical Earth Material Cycling, Nanjing University, 163 Xianlin Avenue, Nanjing, Jiangsu 210023, P.R. China; szshen@nju.edu.cn
L. Angiolini, Dipartimento di Scienze della Terra "A. Desio", Università degli Studi di Milano, Via Mangiagalli 34, I-20133 Milano; lucia.angiolini@unimi.it

KEY WORDS - brachiopod systematics, bivalves, Permian-Triassic boundary, Unitary Associations.

ABSTRACT - The Abadeh section is one of the most important Neotethyan sections, as it records a continuous marine sedimentary succession across the Permian-Triassic boundary. Although this succession yields a rich brachiopod fauna, this has never been studied in detail. Instead most of the studies carried out so far, have been focused on the position of the Permian-Triassic boundary, which is still debated. Here, we present a systematic study of the brachiopod fauna from the Hambast Formation, which comprises 30 species of taxa from the orders Productida, Orthotetida, Orthida, Athyridida and Spiriferida. Brachiopod biodiversity is relatively high and constant in the Wuchiapingian part of the section. But in the Changhsingian, just a single species occurs: Paracrurithyris pygmaea. Also, species of bivalves of the genus Claraia *occur in the uppermost Griesbachian-lower Dienerian Elikah Formation.*

Using the Unitary Associations method, we compared the stratigraphic distribution of the brachiopods in the Abadeh section with those in the Julfa section, another important Permian-Triassic succession in North-West Iran. Based on this analysis three Wuchiapingian brachiopod biozones and one Changhsingian brachiopod biozone have been detected and correlated to the

conodont biozonation; these biozone are the Araxilevis intermedius-Leptodus nobilis *Biozone, the* Permophricodothyris ovata-Araxathyris quadrilobata *Biozone, and the* Haydenella kiangsiensis-Transcaucasathyris minor *Biozone in the Wuchiapingian, and the* Paracrurithyris pygmaea *Biozone in the Changhsingian. Most of the biozones can be correlated through Iran and Transcaucasia, showing the potential of brachiopods for correlation at a regional scale in the Upper Permian.*

INTRODUCTION

Since its discovery in 1967 (Taraz, 1969), the Abadeh section has been regarded as one of the most important sections of Iran. This is because it records a complete marine succession across the Permian-Triassic boundary and alsobbecause of its potential to correlate the Tethyan timescale to the International Chronostratigraphic Scale. This has led to intense attention being devoted to the section by many research groups (e.g., Kozur et al., 1978; Taraz et al., 1981; Gallet et al., 2000; Korte et al., 2004; Kozur, 2007; Richoz et al., 2010; Shen & Mei, 2010; Liu et al., 2013; Shen et al., 2013; Chen et al., 2020; Baud et al., 2021). The first investigation focused on its stratigraphy and fossil content (Taraz et al., 1981), and the majority of subsequent studies have focused on the conodont faunas of the section, the geochemistry, and the position of the Permian-Triassic boundary. But, the exact location of the Permian-Triassic boundary in the section has not been resolved, and remains a highly debated topic, as synthesized later in this paper.

Despite the section significance, barely any attention has been given to the study of fossils other than conodonts. In fact, the brachiopods which occur abundantly in the Abadeh section have never been studied before, except for a few species occurrences reported by Taraz et al. (1981). Thus, the present study is focused on providing new data by studying the brachiopod and bivalve fauna collected during fieldwork work in the Yazd Province by an Italian-Chinese-Iranian research team at the end of November 2017 (Angiolini et al., 2017).

Brachiopods are widely recognized as useful tools for paleoecologic, paleogeographic, and paleoclimatic reconstructions, because they are highly sensitive to thermal gradients and geographical barriers, and they are also characterized by a relatively short larval stage, which often ends with the permanent settling of the adults (Shen in Lucas & Shen, 2018). Due to their provinciality and relatively slow evolutionary rates, however, they are not considered to be good index-fossils or very valuable tools for global biostratigraphic correlation. However, brachiopods are widespread in Paleozoic sedimentary successions and are often associated with index-fossils, such as conodonts, fusulines and ammonoids, and the correlation of brachiopod associations with a robust zonation based on these taxa can provide a useful tool for correlation at a regional scale. In this work, besides providing systematic descriptions of the brachiopods from Abadeh, we thus address their

biostratigraphic significance and potential for correlation of the Lopingian of Iran. Besides the brachiopods, bivalves have been analyzed too; although they are less abundant in Abadeh, they provide biostratigraphic data to constrain the age of the Triassic part of the section.

GEOLOGICAL SETTING

The geology of Iran, and in general that of central Asia, is very complex, being the result of a dynamic structural evolution. This is mainly linked to the rifting and drifting of the Cimmerian blocks - that included Iran - from the Gondwana margin in the Early Permian. Followed by the accretion of the blocks to the southern margin of Laurasia in the Late Triassic, which produced the Cimmerian orogeny (e.g., Şengör, 1979; Muttoni et al., 2009; Zanchi et al., 2009a, b, 2016; Zanchetta et al., 2013). The Permian-Triassic drifting of the Cimmerian blocks was in turn related to the opening of the Neotethys Ocean to the south and the progressive subduction of the Paleotethys Ocean northward under the Eurasian margin, in concomitance with the transformation of Pangea from an Irvingian type B to a Wegenerian type A configuration (Muttoni et al., 2009; Muttoni & Kent, 2019). Thus, until the Cisuralian (Early Permian), Iran was located close to the Gondwanan margin. During the Guadalupian (Middle Permian) the northward drift of the Cimmerian terranes was ongoing, along with the reconfiguration of Pangea. By the Lopingian (Late Permian), the latter was completed, in a Pangea A configuration, and the Cimmerian blocks were located at equatorial paleolatitudes (Besse et al., 1998; Gallet et al., 2000; Muttoni et al., 2009; Muttoni & Kent, 2019). In the Late Triassic, Iran was at northern paleolatitudes and set to collide with and become part of the southern Eurasian margin. A dramatic geodynamic reorganization, with a subduction jump to the SW of the accreted microplate, followed by opening and closure of small Neotethys oceanic branches, characterized the complex Mesozoic evolution of the area (Hassanzadeh & Wernicke, 2016 and references therein). In the Oligocene-Miocene (Su & Zhou, 2020 and references therein), Iran underwent tectonic deformation due to the closure of the Neotethys and the collision of the Arabian plate with Eurasia.

Iran, therefore, is a mosaic of blocks sandwiched between Arabia to the south and Eurasia to the north (Fig. 1). The regions of North and Central Iran belong to the same Cimmerian block of Gondwana ancestry (Gaetani et al., 2009; Zanchi et al., 2009a; Berberian, 2014). Indeed, the Alborz Mountains is an upper Paleogene intracontinental belt, a product of the Arabian-Eurasian collision, which reactivated part of the Cimmerian orogen (Allen et al., 2003; Zanchi et al., 2006, 2009b), and its sedimentary successions represent the northern margin of the Iran microplate during the Paleozoic (Wendt et al., 2005; Gaetani et al., 2009; Zanchi et al., 2009a). The Zagros belt, instead, is part of Arabia and it records the collision between Arabia and the Iranian blocks in the Cenozoic. The Gondwanan ancestry of North and Central Iran has been widely discussed and it is based on the

affinity of the Precambrian basement and of the upper Precambrian-Lower Cambrian sedimentary successions with those of Gondwana (Berberian & King, 1981; Saidi et al., 1997; Ramezani & Tucker, 2003; Hassanzadeh et al., 2008; Zanchi et al., 2009a). In addition, the Gondwanan affinity of North and Central Iran has been supported by paleomagnetic and paleontological data (e.g., Angiolini et al., 2007a; Muttoni et al., 2009).

Central Iran is a particularly complex area and of debated interpretation, due to the occurrence of large active intracontinental faults and several ophiolitic belts, as the so-called "Coloured Mélange", an ophiolitic ring of Upper Mesozoic age which defines the most internal part of the region (Zanchi et al., 2009a; Hassanzadeh & Wernicke, 2016) (Fig. 1). The intracontinental fault system affecting Central Iran is very complex and induces a north-south dextral shearing to the region, with some of these faults separating the Yazd, Tabas and Lut blocks; these faults were already active during the Paleozoic evolution of the region (Wendt et al., 2005; Zanchi et al., 2009a). The tectonic setting is further complicated by the occurrence of isolated blocks in Central Iran which show signs of Carboniferous metamorphism (Bagheri & Stampfli, 2008; Zanchi et al., 2015; Berra et al., 2018; Zanchetta et al., 2018). These have been variably interpreted in the literature, but the most recent interpretations favour a large anticlockwise rotation of the Central Iran blocks (Javadi et al., 2013; Mattei et al., 2015; Tadayon et al., 2019).

One of the most complex regions related to Central Iran - and where Abadeh is located (Hassanzadeh & Wernicke, 2016) - is the Sanandaj-Sirjan Zone (SSZ), a narrow belt of strongly polyphase deformed metamorphic rocks located between Central Iran and the Zagros belt, with a NW-SE orientation and both its boundaries marked by discontinuously preserved ophiolites (Berberian & King, 1981; Stöcklin, 1981; Hassanzadeh & Wernicke, 2016). The SSZ, located north-eastward of the Neotethys suture, differs from the other regions of Iran because it contains an extensive record of Mesozoic magmatism and metamorphism attesting to a continuous subduction process since the Late Triassic (Hassanzadeh & Wernicke, 2016). Even though some authors considered the SSZ as part of the Arabian margin or as a distinct microplate due to the presence of an inner ophiolitic belt between the SSZ and Central Iran (Şengör et al., 1993; Alavi, 1994; Glennie, 2000; Shafaii Moghadam & Stern, 2011), others (e.g., Stöcklin, 1968, 1974; Takin, 1972; Berberian & King, 1981; Dercourt et al., 1986; Agard et al., 2005; Ghasemi & Talbot, 2006) and also more recent interpretations (Hassanzadeh & Wernicke, 2016) consider the SSZ as developed at the northern margin of the Neotethys, in continuity with Central Iran, with the inner ophiolites belt emplaced by rifting during mid-Cretaceous times. The SSZ records the fate of the Neotethys, from its opening in the Permian to its NE-dipping subduction, which began in the Early Jurassic, along with the deposition of volcanoclastics and the emplacement of calcalkaline magmas and Jurassic eclogites (Davoudian et al., 2016; Shakerardakani

et al., 2021). During the Cretaceous, arc magmatism continued, mostly at the extremes of the SSZ. The sediments associated with the inner ophiolites belt, which are not older than Late Cretaceous, indicate the presence of small oceanic basins, which, added to the presence of the arc magmatism, testify to the transition from a passive margin to an Andean/Japanese type magmatic arc as a result of the subduction of the Neotethys (Hassanzadeh & Wernicke, 2016).

The Upper Permian sedimentary succession of Abadeh, the object of the present work, was thus deposited along the northern margin of the Neotethys ocean at equatorial paleolatitudes in a tectonic context characterized by strong thermal subsidence (Saidi et al., 1997; Hassanzadeh & Wernicke, 2016).

The sedimentary succession of Abadeh - The Abadeh section is located in the Hambast Valley (Yazd Province), which cuts through the Abadeh-Hambast Range belt (Taraz, 1974).

In the Abadeh-Hambast Range, the Precambrian metamorphic basement is exposed and it is covered by Lower Paleozoic dolostones and quarzitic sandstones, up to the Lower Devonian which is missing. The succession continues with Upper Devonian and Lower Carboniferous limestones and sandstones, sutured by a thick Permian-Triassic succession. Up-section, a gap corresponds to the Jurassic to Lower Cretaceous, followed by the deposition of Aptian to Cenomanian limestones. These are unconfomably covered by Upper Oligocene-Lower Miocene limestones (Taraz et al., 1981).

The Permian-Triassic succession of Abadeh was divided by Taraz (1974) into seven Permian units identified by progressive numbers and five Lower Triassic units identified by a series of lowercase letters (a to e). The total thickness of the Permian succession at Abadeh exceeds 1100 metres, while the Limestone Group, the name given to the Lower Triassic succession, has a total thickness of 682 metres, of which 90 metres belong to Unit a, the most studied and important unit of the Triassic at Abadeh (Taraz et al., 1981). These units have been then grouped into four formations: the Permian Surmaq Formation, Abadeh Formation, Hambast Formation, and the Triassic Elikah Formation.

SURMAQ FORMATION. The Surmaq Formation comprises units 1, 2 and 3 of Taraz (1974). At Abadeh, the base of the Unit 1 is not exposed, but its thickness attains 390 m. The lower part of the unit, with a thickness of 120 m, consists of an alternation of thin-bedded limestones, thin and brownish shales and thick-bedded limestones with thin cherty layers and nodules. The middle part of Unit 1 (200 m-thick) consists of thin-bedded limestones forming beds up to 30 cm-thick with cherty nodules, intercalated with thin red shales. The upper part of Unit 1 at Abadeh (70 m-thick) consists of thick-bedded limestones passing upward to thin-bedded limestones with cherty nodules and with red shales. At the top red volcanic ashes occur. Most of the limestones enclose fusulines, while beneath the ash beds there are fossiliferous beds containing abundant macrofossils, mainly brachiopods.

Unit 2 has a total thickness of 80 m, and it is rich in chert. Unit 2 conformably overlies Unit 1, and it is divided into four subunits on the basis of the amount of chert. Subunits a and b contain shell and crinoid bioclasts, and sponge spicules. Subunits c and d are rich in chert and strongly recrystallized.

Unit 3 has a total thickness of 80 m, and consists mainly of black limestones. The lower 19 m of the unit consist of thick-bedded limestones with three chert beds more than one metre-thick, while the rest of the unit consists of an alternation of thin bedded and thick-bedded limestones. Macrofossils are common in the thin-bedded limestones, while fusulines are present in both facies.

ABADEH FORMATION. The Abadeh Formation, with a total thickness of 458 m, comprises units 4 and 5 of Taraz (1974). This formation is characterized by the presence of thick, black, flaggy shales, with more abundant limestones in the upper part.

Unit 4 is about 400 m-thick and is divided in two parts: 4a and 4b. Unit 4a is 120 m-thick, and it consists of an alternation of shales and massive limestones (algal and bioclastic wackestones). Unit 4b (280 m-thick) consists of black, flaggy shales and calcareous shales interbedded with thin limestones. The limestone beds in the middle part contain discontinuous cherty layers and nodules. At the base of the unit, the limestones are micritic with mat-like stromatolites (Shahinfar et al., 2021) and characteristically abundant macrofossils. The limestones of the lower 80 m are fine bioclastic wackestone, while in the upper 100 m are dasycladacean algal packstones. Unit 4 contains abundant foraminifers, bryozoans, brachiopods and crinoids (Shen et al., 2009).

Unit 5, up to 58 m-thick, consists of limestone with cherty nodules in the lower and upper part, while the middle part consists of bedded limestones. In the lower 15 m, limestones are stratified algal wackestones. The upper part is made by black massive fine dasycladacean algal packstones.

HAMBAST FORMATION. The Hambast Formation (35 m-thick) comprises units 6 and 7 of Taraz (1974). Unit 6 has a thickness of 17 to 18 m, and consists of an alternation of greenish shales and grey massive micritic limestones (wackestones and packstones). The limestones contain bioclasts, mainly fragments of brachiopods and crinoids in the lower part, and have irregular bedding surfaces. The lower part of the unit contains abundant well-preserved brachiopods and it is known as the *Araxilevis* Bed (Shen et al., 2009).

Unit 7 is 17 m-thick, and consists of thin-bedded brownish-reddish nodular limestones. The limestones of Unit 7 are all micritic (mostly wackestones), with birds-eye structures (Taraz et al., 1981). The fossil content of this unit is rich in ammonoids and conodonts (Shen et al., 2009). The uppermost 4 m of Unit 7 have been defined as the *Paratirolites* Limestone because of the abundant presence of the ammonoid *Paratirolites* (Stepanov et al., 1969).

ELIKAH FORMATION. At the top of the *Paratirolites* Limestone, a few to 30 cm-thick unit made of greenish to brownish shales crops out discontinuosly, the so-called Boundary Clay (Korte et al., 2004;

Kozur, 2007) or boundary shale (Horacek et al., 2007; Richoz et al., 2010), referred to as the base of the Triassic by Taraz et al. (1981, p. 78). In the present paper we follow Korte et al. (2004) in defining this shaly interval as the Boundary Clay.

The Triassic succession has been divided into the Lower Triassic Limestone and the Middle Triassic Dolomite (Taraz, 1974), and the former is further divided into five units. Of interest for this work is the base of the Elikah Formation, represented by Unit a. This unit consists of the Boundary Clay followed by microbialites (1.40 m-thick) with fan-like structures, intercalated to argillaceous limestones. This interval consists of at least three main microbialite beds, the first around 25 cm-thick, the second 40 cm-thick and the uppermost 30 cm-thick. The thickness of the intercalated argillaceous limestones is around 20 cm, and they are absent between the second and third bed. Unit a continues with 15 m of well-stratified bioturbated platy limestones, interrupted at 130 cm from their base by 70 cm of argillaceous limestones. Above the first 200 cm, the limestones are fossiliferous and contain bivalves, represented by *Claraia* species and ophiceratid ammonoids.

THE ABADEH SECTION. The Abadeh section sampled for this work (Angiolini et al., 2017) consists of two logs, approximately 100 metres from each other. The first log is named Gulley section, because it was measured in a gulley, and the second is called Saddle section, because it was measured on a prominent saddle located to the north-west (Fig. 2). A description of the logs is given below and in Tables 1-2 and Figures 3-4. A composite section, based on correlation of the two logs, is given in Fig. 5. The range of the brachiopods and bivalves is reported in Supplementary Table 1.

GULLEY SECTION. The base of the Gulley section is located at 30°53’43.2’’N - 53°12’17.5’’E, at the top of the Abadeh Formation, which has not been sampled. The Gulley section comprises the lowermost part of Unit 7 of the Hambast Formation, which is made of grey to pinkish nodular marly limestones (Tab. 1, Figs 3, 5).

SADDLE SECTION. The base of the Saddle section is located at 30°53’46.2’’N - 53°12’15.3’’E, in the Abadeh Formation. It comprises the Abadeh, Hambast and base of the Elikah Fms (Tab. 2, Figs 4-5). At the top of the Saddle section, at 12 m from the base of the Elikah Fm., a bivalve assemblage has been collected in bed ABS13.

Detailed stratigraphic logs of the Gulley and Saddle sections have been published in Viaretti et al. (2021).

THE DEBATED PERMIAN-TRIASSIC BOUNDARY AT THE ABADEH SECTION

The Permian-Triassic boundary interval at the Abadeh section has been the subject of a large number of studies since its discovery in 1967 (e.g., Kozur et al., 1978; Taraz et al., 1981; Gallet et al., 2000;

Korte et al., 2004; Kozur, 2007; Richoz et al., 2010; Shen & Mei, 2010; Liu et al., 2013; Shen et al., 2013; Chen et al., 2020; Baud et al., 2021). Notwithstanding more than 40 years of intense research on the section, the exact position of the boundary has remained a strongly debated topic as outlined by the discussions published in two recent Permophiles issues (Horacek et al., 2021; Chen et al., 2021), and as summed up below and in Tab. 3.

The first comprehensive survey of the Abadeh section was published by the Iranian Japanese Research Group (Taraz et al., 1981), who placed the Permian-Triassic boundary between Unit 7 of the Hambast Formation and Unit a of the Elikah Formation. The top of Unit 7 was assigned to the Dorashamian Stage (the uppermost Permian Stage in the Tethyan Scale), based on the identification of the *Paratirolites* Zone. According to Taraz et al. (1981, p. 91), this was followed in paraconformity by 10-30 cm of greenish-pinkish-grey shales capped by 130-180 cm-thick stromatolitic limestones containing *Anchignatodus parvus* [later recognized as *H. parvus* by Kozur (1995)]. Therefore, the authors stated that "the shale bed is referred to as the base of the Triassic" (Taraz et al., 1981, p. 78). Gallet et al. (2000) sampled and studied the Permian part of the section. They confirmed the Late Permian age of the top of the Hambast Formation, supported by the FO of *Neogondolella subcarinata* [= *Clarkina subcarinata* (Sweet in Teichert et al., 1973)], a marker for the Dorashamian Stage. The authors pointed out that the uppermost Permian was missing in the Abadeh section, confirming the paraconformity at the Permian-Triassic boundary described by Taraz (1974) and by Taraz et al. (1981).

This was then challenged by Korte et al. (2004) who rejected the occurrence of a stratigraphic gap at the boundary, based on a revision of the conodont zones, and placed the Permian-Triassic boundary at 1.4 metres above the base of the Elikah Formation (Korte et al., 2004, fig. 1). Korte et al. (2004) thus recognized the Abadeh section as a continuous sedimentary succession across the Permian-Triassic boundary. Kozur (2007) reinforced this statement, reporting a high resolution stratigraphic log of the Abadeh section, and placing the shaly interval at the base of the Elikah Formation (Boundary Clay of Korte et al., 2004) in the *C. meishanensis-H. praeparvus* Zone, immediately overlain by the *Merrillina ultima-Stepanovites*? *mostleri* Zone in the microbialites. These were therefore located underneath the Permian-Triassic boundary. In contrast, Horacek et al. (2007) placed the Permian-Triassic boundary 30 cm above the shales, thus placing the microbialite beds in the Lower Triassic.

Shen & Mei (2010) applied the sample-population method (Mei et al., 2004) to the conodont succession at the Abadeh C section (sensu Taraz et al., 1981) and other published Iranian conodont successions. They did not find in their study the *M. ultima-S.*? *mostleri* Zone of Kozur (2005). They thus correlated this zone with either the upper part of the *C. meishanensis-H. praeparvus* Zone of

Kozur (2004) or the *C. zhejiangensis* Zone at Meishan of Mei et al. (1998). Their study highlighted the problem of correlation between the Meishan section and the Iranian sections.

Korte et al. (2010, p. 295) retained the conodont zonation of Kozur (2004) as "the only detailed Tethyan conodont zonation of the interval," stressing the endemism that characterizes the South Chinese conodont faunas. Despite this endemism, the index conodont *M. ultima* is present in the Changhsingian of the Meishan section (Korte et al., 2010), an occurrence used by the authors to place the Permian-Triassic boundary at Abadeh between the *M. ultima-S.*? *mostleri* Zone and the *H. parvus* Zone, above the microbialites.

Richoz et al. (2010) criticized the approach of Kozur (2007), stressing the fact that the ammonoids and most of the conodonts of Abadeh show an intra-Tethyan endemism. For these reasons they adopted the Tethyan Scale (but in fact in their paper they used both the Tethyan stages and the International Chronostratigraphic Chart ones). They attributed the lower 13 metres of Unit 7 to the upper Wuchiapingian, and the last 6.3 metres of Unit 7 to the Dorashamian, based on ammonoid correlation with the Iranian Zal and Julfa sections. Based on conodonts, they proposed the occurrence of a stratigraphic gap between Unit 7 and the Elikah Formation, stating: "The gap is best documented in Abadeh with the *jolfensis* interval and the boundary shale sensu stricto missing" (Richoz et al., 2010, p. 247). They placed the Permian-Triassic boundary 25 cm above the base of the Elikah Fm. and discussed the FO of *H. parvus* in previous works, stating that the *C. meishanensis-H. praeparvus* Zone is reduced at the Abadeh section, while the *M. ultima-S.*? *mostleri* Zone of Kozur (2007) belongs to the *H. parvus* Zone.

In a synthesis of broad interest on the distribution of the Permian-Triassic Boundary Microbialites (PTBM), Kershaw et al. (2012) showed that the distribution of the PTBM correlates with the succession from bed 24 to bed 27d in Meishan. From a biostratigraphic point of view, the PTBM range from the *H. praeparvus* Zone to the boundary between the *H. parvus* Zone and *Isarcicella staechei* Zone. In referring to the Abadeh section, Kershaw et al. (2012) followed the stratigraphy published by Richoz et al. (2010), and placed the Permian-Triassic boundary at the base of the microbialites.

More recent works by Shen et al. (2013), Liu et al. (2013) and Dudás et al. (2017) followed the conodont zonation of Shen & Mei (2010), but placed the Permian-Triassic boundary in different stratigraphic positions. Shen et al. (2013) placed the FO of *H. parvus* inside Unit a of the Elikah Formation, while Liu et al. (2013) placed it in the uppermost part of Unit 7, hence in the Hambast Formation. Dudás et al. (2017) placed the Permian-Triassic boundary at the base of the microbialites. In contrast however, it should be noted that Dudás et al. (2017, Fig. S4B) placed the formational

boundary at the top of the microbialites, including all of the interval of shales and microbialites in the Hambast Formation (90 cm).

The discrepancies in the identification of the position of the Permian-Triassic boundary at Abadeh can be in part explained by the lithological variation at the boundary. Here, in fact, the lithology of the beds at the base of the Elikah Formation and in particular the thickness of the Boundary Clay and of the microbialites varies laterally, explaining at least in part the differences observed in the stratigraphic logs of the authors. The Boundary Clay, for example, has a thickness which ranges from a few cm to 30 cm. The microbialites often crop out as several lenticular horizons separated by shales (Fig. 4d). While most of the authors show the microbialite interval as a three layers unit, Chen et al. (2020) suggest that this is not always the situation, and their stratigraphic log shows the intercalation of argillaceous limestones between the microbialite beds.

Chen et al. (2020) proposed a very detailed stratigraphic log, with a focus on the Permian-Triassic transition in the succession and for the most part they followed the conodont zonation of Shen & Mei (2010). However, in fig. 2 of Shen & Mei (2010) the FO of *H. parvus* seems to be located about 80 cm above the top of the *Paratirolites* Limestone, whereas Chen et al. (2020) placed the base of the *H. parvus* Zone at the top of the microbialites (about 1.5 m above the top of the *Paratirolites* bed), in agreement with Korte et al. (2004) and Kozur (2007).

The work of Chen et al. (2020) was criticized by Horacek et al. (2021) mainly for their use of the stratigraphy of Shen & Mei (2010) - considered of low-resolution - and for the absence of figured material for the definition of the conodont zones. Horacek et al. (2021, fig. 1) also discussed the different positions of the Permian-Triassic boundary at Abadeh identified by previous authors, classifying them into two groups; the first group comprising the authors that placed the Permian-Triassic boundary near the base of the microbialites, and the second including authors that placed the boundary above the microbialites.

Chen et al. (2021) answered the criticism, by emphasising that the uncertainty and the complexity of interpretations surrounding the position of the Permian-Triassic boundary at the Abadeh section is so deep that it is impossible to force previous authors into two groups. They discussed the arguments raised by Horacek et al. (2021) and concluded, based on a revision of the conodonts collected in 2009 and 2017 (Shen et al., 2009; Angiolini et al., 2017), that the PTB should be in the middle of the microbialites, 80 cm above the base of the Boundary Clay.

In this paper, we follow Shen & Mei (2010) and Chen et al. (2021) in placing the Permian-Triassic boundary 80 cm above the base of the Boundary Clay (that is at the top of the *Paratirolites* Limestone). An overview of the debate is provided in Tab. 3 and Fig. 6.

THE BIVALVE FAUNA FROM ABADEH

The bivalves collected from the Abadeh section come mainly from bed ABS13 (Fig. 7).

The single specimen collected from bed ABS10 (Hambast Fm.) is represented by a badly preserved internal mould of a left valve which is moderate in size, slightly inflated and retrocrescent. The radial ornamentation is not well preserved and only detectable on the median-ventral part of the disc. It consists of irregularly spaced and rounded ribs, apparently of different orders. The umbo, posterior and anterior auricles are not preserved or clearly detectable. The valve incompleteness prevents any further determination at lower taxonomic categories than Aviculopectinoidea sp. (Fig. 7a).

Two species of *Claraia* occur in bed ABS13 (Elikah Fm.): *Claraia radialis julfensis* Nakazawa, 1977 (Fig. 7b-c) and *Claraia* gr. *aurita* (Hauer, 1850) (Fig. 7d).

The majority of the specimens collected from bed ABS13 belong to *Claraia radialis julfensis.* They are radially ornamented and reach a maximum height of 47 mm. They have unfortunately an incomplete preservation which prevents an accurate description of the shell outline and wing morphology. The valves were probably moderately inflated, slightly oval and retrocrescent. The surface is ornated by dense, about fifty, radial ribs which grow by intercalation and arranged into three orders. Concentric ornaments are almost absent. Few and weak concentric folds occasionally occur only in the umbonal region.

Claraia species with a predominant radial ornamentation have been included into the *C. stachei* group (Ichikawa, 1958). The preserved morphology of the studied specimens corresponds well to *Claraia radialis julfensis* Nakazawa, 1977, a subspecies already described from Julfa and Abadeh (Iran). It has been later attributed to *Claraia stachei* Bittner, 1901 (Yin, 1985). The latter species, however, presents taxonomical problems (Hofmann et al., 2013). Its nomenclatural types have not been figured and the identification is based on Greenland and North American specimens respectively illustrated by Spath (1930) and Newell & Kummel (1942), who interpreted Bittner's species in different ways. For instance, the North American individuals have fewer and more subdued radial ribs than those from Greenland. In absence of an unequivocal original definition of *C. stachei*, Nakazawa's subspecies is here referred to as *Claraia radialis* Leonardi, 1960 from the Dolomites, where *Claraia* shells with a predominant radial sculpture are rare. They occur within the *Claraia clarai* Subzone, latest Griesbachian-early Dienerian in age (Induan; Broglio Loriga et al., 1983; Posenato, 2008).

According to Taraz et al. (1981), in the Abadeh section *C. radialis julfensis* occurs in the lower Elikah Fm. It ranges from 3 m to 17.5 m above the formational boundary with the Hambast Fm. *Isarcicella isarcica*, a marker for the late Griesbachian, appears at 2 m (Taraz et al., 1981) or 2.3 m (Korte et al., 2004) above the formational boundary while the first appearance of *Neospathodus dieneri*, marker for the base of the Dienerian, has been found at 15 m above the Boundary Clay

(e.g., Korte et al., 2004; Horacek et al., 2007; Richoz et al., 2010). The *Claraia*-bearing bed ABS13 belongs to the *I. isarcica* Zone (Fig. 5), that is late Griesbachian in age.

The other species that occurs, *Claraia* gr. *aurita*, is represented only by the median part of a left valve. It shows an ornamentation pattern quite different from the other radially ribbed individuals coming from bed ABS13. The sculpture consists of predominant thin, slightly waived and regularly spaced concentric ribs and very weak and irregular radial ribs with rounded apex. Predominant concentric ribs are a typical feature of the *Claraia aurita* group (Ichikawa, 1958) which also contains species with faint radial ornamentation (e.g., *C. bittneri* Ichikawa, 1958; *C. griesbachi* Bittner, 1899; *C. guizhouensis* Chen in Liu, 1964). The classification of these species is also based on shell outline and wing morphology. In the absence of preservation of these features a specific determination of this fragment is impossible.

THE BRACHIOPOD FAUNA FROM ABADEH

The studied brachiopod fauna comprises 30 species belonging to 14 genera: *Spinomarginifera helica*, *S. iranica*, *S. pygmaea*, *S. spinosocostata*, *Spinomarginifera* sp., *Araxilevis intermedius*, *Tschernyschewia typica*, *Leptodus* cf. *richtofeni*, *L. nobilis*, *Leptodus* sp., *Permianella* sp., *Orthothetina persica*, *Orthothetina* sp., *Perigeyerella* aff. *costellata*, *P.* aff. *tricosa*, *Perigeyerella* sp., *Araxathyris abichi*, *A. bruntoni*, *A. felina*, *A. quadrilobata*, *Araxathyris* spp., ?*Rectambitus* sp., *Gruntallina* sp., ?*Spirigerella* sp., *Transcaucasathyris araxensis*, *T. kandevani*, *T. lata*, *Transcaucasathyris* spp., *Paracrurithyris pygmaea* and ?*Permophricodothyris* sp. Several poorly preserved specimens have been identified as belonging to the Tyloplectini, Schizophoriidae and to the Athyrididae. The systematic study presented in this paper represents a step forward from the first survey by Taraz et al. (1981) who listed only 14 brachiopod species.

Five brachiopod orders are represented in this fauna: Productida, Orthotetida, Orthida, Athyridida and Spiriferida. Two of them, Orthida and Spiriferida, are subordinated being represented by a single specimen each. Among the other three orders, Productida and Athyridida are dominant, being respectively 37.2% and 60.8% of the described specimens. The Orthotetida represents only 1.6% of the described specimens.

The representatives of the two main orders, Productida and Athyridida, are characterized by different life styles, the former is seminfaunal and better adapted to soft substrates, while the latter is pedicle-attached and ubiquitary, but requiring small hard substrates (shells, bioclasts) to attach. The depositional environment of the Hambast Fm. is a low energy one, at a depth below the storm wave base. The relative abundance of the representatives of the two orders (Fig. 5) seems not to strictly correlate to the lithology, with both taxa being variably present in muddy or in more bioclastic

sediments. However, in beds ABS0, ABS15, ABS5, ABS6, ABS7 which are shales (mostly covered), the brachiopod fauna is dominated or represented only by semi-infaunal taxa which thrive better in these conditions.

The five orders are also characterized by two different microstructures of the shell. The Productida and Orthotetida have a laminar secondary layer, and the Orthida, Athyridida and Spiriferida have a fibrous one. The distribution of these orders along the stratigraphic succession shows an alternation in the prevalence of one microstructural type over the other, but in the upper part of the section, from the base of the *Clarkina transcaucasica* Zone upward, only brachiopods with a fibrous microstructure are present (Fig. 8). To better investigate the distribution of the brachiopods in terms of change in biodiversity and in microstructure, we have calculated the Margalef and Shannon-Wiener diversity indices and the percentage of the brachiopod shell microstructural types bed by bed (Tab. 4). The diversity indices show that there is no biodiversity decline up to bed ABS25 at the base of the *Clarkina orientalis* Zone, in the upper Wuchiapingian (Shen et al., 2019). Also, there is no correlation between biodiversity variations and microstructural change (Fig. 8). When the indices are high there is alternation in the dominance by laminar vs fibrous taxa, whereas, when the indices are low, the laminar taxa dominate. This could be linked to local facies change, i.e. the advantage of laminar concave-convex shells on soft shaly substrates such as ABS0, ABS15, ABS5, ABS6, ABS7. However, in the *Paratirolites* Limestones, brachiopod biodiversity drops to just one species, the disaster taxon *Paracrurithyris pygmaea*, characterized by a fibrous secondary layer.

Biostratigraphy and correlation - The stratigraphic distribution of brachiopods from the composite Abadeh section produced in this study has been compared with that of the Julfa section of NW Iran published by Ghaderi et al. (2014). The comparison has been made using the Unitary Association (UA) method of Guex (1991), a deterministic mathematical model that, based on the relations of coexistence and superposition of taxa, defines consistent associations of taxa which can be used to build a biozonation and to correlate different successions (Tab. SOM 2).

Before the computation of data, we added the occurrence of *Paracrurithyris pygmaea* in bed ABS11, represented by few small specimens recorded in thin section and not reported in the systematic descriptions. As a result, eight UAs have been found, merged into five due to high similarity in the taxonomical composition. Three UAs are recorded in both sections, showing their potential role to correlate the Upper Permian of NW Iran (Julfa) and Central Iran (Abadeh) (Fig. 9). The first biozone is represented by UA1-2, which correlates the base of the Hambast Formation at the Abadeh section with the lower Lower Julfa Beds. This biozone is here named *Araxilevis intermedius-Leptodus nobilis* Biozone, corresponding to the *Araxilevis intermedius* Biozone described by Ghaderi et al. (2014), ranging from bed G125 to bed G139 in Julfa and from from beds ABS0/ABS15 to beds ABS5/ABS6

in Abadeh, and Wuchiapingian in age. The UA analysis shows the occurrence of UA3, characterized by *Orthothetina eusarkos*, only in the Julfa section. This interval, which is absent at Abadeh, was not considered by Ghaderi et al. (2014) and it was included mostly in the lower part of the *Permophricodothyris ovata* Biozone. The following biozone is represented by UA4-5, which in Abadeh spans the beds ABS7 to ABS25, in the central part of the Hambast Formation. At Julfa, UA4-5 spans the beds G143b to G161, in the upper Lower Julfa Beds and the lower Upper Julfa Beds. This UA can be defined as the *Permophricodothyris ovata-Araxathyris quadrilobata* Biozone and it corresponds to the middle-upper part of the *Permophricodothyris ovata* Biozone defined by Ghaderi et al. (2014) at Julfa. According to the conodont zonation of Shen & Mei (2010), this zone roughly corresponds to the *Clarkina transcaucasica* Zone and partially to the upper *C. guangyuanensis* Zone and it is middle to late Wuchiapingian in age. Another UA exclusively present in Julfa is UA6-7, here defined as *Haydenella kiangsiensis-Transcaucasathyris minor* Biozone, which corresponds to the *Haydenella kiangsiensis* Biozone defined by Ghaderi et al. (2014). The absence of this biozone in Abadeh is possibly due to outcrop conditions. Finally, UA8 has been detected in the *Paratirolites* Limestone of both sections, correlating bed ABS11 at Abadeh with bed G271 at Julfa. UA8 is taxonomically identified by the presence of *Paracrurithyris pygmaea*, and establishes the *P. pygmaea* Biozone, the uppermost brachiopod biozone that can be found in the Permian of Iran, late Changhsingian in age.

Ghaderi et al. (2014) supported the correlation of the Julfa beds with the faunal succession of Dorasham, Transcaucasia (Ruzhentsev & Sarytcheva, 1965) proposed by Stepanov et al. (1969). According to Ghaderi et al. (2014), the *Araxilevis intermedius* Biozone in Julfa correlates with the *Araxilevis* beds in Dorasham, the *Permophricodothyris ovata* Biozone correlates with the *Araxoceras-Oldhamina* beds in Dorasham and the *Haydenella kiangsiensis* Biozone correlates with the *Haydenella-Pseudowellerella* (= *Prelissorhynchia*) beds in Dorasham. Consequently, based on our revised biozonation, the newly proposed *Araxilevis intermedius-Leptodus nobilis* Biozone correlates with the *Araxilevis* beds of Dorasham and the *Permophricodothyris ovata-Araxathyris quadrilobata* biozone correlates with the *Araxoceras-Oldhamina* beds of Dorasham.

The correlation between the succession of the Alborz Mountains in North Iran (Gaetani et al., 2009; Angiolini & Carabelli, 2010) and those of Central and North-West Iran, as well as with Transcaucasia, is more difficult, given the different depositional settings - shallow water in North Iran vs deeper water in Abadeh and Julfa - as already discussed by Angiolini & Carabelli (2010) and Ghaderi et al. (2014). The *Araxilevis intermedius* Biozone of the lower member of the Nesen Formation in the Alborz mountains has been correlated to the *Araxilevis* Biozone of Transcaucasia and Julfa (Gaetani et al., 2009; Angiolini & Carabelli, 2010; Ghaderi et al., 2014). Consequently, the *Araxilevis*

intermedius Biozone should correlate with the newly proposed *Araxilevis intermedius-Leptodus nobilis* Biozone. The *Haydenella* Biozone of the Alborz Mountains correlates with the *Haydenella kiangsiensis* Biozone of Julfa, which is missing at Abadeh. The main problem is the correlation of the *Permophricodothyris ovata* Biozone, which in North Iran has been found above the *Haydenella* Biozone and it has been given a Changhsingian age. Also, the *Paracrurithyris pygmaea* Biozone which is very characteristic of the uppermost Changhsingian beds in Julfa, Abadeh and South China has not been recorded in the Alborz Mountains.

CONCLUSIONS

To conclude, in this paper we show that:

1. The position of the Permian-Triassic boundary at the Abadeh section is still debated. However, latest conodont data, field observations and literature analysis suggest that the boundary is most likely placed at 80 cm above the base of the Elikah Fm.
2. The newly described Wuchiapingian brachiopod fauna from the Hambast Fm. consists of 30 described species belonging to 14 genera, a significant improvement compared to the first list provided by Taraz et al. (1981).
3. In the Abadeh section, there is no biodiversity decline in the brachiopod fauna during the Wuchiapingian, and no correlation between biodiversity and shell microstructural changes. However, in the Changhsingian part of the succession, brachiopods are very rare and represented only by a fibrous shelled species *Paracrurithyris pygmaea*. This species is very characteristic of the uppermost Permian beds in Julfa and South China, and it has been recovered also from the Boundary Clay.
4. The Abadeh section has been correlated to the Julfa section in NW Iran using the Unitary Associations method. The analysis allowed the identification of four biozones. Three of them are present in both sections: the Wuchiapingian *Araxilevis intermedius-Leptodus nobilis* Biozone, extending from the *Clarkina asymmetrica* Zone to the *C. guangyuanensis* Zone; the Wuchiapingian *Permophricodothyris ovata-Araxathyris quadrilobata* Biozone, roughly corresponding to the *C. transcaucasica* Zone; the Changhsingian *Paracrurithyris pygmaea* Biozone, from the base of the *C. abadehensis* Zone. One biozone, the Wuchiapingian *Haydenella kiangsiensis-Transcaucasathyris minor* Biozone, has been found only in the Julfa section, but it is considered important for regional correlation with Transcaucasia and North Iran. These results indicate that brachiopods can be useful tools in biostratigraphy, and show their potential for correlation at a regional scale in the Upper Permian.

5. The *Claraia* bed, containing *Claraia radialis julfensis* and *Claraia* gr. *aurita*, is late Griesbachian in age.

SYSTEMATIC PALEONTOLOGY

Class STROPHOMENATA Williams, Carlson, Brunton, Holmer & Popov, 1996
Order PRODUCTIDA Sarytcheva & Sokolskaya, 1959
Suborder PRODUCTIDINA Waagen, 1883
Superfamily PRODUCTOIDEA Gray, 1840
Family PRODUCTELLIDAE Schuchert, 1929
Subfamily MARGINIFERINAE Stehli, 1954
Tribe MARGINIFERINI Stehli, 1954

Genus *Spinomarginifera* Huang, 1932
Type species *Spinomarginifera kueichowensis* Huang, 1932

Remarks - The genus *Spinomarginifera* Huang, 1932 differs from *Marginifera* Waagen, 1884 because of the spine bases not arranged in rows along the flanks, and from *Entacanthadus* Grant, 1993 because of the occurrence of spine bases on the dorsal valve. The species of the genus *Spinomarginifera* are distinguished by the spine bases shape and arrangment, the presence and distribution of ridges and presence/absence of a ventral sulcus.

Spinomarginifera helica (Abich, 1878)
(Pl. 1, figs 1-5)

1878 *Productus intermedius helicus* ABICH, p. 44, Pl. 5, fig. 7; Pl. 10, figs 3, 12-13, 17, 19-20.
1878 *Productus aculeatus* ABICH, p. 50, Pl. 5, fig. 12; Pl. 10, fig. 21.
1878 *Productus spinulosus* ABICH, p. 51, Pl. 5, fig. 9.
1878 *Productus indeterminatus* ABICH, p. 47, Pl. 10, fig. 16; p. 48, Pl. 10, figs 4-18.
1900 *Marginifera intermedia helica* (Abich) - ARTHABER, p. 265, Pl. 20, figs 10-12.
1903 *Marginifera helica* (Abich) - DIENER, p. 74, Pl. 3, fig. 9.

1933 *Marginifera intermedia helica* (Abich) - SIMIĆ, p. 42, Pl. 3, fig. 9.
1937 *Productus* (*Marginifera*) *intermedius-helicus* var. *multispinosa* (Abich) - LICHAREW, p. 95, Pl. 22, fig. 9.
1958 *Marginifera helica helica* (Abich) - RAMOVS, p. 501, Pl. 2, fig. 8.
1960 *Spinomarginifera intermedia-helica* (Abich) - SARYTCHEVA et al., p. 228, Pl. 38, fig. 14.
1963 *Spinomarginifera intermedia-helica* (Abich) - SCHRÉTER, p. 118, Pl. 5, figs 3-11.
1965b *Spinomarginifera helica* (Abich) - FANTINI SENTINI, p. 47, Pl. 5, figs 6-7.
1965 *Spinomarginifera helica* (Abich) - SARYTCHEVA & SOKOLSKAYA in Ruzhentsev & Sarytcheva, p. 226, Pl. 37, figs 9-11.
1966 *Spinomarginifera helica* (Abich) - FANTINI SESTINI & GLAUS, p. 904, Pl. 64, fig. 6.
1969 *Spinomarginifera helica* (Abich) - STEPANOV et al., Pl. 5, fig. 3a-b.
2010 *Spinomarginifera helica* (Abich) - ANGIOLINI & CARABELLI, p. 53, Pl. 1, figs 10-11.
2011 *Spinomarginifera helica* (Abich) - VERNA & ANGIOLINI in Verna et al., p. 78, Pl. 3, figs 1-7; Pl. 6, figs 5-6.
2014 *Spinomarginifera helica* (Abich) - GARBELLI & ANGIOLINI in Ghaderi et al., p. 38, Pl. 1, figs 9-12.

Material - Five figured articulated shells: MPUM12170 (ABS3-1), MPUM12171 (ABS16-18), MPUM12172 (ABS17-70), MPUM12173 (ABS22-1), MPUM 12174 (ABS25-4); five articulated shells: MPUM12175 (ABS7-12, ABS8-21, ABS16-17, ABS17-4, ABS22-6); one internal mould: MPUM12176 (ABS17-2).

Description - Small to medium sized, concave-convex shell with transverse sub-oval outline. Trail long and slightly geniculated. Cardinal margin long and straight, ending with small ears. Maximum width anteriorly, 10.3-19.4 mm; shell length: 9.2 -14.5 mm. Ventral umbo broad and only moderately projecting on the cardinal margin. Ventral valve with a very slight and shallow median sulcus. Ornamentation of ventral valve of widely spaced spines. Spine bases rounded, forming elongated ridges on the trail, 0.6 mm wide. Ornamentation of dorsal valve of fine rugae, few spines. Dorsal valve interior with a bilobed cardinal process and cardinal ridges, pear-shaped adductor scars.

Remarks - *Spinomarginifera helica* (Abich, 1878) is a very variable species and, according to Sarytcheva & Sokolskaya in Ruzhentsev & Sarytcheva (1965), this variability is mostly due to ontogenetic variation. Intraspecific variability is detected in features such as size, outline and

dimensions, number and position of spines, and it also shows substantial differences from the other species of the genus. *S. helica* differs from *S. ciliata* (Arthaber, 1900) because of the larger spine bases and spine ridges not uniformly distributed; from *S. iranica* Fantini Sestini, 1965a because the spines are widely spaced, with no clustering on the ears and because of the presence of spine ridges; from *S. pygmaea* Sarytcheva in Ruzhentsev & Sarytcheva, 1965, because of the larger size and the elongated spine bases forming ridges on the anterior trail; from *S. spinosocostata* (Abich, 1878) because the spine bases form ridges only on the anterior trail, without giving origin to ribs; from *S. sulcata* Shen et al., 1992, because of the absence of a distinct ventral sulcus.

Occurrence - Hambast Formation, Unit 6, Abadeh section, Central Iran. Wuchiapingian.

Distribution - Wuchiapingian *Araxilevis, Oldhamina* and *Haydenella* beds of Transcaucasia (Ruzhentsev & Sarytcheva, 1965); Guadalupian to lower Changhsingian of North and North-West Iran (Fantini Sestini, 1965b; Angiolini & Carabelli, 2010; Ghaderi et al., 2014); Lopingian of Himalaya (Diener, 1903), of North Caucasus (Licharew, 1937, 1939) and of South-East Europe (Simić, 1933; Ramovs, 1958). Specimens of *S.* cf. *helica* have been found in the Wuchiapingian of Turkey (Angiolini et al., 2007b).

Spinomarginifera iranica Fantini Sestini, 1965a
(Pl. 1, figs 6-9)

1965a *Spinomarginifera iranica* FANTINI SESTINI, p. 992, Pl. 94, figs 2-5.
2010 *Spinomarginifera iranica* Fantini Sestini - ANGIOLINI & CARABELLI, p. 56, Pl. 1, figs 12-18.
2011 *Spinomarginifera iranica* Fantini Sestini - VERNA et al., p. 65, Pl. 1, fig. 23.
2014 *Spinomarginifera iranica* Fantini Sestini - GARBELLI & ANGIOLINI in Ghaderi et al., p. 39, Pl. 1, figs 13-16.

Material - Four figured articulated shells: MPUM12177 (ABS8-37), MPUM12178 (ABS17-43), MPUM12179 (ABS17-46), MPUM12180 (ABS17-61); seven articulated shells: MPUM12181 (ABS1-1), MPUM12182 (ABS7-8), MPUM12183 (ABS8-20, ABS8-28, ABS8-35, ABS8-70), MPUM12184 (ABS17-8).

Description - Small to medium sized, concave-convex shell with a subtriangular outline. Corpus cavity deep and trail slightly geniculated. Maximum width: 9.7-17.3 mm; length: 8.6-12.5 mm.

Cardinal margin straight, ending with small and angulate ears. Anterior commissure rectimarginate. Ventral umbo broad, recurved, slightly projecting on the cardinal margin. Ornamentation of ventral valve of several closely spaced spines, denser on the ears. Spine bases rounded, not forming ridges. Growth lamellae on the anterior trail and dense growth lines. On the dorsal valve spines are less dense. Dorsal valve interior with pear-shaped muscle scars projecting antero-laterally and median septum extending up to shell mid-length.

Remarks - *Spinomarginifera iranica* Fantini Sestini, 1965a, has been considered a transitional species between *S. ciliata* (Arthaber, 1900) and *S. helica* (Abich, 1878) by Angiolini & Carabelli (2010). It differs from *S. ciliata* for its coarser and more widely spaced spines; and from *S. helica* because of the spines, which have oval bases, do not form ridges and are more densely spaced.

Occurrence - Hambast Formation, Unit 6, Abadeh section, Central Iran. Wuchiapingian.

Distribution - Guadalupian-Lopingian of Turkey (Angiolini et al., 2007b; Verna & Angiolini in Verna et al., 2011); Wuchiapingian and lower Changhsingian of North and North-West Iran (Angiolini & Carabelli, 2010; Ghaderi et al., 2014).

Spinomarginifera pygmaea Sarytcheva in Ruzhentsev & Sarytcheva, 1965
(Pl. 1, figs 10-13)

1965 *Spinomarginifera pygmaea* SARYTCHEVA in Ruzhentsev & Sarytcheva, p. 227, Pl. 37, figs 13-15.
2010 *Spinomarginifera pygmaea* Sarytcheva in Ruzhentsev & Sarytcheva - ANGIOLINI & CARABELLI, p. 56, Pl. 1, figs 19-20.

Material - Four figured articulated shells: MPUM12185 (ABS7-7), MPUM12186 (ABS8-27), MPUM12187 (ABS8-29), MPUM12188 (ABS8-39); two articulated shells: MPUM12189 (ABS8-16, ABS8-36).

Description - Small-sized, concave-convex shell with short and slightly geniculated trail. Maximum width: 8-11.4 mm; length: 6.7-12.4 mm. Outline sub-oval, cardinal margin straight, shorter than maximum width, ending with slightly enrolled ears. Ventral umbo pointed, strongly recurved on the cardinal margin, projecting over it. Ventral valve with a subquadrate visceral disc. Dorsal valve

strongly concave, with sub-oval visceral disc. Ornamentation of the ventral valve of equally spaced spines with rounded bases, weak and flat ribs and rugae. Growth lamellae on the anterior trail. Ornamentation of the dorsal valve of strong concentric rugae with few spine bases.

Remarks - *Spinomarginifera pygmaea* Sarytcheva in Ruzhentsev & Sarytcheva, 1965 differs from *S. ciliata* (Arthaber, 1900), *S. helica* (Abich, 1878) and *S. spinosocostata* (Abich, 1878) because its spine bases are rounded and do not form ridges; from *S. sulcata* Shen et al., 1992, because of the absence of a ventral sulcus and; from *S. iranica* Fantini Sestini, 1965a because of its smaller size.

Occurrence - Hambast Formation, Unit 6, Abadeh section, Central Iran. Wuchiapingian.

Distribution - Wuchiapingian *Oldhamina* beds and Changhsingian beds of Transcaucasia (Ruzhentsev & Sarytcheva, 1965); Wuchiapingian and lower Changhsingian of North Iran (Angiolini & Carabelli, 2010).

Spinomarginifera spinosocostata (Abich, 1878)
(Pl. 1, figs 14-16)

1878 *Productus spinoso-costatus* ABICH, p. 41, Pl. 10, figs 6-7, 10.
1878 *Productus spinoso-costatus* var. *cariniferus* ABICH, p. 41, Pl. 10, fig. 8.
1878 *Productus spinoso-costatus* var. *expansus* ABICH, p. 42, Pl. 5, figs 8, 11.
1900 *Marginifera spinosocostata* (Abich) - ARTHABER, p. 262, Pl. 20, figs 5-8.
1911 *Productus (Marginifera) spinuloso-costatus* Abich - FRECH, p. 175, Pl. 27, figs 1-2.
1937 *Productus (Marginifera) spinosocostatus* Abich - LICHAREW, p. 71, Pl. 10, fig. 37.
1965b *Marginifera spinosocostata* (Abich) - FANTINI SESTINI, p. 43, Pl. 5, figs 2-3.
1965 *Spinomarginifera spinosocostata* (Abich) - SARYTCHEVA & SOKOLSKAYA in Ruzhentsev & Sarytcheva, p. 225, Pl. 37, figs 6-8.
1966 *Spinomarginifera spinosocostata* (Abich) - FANTINI SESTINI & GLAUS, p. 905, Pl. 64, fig. 5.
2010 *Spinomarginifera spinosocostata* (Abich) - ANGIOLINI & CARABELLI, p. 56, Pl. 1, figs 21-22.
2011 *Spinomarginifera spinocostata* (Abich) - VERNA & ANGIOLINI in Verna et al., p. 65, Pl. 1, figs 31-33.
2014 *Spinomarginifera spinosocostata* (Abich) - GARBELLI & ANGIOLINI in Ghaderi et al., p. 39, Pl. 1, figs 17-22.

Material - Three figured articulated shells: MPUM12190 (ABS8-24), MPUM12191 (ABS25-5), MPUM12192 (ABS25-10); three articulated shells: MPUM12193 (ABS0-35), MPUM12194 (ABS25-2, ABS25-45).

Description - Small to medium-sized, concave-convex shell. Trail geniculated and outline transversely sub-oval. Cardinal margin straight, with angular extremities, shorter than the maximum width. Anterior commissure rectimarginate. Maximum width: 10.4-15.5 mm; length: 9-12.5 mm. Ventral valve with long and geniculated trail. Umbo broad, strongly recurved on the cardinal margin, but not projecting over it. Visceral disc with a slight median depression. Dorsal valve with a short trail and a transversely sub-oval visceral disc. Ornamentation of the ventral valve of spines with rounded bases placed on ribs. Ribs coarse, up to 1.4 mm wide. Ornamentation of the dorsal valve with few spines without ridges and concentric fine rugae.

Remarks - The presence of long spine ridges forming ribs is a diagnostic feature present only in the species *Spinomarginifera spinosocostata* (Abich, 1878).

Occurrence - Hambast Formation, Unit 6, Abadeh section, Central Iran. Wuchiapingian.

Distribution - Wuchiapingian *Araxilevis* and *Oldhamina* beds of Transcaucasia (Ruzhentsev & Sarytcheva, 1965); Guadalupian-Lopingian Ruteh and Nesen Formation of the Alborz Mountains, North Iran (Fantini Sestini, 1965b; Fantini Sestini & Glaus, 1966; Angiolini & Carabelli, 2010); Wuchiapingian of North-West Iran (Ghaderi et al., 2014); Lopingian of North Caucasus (Licharew, 1937). Specimens of *S.* cf. *spinosocostata* have been found in the Wuchiapingian of Turkey (Angiolini et al., 2007b).

Spinomarginifera sp.

(Pl. 1, fig. 17)

Material - One figured interior dorsal valve attached to the exterior of a ventral valve: MPUM12195 (ABS16-1); sixty-nine articulated shells: MPUM12196.

Remarks - The specimens are poorly preserved. In most of the specimens the shell is almost entirely decorticated, leaving internal moulds with just small portions of shell where a few of the spine bases are preserved, hampering their identification at specific level.

Occurrence - Hambast Formation, Unit 6, Abadeh section, Central Iran. Wuchiapingian.

Family PRODUCTIDAE Gray, 1840
Subfamily LEIOPRODUCTINAE Muir-Wood & Cooper, 1960
Tribe TYLOPLECTINI Termier & Termier, 1970

Genus *Araxilevis* Sarytcheva & Sokolskaya in Ruzhentsev & Sarytcheva, 1965
Type species *Productus intermedius* Abich, 1878

Remarks - The genus *Araxilevis* Sarytcheva & Sokolskaya in Ruzhentsev & Sarytcheva, 1965 differs from *Tyloplecta* Muir-Wood & Cooper, 1960 because of its longer and lamellose trail, the swollen spine bases, the absence of ribbing and the larger size.

Araxilevis intermedius (Abich, 1878)
(Pl. 2, figs 1-5)

1878 *Productus intermedius* ABICH, p. 27, Pl. 4, figs 10-12; Pl. 7, fig. 1; Pl. 10, figs A-B.
1878 *Productus intermedius* var. *plano-convexus* ABICH, p. 31, Pl. 4, fig. 13; Pl. 9, fig. 6.
1878 *Productus martini* ABICH, p. 32, p. 5, fig. 1; Pl. 9, fig. 4.
1900 *Productus intermedius* (Abich) - ARTHABER, p. 254, Pl. 19, figs 7-8.
1939 *Productus intermedius* (Abich) - LICHAREW, p. 93, Pl. 21, fig. 1.
1960 *Plicatifera intermedia* (Abich) - SARYTCHEVA et al., p. 227, Pl. 35, fig. 3.
1965 *Axarilevis intermedius* (Abich) - SARYTCHEVA & SOKOLSKAYA in Ruzhentsev & Sarytcheva, p. 222, Pl. 35, fig. 4; Pl. 36, figs 1-4.
1969 *Araxilevis intermedius* (Abich) - STEPANOV et al., Pl. 3, fig. 1a-c.
2010 *Araxilevis intermedius* (Abich) - ANGIOLINI & CARABELLI, p. 60, Pl. 2, fig. 8.
2014 *Araxilevis intermedius* (Abich) - GARBELLI & ANGIOLINI in Ghaderi et al., p. 40, Pl. 1, figs 27-28.

Material - Five figured articulated shells: MPUM12197 (ABS0-1), MPUM12198 (ABS0-25), MPUM12199 (ABS0-28), MPUM12200 (ABS5-12), MPUM12201 (ABS5-14); seven articulated shells: MPUM12202 (ABS0-27), MPUM12203 (ABS5-3, ABS5-5, ABS5-7, ABS5-8, ABS5-9,

ABS5-11); six articulated fragments: MPUM12204 (ABS5-4, ABS5-10, ABS5-13), MPUM12205 (ABS8-5, ABS8-6, ABS8-7); one internal mould: MPUM12206 (ABS5-12).

Description - Medium sized, concave-convex shell with sub-rectangular outline. Trail slightly geniculate. Cardinal margin straight and long, corresponding to the maximum width, cardinal extremities angular with well-developed ears. Shell substance thicker in the ventral than in the dorsal valve. Maximum width: 40-74 mm; length: 39-52.5 mm. Shell thickness: 20-34 mm. Ventral umbo broad and recurved on the cardinal margin. Ventral median sulcus shallow and flat, more evident near the umbo and fading on the trail. Dorsal valve with a longitudinally elongated sub-elliptical outline. Ornamentation of the ventral valve of spines with elongated bases on ribs. Spine bases 0.2-0.35 mm long and 0.15-0.2 mm wide, not arranged in a definite pattern. Ribs numbering 5-8 per 10 mm; in the anterior third of the ventral valve the ribs are substituted by well-developed growth lamellae. Ornamentation of the dorsal valve with ribs, growth lamellae and pustules. Dorsal valve interior with a median septum extending for 2/3 of the valve length. On each side of the septum near the hinge, rounded triangular shaped muscular impressions are present, characterized by fine branching. In the middle part of the dorsal valve there are brachial ridges, extending laterally and ending with a closed loop near the lateral margin of the valve.

Remarks - The specimens under study belong to *Araxilevis intermedius* (Abich, 1878) based on the sub-rectangular outline, the concave-convex morphology with a slight geniculation on the anterior trail, the strongly lamellose anterior trail and the shape of the muscle field and the brachial loops. *Araxilevis* comprises two species: *A. intermedius* and *A. minor*. While the first one is well known in the literature, the second one was described by Termier & Termier in Montenat et al. (1976) from the Murgabian of the Saiq Plateau, Oman, and it is cited only in Weidlich & Bernecker (2007). There are three syntypes of *A. minor* in the National History Museum in Paris, but there are no traces of the holotype (Pacaud, 2015). It is thus difficult to make an objective comparison with the other species. Specimens labelled MPUM12207 are characterized by a longer shape resulting in a sub-quadrate outline, a less convex ventral valve resulting in a less thick shell and a longer median sulcus, characters which prevent a reliable generic identification for these specimens. Therefore, they have been identified as indeterminate Tyloplectini.

Occurrence - Hambast Formation, Unit 6, Abadeh section, Central Iran. Wuchiapingian.

Distribution - Lower Wuchiapingian *Araxilevis* beds of Transcaucasia (Ruzhentsev & Sarytcheva, 1965); Wuchiapingian and lower Changhsingian of North Iran (Angiolini & Carabelli, 2010); Wuchiapingian of Ali Bashi Mountains, North-West Iran (Ghaderi et al., 2014).

Suborder STROPHALOSIIDINA Schuchert, 1913

Superfamily AULOSTEGOIDEA Muir-Wood & Cooper, 1960

Family SCACCHINELLIDAE Licharew, 1928

Subfamily TSCHERNYSCHEWIINAE Muir-Wood & Cooper, 1960

Genus *Tschernyschewia* Stoyanov, 1910

Type species *Tschernyschewia typica* Stoyanov, 1910

Remarks - The genus *Tschernyschewia* Stoyanov, 1910 can be recognised by the presence of a high ventral median septum inserted between the lobes of the cardinal process and the ornamentation of the ventral valve, made of very closely set spine bases.

Tschernyschewia typica Stoyanov, 1910

(Pl. 3, figs 1-2)

1878 *Productus scabriculus* ABICH (non Martin, 1809), p. 33, Pl. 5, fig. 3.

1900 *Productus abichi* ARTHABER, p. 252, Pl. 20, fig. 1.

1910 *Tchernyschewia typica* STOYANOV, p. 853.

1915 *Tschernyschewia typica* Stoyanov - STOYANOV, p. 77, Pl. 1, figs 1-5; Pl. 2, figs 1-12; Pl. 4, fig. 1.

1933 *Tschernyschewia typica* Stoyanov - SIMIĆ, p. 95, Pl. 1, figs 15-18.

1944 *Productus* (*Tschernyschewia*) *typica* Stoyanov - REED, p. 83, Pl. 12, fig. 13; Pl. 13, fig. 7; Pl. 18, fig. 6.

1958 *Tschernyschewia typica* Stoyanov - RAMOVS, p. 524, Pl. 9, figs 3-4.

1960 *Tschernyschewia typica* Stoyanov - MUIR-WOOD & COOPER, p. 127, Pl. 25, figs 1-9.

1963 *Tschernyschewia typica typica* Stoyanov - SCHRÉTER, p. 109, Pl. 3, figs 9-17; Pl. 4, figs 1-2.

1965 *Tschernyschewia typica typica* Stoyanov - AMIOT et al., p. 176, Pl. 21, figs 22-24.

1965 *Tschernyschewia typica* Stoyanov - SARYTCHEVA & SOKOLSKAYA in Ruzhentsev & Sarytcheva, Pl. 33, figs 8-9.
2010 *Tschernyschewia typica* Stoyanov - ANGIOLINI & CARABELLI, p. 63, Pl. 2, fig. 12; Pl. 3, fig. 1.
2014 *Tschernyschewia typica* Stoyanov - GARBELLI & ANGIOLINI in Ghaderi et al., p. 41, Pl. 1, figs 33-39.

Material - Two figured articulated shells: MPUM12208 (ABS7-1), MPUM12209 (ABS8-8); one articulated fragment: MPUM12210 (ABS0-30).

Description - Medium-sized, plano- to concave-convex shell with a transversally elliptical outline. Trail is geniculated. Maximum width: 20.7-33.5 mm; length: 13.4-25.7 mm. Ventral valve convex with steep flanks, with a broad but shallow median sulcus, more enhanced near the anterior commissure, where it forms a slight fold. Ventral umbo small and recurved on the cardinal margin, leaving a small and anacline interarea. Dorsal valve plano to slightly concave, dorsal umbo small and pointed. Ornamentation mainly made by spines. On the ventral valve the spines are very close and numerous, with small but elongated bases, ranging from 0.5 to 1 mm in length; on the dorsal valve spines are rare. Ventral valve interior with a very long and high median septum, inserted between the lobes of the cardinal process and touching the interior of the dorsal valve. Dorsal valve interior with a bilobed cardinal process, very prominent and with long lobes.

Remarks - The genus *Tschernyschewia* can be used as a marker for the Upper Permian in Europe and Asia, as observed by Cooper & Grant (1975, p. 914); the only species described in the literature from these areas of study is *T. typica*. Given the presence of highly diagnostic characters such as the internal of the valves and the spines distribution, the specimens here described belong to this taxon.

Occurrence - Hambast Formation, Unit 6, Abadeh section, Central Iran. Wuchiapingian.

Distribution - Wuchiapingian *Araxilevis* and *Oldhamina* beds of Transcaucasia (Ruzhentsev & Sarytcheva, 1965); Changhsingian Nesen Formation of the Alborz Mountains, North Iran (Angiolini & Carabelli, 2010); Lopingian of South-East Europe (Simić, 1933; Ramovs, 1958; Schréter, 1963); Lopingian of Salt Range, Pakistan (Reed, 1944); Changhsingian of Sichuan, China (Shen et al., 1992); Wuchiapingian of North-West Iran (Ghaderi et al., 2014).

Suborder LYTTONIIDINA Williams, Harper & Grant, 2000

Superfamily LYTTONIOIDEA Waagen, 1883

Family LYTTONIIDAE Waagen, 1883

Subfamily LYTTONIINAE Waagen, 1883

Genus *Leptodus* Kayser, 1883

Type species *Leptodus richtofeni* Kayser, 1883

Remarks - The genus *Leptodus* is a problematic taxon mainly because of the poor preservation of the type material of *L. richthofeni*. Also, the simultaneous institution in 1883 of *Lyttonia* Waagen (type *L. nobilis*) for a congeneric species and the subsequent publications of subjective synonyms, *Spinolyttonia* Sarytcheva, 1964, *Juxholdamina* Liang, 1990, and *Semigluberina* Liang, 1990, make the study of this taxon quite difficult (Williams et al., 2000). *Leptodus* differs from the allied genus *Oldhamina* Waagen, 1883 based on the angle of insertion of the lateral septa to the median ridge: in *Leptodus* the angle is roughly 90°, while in *Oldhamina* the lateral septa are inclined forward forming an acute angle. Another similar genus is *Collemataria* Cooper & Grant, 1974, from West Texas, USA which differs from *Leptodus* in lacking muscle scars or bounding plates in the apical region of the ventral valve; the attachment area is similar in the two genera, but in *Collemataria* the anterior margin of the cowl (anterodorsally growing shell producing conical shape of holoperipheral ventral valve) becomes the lip of the hinge. However, there is no clear distinction between the lateral septa of *Collemataria* and *Leptodus*.

Leptodus cf. *richthofeni* Kayser, 1883

(Pl. 3, figs 3-4)

Material - One figured ventral valve fragment: MPUM12211 (ABS20-7); one figured articulated fragment: MPUM12212 (ABS100-2); three ventral valve fragments: MPUM12213 (ABS6-9, ABS6-11, ABS20-6).

Description - The only characters that are visible are the septa, sharp and tilted forward [anguliseptate sensu Cooper & Grant (1974)]. Septa are arcuate and hooked at their end near the median ridge. Average distance between septa is 2 mm.

Remarks - The preservation of the specimens hampers the classification at the species level; however, the orientation of the septa is a diagnostic character that enables the specimens to be

excluded from the species *Leptodus nobilis* (Waagen, 1883) and *L. tenuis* (Waagen, 1883), in which straight septa intersect the median ridge at roughly 90° and between 75-90°, respectively. The septa of the described specimens are arcuate and get close to the median ridge with an angle of around 45°, in the range of *L. richthofeni*. The presence of hooked ends on the septa is also very similar to *L. richthofeni*.

Occurrence - Hambast Formation, Unit 6, Abadeh section, Central Iran. Wuchiapingian.

Leptodus nobilis (Waagen, 1883)
(Pl. 3, figs 5-7)

1883 *Lyttonia nobilis* WAAGEN, p. 398, Pl. 29, figs 1-3; Pl. 30 figs 1-2, 5-6, 8, 10-11.
1897 *Lyttonia nobilis* Waagen - DIENER p. 37, Pl. 1, figs 5-7.
1905 *Lyttonia nobilis* Waagen - NOETLING, p. 140, Pl. 17, figs 1-2; Pl. 18, figs 1-11; text-fig. 2.
1913 *Lyttonia nobilis* Waagen - MANSUY, p. 123, Pl. 13, fig. 10.
1924 *Lyttonia nobilis* Waagen - ALBRECHT, p. 289, fig. 1a-b.
1931 *Lyttonia nobilis* Waagen - GRABAU, p.285, Pl. 28, figs 4-5.
1932 *Lyttonia nobilis* Waagen - HUANG, p. 89, Pl. 7, figs 9-10; Pl. 8, figs 8-9; Pl. 9, figs 1-8.
1933 *Lyttonia nobilis* Waagen - HUANG, p. 93, Pl. 11, fig. 22.
1933 *Lyttonia nobilis* Waagen - SIMIĆ, p. 49, Pl. 4, fig. 1.
1958 *Leptodus nobilis* (Waagen) - RAMOVS, p. 497, Pl. 2, fig. 3.
1960 *Leptodus nobilis* (Waagen) - TERMIER & TERMIER, p. 241, Pl. 3, figs 1-10.
1961 *Leptodus nobilis* (Waagen) - CHI-THUAN, p. 274, Pl. 1, fig. 1.
1962 *Leptodus nobilis* (Waagen) - CHI-THUAN, p. 488, Pl. 1, fig. 1.
1963 *Leptodus nobilis* (Waagen) - SCHRÉTER, Pl. 3, figs 5-8.
1964 *Leptodus nobilis* (Waagen) - GLAUS, p. 504, Pl. 1; Pl. 2, fig. 1.
1965 *Leptodus nobilis* (Waagen) - SARYTCHEVA & SOKOLSKAYA in Ruzhentsev & Sarytcheva, Pl. 39, figs 6-8.
1974 *Leptodus nobilis* (Waagen) - COOPER & GRANT, Pl. 191, figs 8-9.
1976 *Leptodus nobilis* (Waagen) - GRANT, Pl. 43, figs 18-19.
1978 *Leptodus nobilis* (Waagen) - FENG & JIANG, p. 269, Pl. 100, fig. 2.
1979 *Leptodus nobilis* (Waagen) - JIN & YE in Jin et al., p. 82, Pl. 23, fig. 15.
1984 *Leptodus nobilis* (Waagen) - YANG, p. 226, Pl. 35, fig. 12.
1986 *Leptodus nobilis* (Waagen) - SREMAC, p. 30, Pl. 10, figs 1-2.

1987 *Leptodus nobilis* (Waagen) - TAZAWA, fig. 30.5; fig. 31.2.
1990 *Leptodus nobilis* (Waagen) - LIANG, p. 225, Pl. 40, figs 1, 5.
1990 *Semigluberina* sp. 1 LIANG, p. 233, Pl. 42, figs 1-2.
1990 *Semigluberina flabelata* LIANG, p. 231, Pl. 41, figs 4-8.
1990 *Semigluberina gabata* LIANG, p. 232, Pl. 41, fig. 9.
1990 *Semigluberina ovata* LIANG, p. 233, Pl. 41, fig. 10.
1994 *Leptodus nobilis* (Waagen) - LEMAN, Pl. 1, figs 3-4.
1995 *Leptodus nobilis* (Waagen) - ZENG et al., Pl. 11, fig. 3.
1998 *Leptodus nobilis* (Waagen) - TAZAWA et al., p. 241, figs 2.1-2.2, 4.
2001 *Leptodus nobilis* (Waagen) - TAZAWA, p. 297, figs 7.13-7.14.
2002 *Leptodus nobilis* (Waagen) - SHEN et al., p. 679, fig. 5.28.
2003 *Leptodus nobilis* (Waagen) - TAZAWA, p. 31, figs 4.1-4.2.
2005 *Leptodus nobilis* (Waagen) - CAMPI et al., p. 125, Pl. 4A-B.
2010 *Leptodus nobilis* (Waagen) - ANGIOLINI & CARABELLI, p. 63, Pl. 2, figs 13-15; Pl. 3, fig. 23.
2016 *Leptodus nobilis* (Waagen) - TAZAwa, p. 29, fig. 10.
2018 *Leptodus nobilis* (Waagen) - TAZAWA et al., p. 915, fig. 2.

Material - Two figured ventral valve fragments: MPUM12214 (ABS6-6), MPUM12215 (ABS20-8); one figured dorsal valve: MPUM12216 (ABS15-1); three fragments: MPUM12217 (ABS5-1, ABS6-8, ABS6-10).

Description - Ventral valve with conical shape, width up to 28.7 mm and length up to 73.6 mm. Septa are solidiseptate, straight and slightly tilted towards the umbo at their end; they intersect the median ridge at roughly 90°. The average distance between septa is 1.5 mm. Ornamentation of the ventral valve of fine growth lines.

Remarks - Waagen (1883, p. 398, pl. 29, figs 1-3; pl. 30, figs 1-2, 5-6, 8, 10-11) described *L. nobilis* as a highly variable shell, its shape and outline depending on the surface where it was attached and it has grown. He described specimens with length up to 145 mm and normally longer than wide. Despite the assertion by Williams et al. (2000) of species of the genus *Leptodus* being normally transversely oval, they figured the specimens of *L. nobilis* described by Grant (1976, specimens from the Kalabagh Member, Khisor Range, Pakistan), which show variability in outline reinforcing Waagen's statement.

Occurrence - Hambast Formation, Unit 6, Abadeh section, Central Iran. Wuchiapingian.

Distribution - *Leptodus nobilis* (Waagen, 1883) occurs in the Wuchiapingian *Araxilevis*, *Oldhamina* and *Haydenella* beds of Transcaucasia (Ruzhentsev & Sarytcheva, 1965); Guadalupian-Lopingian of South China, Salt Range, Malaysia, Cambodia, Transcaucasia, Japan, Mongolia, Baoshan Block, Kashmir, Timor and South-East Europe (Tazawa, 2003; Campi et al., 2005); Wuchiapingian and lower Changhsingian of North Iran (Angiolini & Carabelli, 2010).

Leptodus sp.

Material - Three ventral valve fragments: MPUM12217 (ABS6-4, ABS6-7, ABS6-12).

Remarks - These specimens are poorly preserved with only a couple of septa visible on each specimen. Septa are visible in the interior of the valves, they are anguliseptate and straight or slightly arcuate. Given the poor preservation, the nomenclature is left open.

Occurrence - Hambast Formation, Unit 6, Abadeh section, Central Iran. Wuchiapingian.

Superfamily PERMIANELLOIDEA He & Zhu, 1979
Family PERMIANELLIDAE He & Zhu, 1979

Genus *Permianella* He & Zhu, 1979
Type species *Permianella typica* He & Zhu, 1979

Remarks - *Permianella* He & Zhu, 1979, *Sicyusella* Liang, 1990 and *Tenerella* Liang, 1990 are very similar permianellid genera. The most important feature to distinguish *Sicyusella* from the other permianellid genera is the curved longitudinal profile, a character displayed on the specimen described here. Other features of the genus, such as the boat shaped outline with the maximum width placed at shell mid-length, are not recorded in the specimen under study. However, Shen et al. (2017) consider *Sicyusella* as a junior synonym of *Permianella*, because of the great morphological plasticity of the genus with its shape depending on the growth environment. Williams et al. (2000) treated *Sicyusella* as a synonym of *Tenerella*, which is in turn considered a synonym of *Permianella* or *Dicystoconcha* Termier et al., 1974 by Shen et al. (2017). The genus

Tenerella is not well defined, as the most important distinguishing characters indicated by Liang (1990) are the general features for the family Permianellidae, like the strongly recurved shell and the deep incision of the anterior margin. Its internal structures recall those of *Dicystoconcha* (Shen et al., 2017). The stratigraphic range of *Sicyusella* and *Tenerella* is restricted to the Capitanian, whereas *Permianella* is the only genus of the family Permianellidae occurring also in the Lopingian.

Permianella cf. *grunti*

(Pl. 3, fig. 8)

Material - One figured articulated shell: MPUM12219 (ABS25-10).

Description - Concave-convex shell, with curved longitudinal profile. Width: 11.5 mm; length: 27.8 mm. The ventral valve is divided by a long, deep and narrow sulcus, covered with fine growth lines characterized by a strong convexity pointing backwards. Anteriorly the shell is divided into two lobes. There are two small bulges on the lateral margin of the shell, one each side. Ventral valve and dorsal valve interior are not visible.

Remarks - All the published figures of specimens of *Permianella* species record great variability of shape, depending on the growth condition of the specimens, and there is a whole spectrum of positions of the point of separation, degree of separation and length of the two anterior lobes. Also, their direction of growth compared to the orientation of the proximal part of the shell is very variable. For instance, the specimen UKM/JG/F301 described as *Permianella typica* by Campi et al. (2000, fig. 5, p. 41) shows that the portion of the shell between the attachment ring and the anterior incision is, at least, 2 cm long, roughly the length of the specimen under study. Another diagnostic feature of the genus *Permianella* is the lateral marginal brim, being incomplete in most of the described specimens. This feature may be represented by the two lateral bulges on the specimen here described, which are similar to features described in the diagnosis of *Permianella grunti* Shen & Shi, 1997 from the Wuchiapingian of Dorasham. The specimen MPUM12219 is also very similar to the holotype figured by Shen & Shi (1997, pl.1, figs 1-2). The absence of a well-developed marginal brim, however, could be a taphonomic artifact, therefore, given the problems in the taxonomy of the family Permianellidae (Shen et al., 2017), the morphological variability and stratigraphic range of these genera, the nomenclature is here left open.

Occurrence - Hambast Formation, Unit 6, Abadeh section, Central Iran. Wuchiapingian.

Order ORTHOTETIDA Waagen, 1884

Suborder ORTHOTETIDINA Waagen, 1884

Superfamily ORTHOTETOIDEA Waagen, 1884

Family MEEKELLIDAE Stehli, 1954

Subfamily MEEKELLINAE Stehli, 1954

Genus *Orthothetina* Schellwien, 1900

Type species *Orthotetes persicus* Schellwien, 1900

Remarks - The genus *Orthothetina* Schellwien, 1900 differs from the other genera in the subfamily by having strong sub-parallel dental plates, always separated and slightly converging to the valve floor only near the umbo.

Orthothetina persica (Schellwien, 1900)

(Pl. 3, fig. 9)

1900 *Orthotetes (Orthothetina) persicus* SCHELLWIEN, p. 8, Pl. 1, fig. 2.

1911 *Orthotetes (Orthothetina) persicus* Schellwien - FRECH, p. 123, Pl. 26, fig. 3.

1965 *Orthothetina persica* (Schellwien) - SOKOLSKAYA in Ruzhentsev & Sarytcheva, p. 206, Pl. 30, figs 4-5.

2010 *Orthothetina persica* (Schellwien) - ANGIOLINI & CARABELLI, p. 65, Pl. 4, figs 4-5.

2014 *Orthothetina persica* (Schellwien) - GARBELLI & ANGIOLINI in Ghaderi et al., p. 42, Pl. 2, figs 1-4.

Material - One figured articulated shell: MPUM12220 (ABS20-2).

Description - Biconvex shell, with stronger convexity in the dorsal valve, outline transversely elliptical and cardinal margin straight and shorter than maximum width. Maximum width: 64.6 mm, located in the anterior half of the shell; length >43.3 mm. Anterior commissure uniplicate. Ventral umbo small, convex and with rounded slopes. Ventral interarea apsacline, sub-triangular, short and wide, with slightly concave margins. Dorsal valve strongly convex with a sub-rectangular outline. Ornamentation of two orders of fine regularly arranged costellae. First order costellae are coarser, 0.3 mm wide at mid-length and at anterior margin. Two to four second order costellae occur

between two first order ones. Near the anterior margin costellae number 10-11 per 5 mm. Ventral valve interior with nearly parallel thin dental plates.

Remarks - The specimen here described is similar to *Orthothetina persica* (Schellwien, 1900), particularly the specimens described and figured by Ghaderi et al. (2014, pl. 2, figs 1-4) for the number and arrangement of costellae. The allied species *Orthothetina eusarkos* (Abich, 1878) is characterized by thick concentric growth lines at the anterior margin, a feature missing in the specimen under study; costellae in *O. eusarkos* are also less numerous (9-10 in 5 mm).

Occurrence - Hambast Formation, Unit 6, Abadeh section, Central Iran. Wuchiapingian.

Distribution - Wuchiapingian *Oldhamina* beds of Transcaucasia (Ruzhentsev & Sarytcheva, 1965); Wuchiapingian-Changhsingian of the Alborz Mountains, North Iran (Angiolini & Carabelli, 2010); Wuchiapingian of North-West Iran (Ghaderi et al., 2014).

Orthothetina sp.

Material - One articulated shell: MPUM12221 (ABS21-6).

Description - Biconvex shell, with transversely suboval outline, cardinal margin short and straight. Anterior commissure unisulcate. Ventral valve less convex than the dorsal valve, with sub-trapezoidal outline. Cardinal extremities pointed. Ventral interarea short and wide, between aspacline and orthocline. Dorsal valve with a transversely sub-oval outline. Dorsal umbo small, dorsal interarea small and triangular. Ornamentation of costellae, uniform in width and increasing in number anteriorly, up to 11-12 per 5 mm. Ventral valve interior with parallel dental plates, 1.3 mm set apart.

Remarks - The preservation of the specimen under study does not allow an identification at the species level.

Occurrence - Hambast Formation, Unit 6, Abadeh section, Central Iran. Wuchiapingian.

Genus *Perigeyerella* Wang, 1955

Type species *Perigeyerella costellata* Wang, 1955

Remarks - The main feature of the genus *Perigeyerella* Wang, 1955 is the interior of the ventral valve, in particular the dental plates: they are thin and near the umbo they form a spondylium supported by a median septum, which decreases in height going towards the anterior. The dental plates then reach the floor of the ventral valve, and progressively diverge from each other. The growth of the dental plates goes through three stages, similar to other genera in the family: elevated spondylium near the umbo similar to *Sicelia* Gortani & Merla, 1934, *Geyerella* Schellwien, 1900 and *Ombonia* Caneva, 1906, then the spondylium becomes sessile and anteriorly the dental plates are separated as in *Meekella* and *Orthothetina*.

Perigeyerella aff. *costellata* Wang, 1955

(Pl. 3, fig. 10; Pl. 4, fig. 1)

Material - Two figured articulated shells: MPUM12222 (ABS20-1), MPUM12223 (ABS21-10); one articulated shell: MPUM12224 (ABS0-29).

Description - Medium-sized, biconvex shell with a more convex dorsal valve, a pear-shaped outline, and a broadly unisulcate anterior commissure. Cardinal margin straight, equal or shorter than half the maximum shell width, which is located near mid-length; obtuse angular extremities. Maximum width: 45.8-57.2 mm; length: 41-44.6 mm. Ventral valve convex, with a sub-triangular outline. Ventral interarea high and triangular, apsacline and slightly concave. Pseudodeltidium flat and triangular, with a convex monticulus in the middle. Dorsal valve more convex than the ventral valve, with a sub-circular outline. Dorsal umbo short, recurved on the cardinal margin. Occasionally a very shallow dorsal sulcus is present. Ornamentation of both valves of fine costellae increasing anteriorly by intercalation or bifurcation; they can be divided into two orders, with second order costellae finer than the first order costellae, but lacking a regular arrangement. Costellae number 12-14 per 5 mm near the anterior margin of both valves and are cancellated by strongly concentric fila. On the ventral valve there are also strong growth lamellae irregularly arranged. Ventral valve interior with dental plates apically forming an elevated spondylium with the median septum, then joining at the ventral valve floor and finally becoming separated and almost parallel.

Remarks - The medium size, the pear-shaped outline and the number of costellae are diagnostic features of *Perigeyerella costellata* Wang, 1955 from the Changhsing Formation of northern Guizhou, China. The outline itself is enough to distinguish this species from the species *P.*

guangxiensis Chen & Liao, 2007 and *P. tricosa* Grant, 1976. *P. costellata* differs from *P. altilosina* Xu & Grant, 1994 because of the apsacline ventral interarea. Another character distinguishing *P. costellata* from the other three species is the presence of a shallow sulcus on the dorsal valve. This character is, however, variable in the specimens described in the literature; in particular Shen & Shi (2007) described for the species a shallow sulcus originating from the umbo and widening anteriorly, whereas Angiolini & Carabelli (2010) described only a shallow sulcus. In fact, in the specimens figured by Shen & Shi (2007, pl.8, figs 1-16) the sulcus is deeper, well defined and much more visible than in the specimen MPUM9991 figured by Angiolini & Carabelli (2010, pl. 4, figs 10-11). Based on the depth of the dorsal sulcus, present on a single specimen, the specimens under study are described as *Perigeyerella* aff. *costellata*.

Occurrence - Hambast Formation, Unit 6, Abadeh section, Central Iran. Wuchiapingian.

Perigeyerella aff. *tricosa* Grant, 1976

(Pl. 4, fig. 2)

Material - One figured articulated shell: MPUM12225 (ABS7-2).

Description - Small-sized, biconvex shell, with a transversely elliptical outline. Maximum width: 33.7 mm, placed at shell mid-length; length: 28.1 mm. Anterior commissure slightly unisulcate, cardinal margin straight and short and cardinal extremities slightly auriculate. Ventral valve slightly convex, with a sub-oval outline. Ventral umbo pointed, interarea apsacline, short, wide and sub-triangular, with slightly concave margins. Dorsal valve convex, with maximum convexity posterior to shell mid-length and sub-rectangular outline. Dorsal umbo short and low, with slopes almost flat, forming a small, narrow and triangular interarea. Ornamentation of both valves costellate, increasing by intercalation towards the anterior margin. Some of them are slightly higher, and they are irregularly arranged. Costellae number 9 per 2 mm near the anterior margin. Costellae are cancellated by strong concentric fila. On the ventral valve there are strong, irregularly spaced growth lamellae. Ventral valve interior with thick dental plates converging at the floor of the valve.
Remarks - The outline and the convexity of the dorsal valve are similar to *Perigeyerella tricosa* Grant, 1976, from the Artinskian of Southern Thailand. Other characters shared with *P. tricosa* are the maximum width at shell mid-length, the strongly apsacline ventral interarea, the irregular costellae, as well as their arrangement and density on the valves, and the slightly unisulcate anterior commissure. However, the specimen under study is larger than the specimens described in the

literature (Grant, 1976; Shen & Shi, 2007), the dorsal umbo is less convex and there is no trace of a sulcus on the dorsal valve. Therefore, the specimen under study is identified as *P*. aff. *tricosa*.
Occurrence - Hambast Formation, Unit 6, Abadeh section, Central Iran. Wuchiapingian.

Perigeyerella spp.

Material - One articulated shell: MPUM12226 (ABS21-7); one ventral valve: MPUM12227 (ABS21-2).

Description - Biconvex shell, outline somewhat sub-triangular, more elongated longitudinally. Cardinal margin straight, anterior commissure unisulcate. Ventral interarea orthocline or apsacline. Strong median sulcus on the dorsal valve, starting at shell mid-length. Ornamentation made by two orders of costellae, increasing mainly by branching and without a clear arrangement. Costellae number 12-14 per 5 mm.

Remarks - The preservation of the specimens under study prevent any attempt of identification. However, they are clearly two different species on the basis of the valve shape, the interarea orientation and the ornamentation.

Occurrence - Hambast Formation, Unit 6, Abadeh section, Central Iran. Wuchiapingian.

Order ATHYRIDIDA Boucot, Johnson & Staton, 1964
Suborder ATHYRIDIDINA Boucot, Johnson & Staton, 1964
Superfamily ATHYRIDOIDEA Davidson, 1881
Family ATHYRIDIDAE Davidson, 1881
Subfamily ARAXATHYRIINAE Shen, Grunt & Jin, 2004

Genus *Araxathyris* Grunt in Ruzhentsev & Sarytcheva, 1965
Type species *Spirigera protea* Abich, 1878

Remarks - The subfamily Araxathyriinae Shen et al., 2004 includes the genera *Araxathyris* Grunt in Ruzhentsev & Sarytcheva, 1965, *Rectambitus* Xu & Grant, 1994, and *Tongzithyris* Jin et al., 1974, all characterized by the occurrence of a spondylium in the ventral valve. *Araxathyris* differs from

Rectambitus because of its parasulcate anterior commissure and the lack of a median ridge supporting anteriorly the spondylium; from *Tongzithyris* because of the smaller size and the absence of folds on the lateral slopes. *Araxathyris* is very similar to the genus *Transcaucasathyris* Shen et al., 2004, from which it differs mainly because of the internal characters, which consist of a spondylium in the genus *Araxathyris* vs separated dental plates in the genus *Transcaucasathyris*. Externally the two genera are almost identical, with species of *Transcaucasathyris* being generally smaller. Angiolini & Carabelli (2010) discussed the phylogenetic relation between the two genera, proposing that *Transcaucasathyris* might have evolved from *Araxathyris* through paedomorphism, with the lack of junction of the dental plates to form the spondylium. In particular, they suggested that *T. kandevani* (Fantini Sestini & Glaus, 1966) could have evolved from *A. bruntoni* Angiolini & Carabelli, 2010, based on the stratigraphic range of the two species; they found that the first occurrence of *Araxathyris* in the Nesen Formation (North Iran) is in bed IR 164, while the first occurrence of *Transcaucasathyris* is in bed IR 166, 7.1 m above. Garbelli et al. (2014) addressed this hypothesis showing that the stratigraphic ranges of the species of the two genera in Transacaucasia (Ruzhentsev & Sarytcheva, 1965) and in the Ali Bashi Mountains in Iran (Ghaderi et al., 2014) do not support this evolutionary pattern, as in the Julfa section, the first occurrence of *Transcaucasathyris* is in bed G134, while the first occurrence of *Araxathyris* is 3 m above, in bed G 140. They proposed instead that the genus *Araxathyris* was derived from *Transcaucasathyris*, based on the fact that the subfamily Araxathyriinae is one of the youngest subfamilies among the Comelicaniidae Merla, 1930 *sensu* Shen et al. (2004). As the other subfamilies, which developed earlier, are characterized by the presence of separated dental plates, they interpreted the spondylium as a derived character. However, the subfamilies Araxathyriinae, Comelicaniinae and Transcaucasathyriinae have the same stratigraphic range, i.e. Wuchiapingian-Changhsingian, as shown by the specimens here described. Moreover, Garbelli et al. (2014) highlighted that the acquisition of a spondylium through evolution is shown in the fossil record of Meristidae and Clitambonitidina (Garbelli et al., 2014 and reference therein). However, the Ordovician genera of the Meristidae have dental plates with a high shoe-lifter process which is also present in Silurian and Devonian genera; Silurian and Devonian genera can have a spondylium and Devonian genera (Septathyridinae) have separate dental plates (Alvarez & Rong in Williams et al., 2002). Vinn & Rubel (2000) showed that in the Clitambonitoidea, the Clitambonitidae possess a spondylium which is not derived from dental plates, but the Polytoechioidea have dental plates forming a pseudospondylium. In conclusion, there is no robust evidence that the spondylium is a derived character. The stratigraphic distribution of the two genera in Abadeh supports the hypothesis of Angiolini & Carabelli (2010), with the first occurrence of species of the genus *Araxathyris* being

located in the bed ABS0, whereas the first occurrence of species of the genus *Transcaucasathyris* are located in bed ABS7, stratigraphically above. In the Abadeh section, however, there are many specimens assigned to the family Athyrididae Davidson, 1881, which are badly preserved and impossible to identify at the genus level. Therefore, at the moment, there is no conclusive evidence of the phylogenetic relationship between the two taxa.

Araxathyris abichi (Arthaber, 1900)

(Pl. 4, fig. 3; t

Fig. 10)

1878 *Spirigera royssii* ABICH, p.62, Pl. 7, fig. 8.
1878 *Spirigera protea* var. *ambigua* ABICH, p. 62, Pl. 6, fig. 9.
1878 *Spirigera protea* var. *subtilita* ABICH, pag. 63, Pl. 6, figs 11-12.
1878 *Spirigera plano sulcata* ABICH, p. 63, Pl. 8, fig. 4.
1878 *Spirigera plano sulcata* var. *rugosa* ABICH, p. 64, Pl. 8, fig. 3.
1900 *Spirigera abichi* ARTHABER, p. 280, Pl. 22, figs 10-12.
1965 *Araxathyris abichi* (Arthaber) - GRUNT in Ruzhentsev & Sarytcheva, p. 244, Pl. 43, figs 2-3.
1986 *Araxathyris abichi* (Arthaber) - GRUNT, p. 113, Pl. 15, fig. 7; Pl. 27, fig. 1.
2014 *Araxathyris abichi* (Arthaber) - GARBELLI & ANGIOLINI in Ghaderi et al., p. 50, Pl. 3, figs 56-62.

Material - Two figured articulated shells: MPUM12229 (ABS8-53), MPUM12230 (ABS17-68); one articulated shell: MPUM12231 (ABS0-9).

Description - Small-sized, sub-equally biconvex shell with a longitudinally sub-oval outline. Cardinal margin short, anterior commissure slightly parasulcate. Maximum width: 8.4-9.3 mm; length: 8.2-9.2 mm. Ventral valve convex, sub-pentagonal in outline. Umbo short and recurved on the cardinal margin, without extending over it or touching the dorsal one, bearing a small circular foramen. Median sulcus very shallow, starting narrow at the umbo and widening anteriorly, forming a low and shallow tongue. Palintrope orthocline, very small and triangular. Dorsal valve sub-oval, inflated and with a gentle rounded median fold, better expressed near the anterior commissure. Dorsal umbo very low on the cardinal margin. Ornamentation made by several growth lamellae near the anterior margin, particularly visible on the sulcal tongue. Ventral valve interior with a sessile spondylium with a low median septum.

Remarks - *Araxathyris abichi* (Arthaber, 1900) is easily distinguishable from the congeneric species because of its smaller size and the uniplicate to slightly parasulcate anterior commissure.

Occurrence - Hambast Formation, Unit 6, Abadeh section, Central Iran. Wuchiapingian.

Distribution - Wuchiapingian *Oldhamina* beds of Transcaucasia (Ruzhentsev & Sarytcheva, 1965); Wuchiapingian of the Ali-Bashi Mountains, North-West Iran (Ghaderi et al., 2014).

Araxathyris bruntoni Angiolini & Carabelli, 2010
(Pl. 4, figs 4-5)

1966 *Araxathyris araxensis* Grunt in Ruzhentsev & Sarytcheva - FANTINI SESTINI & GLAUS, p. 911, Pl. 65, fig. 6a-b.
2010 *Araxathyris bruntoni* Grunt - ANGIOLINI & CARABELLI, p. 79, Pl. 3, figs 13-16; Pl. 5, figs 4-7; text-fig. 12.

Material - Two figured articulated shells: MPUM12232 (ABS17-9), MPUM12233 (ABS25-40); seven articulated shells: MPUM12234 (ABS8-72), MPUM12235 (ABS17-17, ABS17-48, ABS17-54, ABS17-78), MPUM12236 (ABS22-15), MPUM12237 (ABS 25-46).

Description - Small sized, unequally biconvex shell, with a sub-oval to sub-pentagonal outline. Cardinal margin very short, anterior commissure strongly parasulcate, with a high and squared sulcal tongue. Maximum width: 7.9-11.8 mm; length: 7.5-11.1 mm. Ventral valve sub-pentagonal and more convex at the umbo. Umbo short and strongly recurved on the cardinal margin, touching the dorsal one. Median sulcus starting at the umbo as a weak and narrow groove, and becoming deeper and wider at mid-length, forming a high and squared sulcal tongue. The sub-rectangular outline of the tongue is variable, from clearly defined by right angles to a more rounded shape. The flanks of the valve are steep, forming two diverging rounded folds at the sides of the sulcus. Dorsal valve inflated, with a sub-rectangular to sub-oval outline. Median fold visible only at the anterior margin, due to the strong convexity of the valve, and variably squared following the outline of the sulcal tongue. On the median fold there is a faint groove, starting from mid-length. Ornamentation of weak growth lines and growth lamellae, more evident anteriorly. Ventral valve interior with dental plates converging at the valve floor forming a spondylium.

Remarks - The specimens under study have been compared to the type material of *Araxathyris bruntoni* Angiolini & Carabelli, 2010. The analysis of the type material confirmed that *A. bruntoni* is characterized by a strongly parasulcate anterior commissure and a markedly squared sulcal tongue. Externally, *A. bruntoni* is similar to *Transcaucasathyris kandevani* (Fantini Sestini & Glaus, 1966) and *T. lata* (Grunt in Ruzhentsev & Sarytcheva, 1965), but from the latter it differs because of its sub-pentagonal outline and the less evident dorsal groove. The small size and the outline of the sulcal tongue distinguish *A. bruntoni* from all other congeneric species.
Occurrence - Hambast Formation, Unit 6, Abadeh section, Central Iran. Wuchiapingian.
Distribution - Wuchiapingian-Changhsingian of the Alborz Mountains, North Iran (Angiolini & Carabelli, 2010).

Araxathyris felina (Arthaber, 1900)
(Pl. 4, fig. 6)

1878 *Spirigera protea* var. *globularis* ABICH, p. 58, Pl. 7, fig. 7; Pl. 8, fig. 12.
1878 *Spirigera protea* var. *subtilita* ABICH, p. 59, Pl. 8, figs 10-11.
1900 *Spirigera protea* var. *alata* Abich - ARTHABER, p. 275, Pl. 22, fig. 2.
1900 *Spirigera protea* var. *armeniaca* Abich - ARTHABER, p. 277, Pl. 22, figs 6-7.
1900 *Spirigera felina* Abich - ARTHABER, p. 279, Pl. 22, figs 8-9.
1965 *Araxathyris felina* (Arthaber) - GRUNT in Ruzhentsev & Sarytcheva, p. 244, Pl. 43, fig. 4; text-fig. 42.
1966 *Araxathyris felina* (Arthaber) - FANTINI SESTINI & GLAUS, p. 911, Pl. 65, fig. 3.
1986 *Araxathyris felina* (Arthaber) - GRUNT, p. 112, fig. 57.
2010 *Araxathyris felina* (Arthaber) - ANGIOLINI & CARABELLI, p. 80, Pl. 5, figs 8-11.
2014 *Araxathyris felina* (Arthaber) - GARBELLI & ANGIOLINI in Ghaderi et al., p. 51, Pl. 3, figs 63-65.

Material - One figured articulated shell: MPUM12238 (ABS8-3); one articulated shell: MPUM12239 (ABS20-4).

Description - Medium sized, biconvex shell, with a sub-oval to sub-pentagonal outline. Anterior commissure parasulcate with a high sulcal tongue, cardinal margin curved and shorter than the maximum width. Maximum width: 15.7 mm; length: 15.4-16.8 mm. Ventral valve more convex at

the umbo, longitudinally elongated and suboval. Ventral umbo recurved on the cardinal margin being in contact with the dorsal one. Median sulcus starting at the umbo, where it is narrow and shallow, becoming wider and deeper at mid-length. Sulcus flanked by two rounded folds. Anterior commissure forming a high sulcal tongue. Dorsal valve with sub-pentagonal outline. Dorsal umbo short and recurved. Median fold more evident at the anterior margin where it is flanked by two depressions corresponding to the sides of the sulcal tongue. Ornamentation of weak growth lamellae anteriorly. Ventral valve interior with dental plates converging and joining to form a spondylium supported by a low median septum.

Remarks - *Araxathyris felina* (Arthaber, 1900) differs from the congeneric species mainly because of its more elongated outline. Other characters are the absence of a dorsal sulcus, which distinguishes it from *A. protea* (Abich, 1878) and the two rounded folds at the sides of the ventral median sulcus, which are absent in *A. quadrilobata* (Abich, 1878); the latter is also different because of the presence of a thin median furrow on the dorsal fold.

Occurrence - Hambast Formation, Unit 6, Abadeh section, Central Iran. Wuchiapingian.

Distribution - Wuchiapingian *Oldhamina* beds of Transcaucasia (Ruzhentsev & Sarytcheva, 1965); Wuchiapingian-Changhsingian of the Alborz Mountains, North Iran (Angiolini & Carabelli, 2010); Wuchiapingian of the Ali-Bashi Mountains, North-West Iran (Ghaderi et al., 2014).

Araxathyris quadrilobata (Abich, 1878)
(Pl. 4, figs 7-8)

1878 *Spirigera protea* var. *quadrilobata* ABICH, p. 53, Pl. 7, fig. 6; Pl. 9, figs 8-9.
1939 *Athyris* (*Composita*) *protea* var. *quadrilobata* (Abich) - LICHAREW, p.117, Pl. 24, fig. 3.
1965 *Araxathyris quadrilobata* (Abich) - GRUNT in Ruzhentsev & Sarytcheva, p. 101, Pl. 43, figs 1a-c, 2a-c.
1969 *Araxathyris quadrilobata* (Abich) - STEPANOV, Pl. 4, fig. 4a-d.
1986 *Araxathyris quadrilobata* (Abich) - GRUNT, Pl. 15, figs 8, 10.
2014 *Araxathyris quadrilobata* (Abich) - GARBELLI & ANGIOLINI in Ghaderi et al., p. 51, Pl. 4, figs 1-4.

Material - One figured articulated shell: MPUM12240 (ABS 8-1); one figured ventral valve: MPUM12241 (ABS21-4); three articulated shells: MPUM12242 (ABS8-2, ABS8-4, ABS8-42).

Description - Medium sized, equally biconvex and inflated shell, with a markedly sub-pentagonal outline. Cardinal margin short and slightly curved, anterior commissure parasulcate, with a wider than higher sulcal tongue. Maximum width: 14.5-19.5 mm; length: 13.4-17.9 mm. Ventral valve sub-pentagonal and strongly convex. Umbo short and recurved on the cardinal margin. Median sulcus starting at the umbo as a narrow groove that deepens after one third of the length. The combination of the deep median sulcus and the strong convexity of the valve forms two ridges with a various degree of sharpness. Dorsal valve sub-oval in outline, inflated and with a high and rounded median fold. On the fold there is a very variable narrow median sulcus. Dorsal umbo small and recurved on the cardinal margin, with steep flanks. Ventral valve interior with a spondylium, formed by two slightly concave dental plates which joins at the valve floor. Dorsal valve interior with spiralia consisting of ten whorls forming a cone pointing laterally.

Remarks - *Araxathyris quadrilobata* is similar to *A. protea* and *A. felina*, but it differs from the former because of its more transverse outline and higher sulcal tongue, and from the second one because of its more transverse outline and the presence of a shallow dorsal sulcus. Another difference between *A. quadrilobata* and *A. felina* is the markedly sub-pentagonal outline in *A. quadrilobata*, while in *A. felina* it is more sub-elliptical.

Occurrence - Hambast Formation, Unit 6, Abadeh section, Central Iran. Wuchiapingian.

Distribution - Wuchiapingian *Oldhamina* beds of Transcaucasia (Ruzhentsev & Sarytcheva, 1965); Wuchiapingian Julfa beds of North Iran (Stepanov et al., 1969); Wuchiapingian of the Ali-Bashi Mountains, North-West Iran (Ghaderi et al., 2014).

Araxathyris spp.

(Fig. 11)

Material - One figured articulated shell: MPUM12245 (ABS25-59); seventeen articulated shells: MPUM12243 (ABS0-31), MPUM12244 (ABS2-4), MPUM12246 (ABS0-5, ABS0-7, ABS0-22, ABS0-39, ABS0-51, ABS1-4, ABS1-7, ABS1-20, ABS1-25, ABS3-16), MPUM12247 (ABS7-19, ABS8-25, ABS8-32, ABS8-52, ABS17-27).

Remarks - The specimens are generally badly preserved. The outline of the specimens is variable, from transversally elliptical to sub-pentagonal or longitudinally sub-oval. The size of the specimens is small for the genus, and the biconvexity of the shell is variable. The spondylium is present in most of the specimens suggesting they belong to species of *Araxathyris.*

Occurrence - Hambast Formation, Unit 6, Abadeh section, Central Iran. Wuchiapingian.

Genus *Rectambitus* Xu & Grant, 1994

Type species *Araxathyris bisulcata* Liao, 1980

Remarks - The genus *Rectambitus* Xu & Grant, 1994 is easily distinguishable from the other genera in the subfamily because of the rectimarginate anterior commissure, the emarginate anterior margin, the smooth surface, the presence of a narrow sulcus on both valves and the spondylium supported anteriorly by a low and broad septum. Although the genus *Rectambitus* was recently placed in the subfamily Spirigerellinae Grunt, 1965 by Shen et al. (2017), here it is considered as a genus belonging to the subfamily Araxathyriinae Shen et al., 2004, because of the presence of a spondylium in the anterior part of the dental plates structure.

?*Rectambitus* sp.

(Pl. 4, figs 9-12)

Material - Five figured articulated shells: MPUM12248 (ABS16-2), MPUM12249 (ABS17-15), MPUM12250 (ABS17-18), MPUM12251 (ABS17-40), MPUM12252 (ABS17-72), eight articulated shells: MPUM12254 (ABS8-41, ABS8-57, ABS8-69), MPUM12255 (ABS17-32, ABS17-69), MPUM12256 (ABS22-20), MPUM12257 (BS25-44, ABS25-68).

Description - Small sized, inequally biconvex shell, with a transversally sub-oval to sub-rectangular outline. Cardinal margin short, anterior commissure rectimarginate to slightly uniplicate and anterior margin slightly emarginate. Maximum width: 5.4-9.3 mm; length: 4.4-9 mm. Ventral valve more convex than the dorsal valve, particularly at the umbo. Outline sub-pentagonal, ventral umbo short and pointed, strongly recurved on the cardinal margin without extending beyond it, bearing a very small foramen. Dorsal valve transversely sub-oval in outline, less convex than the ventral one,

sometimes almost flat. Narrow median sulci on both valves, starting at the umbo and reaching the anterior margin. Shell surface smooth. Ventral valve interior with complex dental plates arrangement. At 0.1 mm from the umbo, the dental plates are placed near the lateral walls of the shell. Starting from 0.5 mm from the umbo the dental plates progressively shift towards the middle of the shell, at 1/4 of the valve width from each side. The dental plates are concave and reach the valve floor.

Remarks - Externally, the specimens under study possess all the diagnostic characters of the genus *Rectambitus*: the rectimarginate anterior commissure, the emarginate anterior margin, the narrow sulcus on both valves and the smooth surface. The only difference is the size, which, in the specimens under study, is half or sometimes 1/3 of the average size for the species of the genus. Some of the specimens under study have a deformed or weakly uniplicate anterior margin; however, the anterior commissure of the type species has not been figured (Xu & Grant, 1994), and Shen et al. (2004) described specimens of species of *Rectambitus* with a weakly uniplicate anterior commissure, therefore some kind of variability might be present in the species of the genus. The specimens under study differ from the species of *Rectambitus* because of the absence of the spondylium. However, comparing the serial sections, a similarity between the dental plates of the specimens under study and the characters of the spondylium of species of *Rectambitus* in the most proximal (i.e. closer to the umbo) sections is evident. In particular, in both cases the dental plates are separate from each other, set close to the lateral walls of the shell, and then come closer to each other, shifting towards the middle of the shell. In both cases, the dental plates reach the floor of the valve. However, the occurrence of a low median septum has not been observed in the specimens under study, so the identification is left open.

Occurrence - Hambast Formation, Unit 6, Abadeh section, Central Iran. Wuchiapingian.

Subfamily COMELICANIINAE Merla, 1930

Genus *Gruntallina* Waterhouse & Gupta, 1986

Type species *Comelicania triangularis* Grunt, 1965 in Ruzhentsev & Sarytcheva, 1965

Remarks - The genus *Gruntallina* was erected on the basis of a taxonomic review, which included the description of another new genus based on material from the Himalayas (*Spitispirifer*), later rejected because of a strong suspicion of falsification of the fossil occurrence made by Gupta (Gaetani

et al., 1990; Posenato, 1991). Later on, the type species of *Gruntallina* was discussed and compared to that of the genus *Comelicania* Frech, 1901 by Posenato (1998), who found consistent differences between the two genera and reassessed the validity of *Gruntallina*. The differences between the two genera mainly relate to the dimensions, which are up to 180 mm in width in species of the genus *Comelicania* and limited to 40 mm in width in species of *Gruntallina*. There are also differences in the internal characters: *Gruntallina* has a lower number of spires in the spiralia compared to *Comelicania*, and low dental ridges instead of the short dental plates that characterize *Comelicania*. Dorsal internal characters of *Gruntallina* include short and nearly flat cardinal flanges nearly parallel to the commissural plane, which are instead longer and perpendicular to the commissural plane in *Comelicania*, and the presence of an anteriorly projected median septum underneath the cardinal plate, which is absent in *Comelicania*.

Gruntallina sp.

(Pl. 4, fig. 13)

Material - One figured articulated shell: MPUM12258 (ABS3-4).

Description - Small sized, biconvex shell with transversely triangular outline. Cardinal margin long with elongated cardinal extremities. Anterior commissure is parasulcate. Ventral valve more strongly convex than the dorsal one. Two well developed folds start from the umbo and reach the anterior margin, separated by a narrow furrow that becomes wider at the anterior margin and shapes the fold in the commissure. Dorsal valve with a faint and narrow sulcus starting from the umbonal region. Shell is generally smooth.

Remarks - The specimen under study shows some differences with the type species *Gruntallina triangularis* (Grunt in Ruzhentsev & Sarytcheva, 1965). The most significant difference is the size, in particular the length, which in the specimen here described is about half the length of the specimens described by Grunt in Ruzhentsev & Sarytcheva (1965). Another difference is the sulcus on the dorsal valve, which is very shallow and narrow, and less defined than in the specimens described by Grunt (pl. 44, figs 5a-d, 6). The different morphology and size could be due to the fact that the single available specimen is a juvenile. The type series of *Gruntallina triangularis* consists of two articulated specimens and one dorsal valve, which are not enough to explore the intraspecific variability and compare it with the specimen under study. Therefore, the nomenclature is left open.

Occurrence - Hambast Formation, Unit 6, Abadeh section, Central Iran. Wuchiapingian.

Subfamily SPIRIGERELLINAE Grunt in Ruzhentsev & Sarytcheva, 1965

Genus *Spirigerella* Brown, 1845
Type species *Spirigerella derbyi* Oehlert, 1887

Remarks - The genus *Spirigerella* Brown, 1845 differs from the genus *Composita* Brown, 1845 by having the maximum width located anterior to midlength, while in species of *Composita* it is located around midlength.

?*Spirigerella* sp.
(Pl. 5, fig. 1)

Material - One figured articulated shell: MPUM12259 (ABS21-7).

Description - Biconvex shell, with a sub-oval outline and medium sized. Cardinal margin curved, anterior commissure uniplicate, with a broad fold on the dorsal valve. Maximum width: 20 mm; length: 20.4 mm. No sulcus on both valves. Ventral umbo short and recurved, bearing a small circular foramen in an epithyrid position. Ventral valve interior with two deep longitudinal diductor scars.

Remarks - Given the poor preservation, the specimen here described can be compared with species of three genera: *Spirigerella* Brown, 1845, *Composita* Brown, 1845 and *Posicomta* Grunt, 1986. Species of the genus *Posicomta* can be easily excluded because of their size, significantly smaller than the specimen ABS 21-7. Grant (1976) described the first Asian *Composita* species, but these were later placed in the genus *Posicomta* by Grunt (1986) because of their smaller size compared to species of the genus *Composita*. The deformation of the specimen under study prevents determination of the position of the maximum width of the shell, which is one of the few diagnostic features useful to discriminate between species of *Composita* and *Spirigerella*. Species of the genus *Spirigerella* are also characterized by the possible presence of a tertiary layer in the apical portion of the shell; in fact, in the ventral umbonal region of the specimen under study, a change in the microstructure of the shell is detected which may suggest it belongs to *Spirigerella*.

Occurrence - Hambast Formation, Unit 6, Abadeh section, Central Iran. Wuchiapingian.

Subfamily TRANSCAUCASATHYRIINAE Angiolini & Carabelli, 2010

Genus *Transcaucasathyris* Shen, Grunt & Jin, 2004
Type species *Araxathyris araxensis* Grunt in Ruzhentsev & Sarytcheva, 1965

Transcaucasathyris araxensis (Grunt in Ruzhentsev & Sarytcheva, 1965)
(Pl. 5, figs 2-5)

1878 *Spirigera protea* var. *globularis* ABICH, p. 58, Pl. 7, fig. 9; Pl. 10, fig. 3.
1965 *Araxathyris araxensis araxensis* GRUNT in Ruzhentsev & Sarytcheva, p. 247, Pl. 43, fig. 6.
1986 *Araxathyris araxensis araxensis* Grunt in Ruzhentsev & Sarytcheva - GRUNT, Pl. 28, figs 1-2.
2004 *Transcaucasathyris araxensis* (Grunt in Ruzhentsev & Sarytcheva) - SHEN et al., p. 893, figs 7.30-7.43.
2014 *Transcaucasathyris araxensis* (Grunt in Ruzhentsev & Sarytcheva) - GARBELLI & ANGIOLINI in Ghaderi et al., p. 48, Pl. 3, figs 23-29; text-fig. 7.

Material - Four figured articulated shells: MPUM12260 (ABS16-6), MPUM12261 (ABS17-37), MPUM12262 (ABS17-51), MPUM12263 (ABS17-71); ten articulated shells: MPUM12264 (ABS8-47, ABS8-56), MPUM12265 (ABS17-39, ABS17-55, ABS17-82), MPUM12266 (ABS22-12, ABS22-25, ABS23-2), MPUM12267 (ABS25-9, ABS25-75).

Description - Small sized, inequally biconvex to plano-convex shell, with a slightly transverse sub-oval outline. Cardinal margin shorter than the maximum width, slightly curved. Anterior commissure variable, from uniplicate to parasulcate, anterior margin slightly emarginate. Maximum width: 7.6-11.7 mm; length: 7.1-11.2 mm. Ventral valve more convex than the dorsal valve, particularly at the umbo, with sub-triangular to sub-pentagonal outline. Ventral umbo short, pointed and recurved, bearing a small foramen, palintrope orthocline to slightly apsacline. Median sulcus starting from the umbo as a groove and widening anteriorly. Depth of the median sulcus near the anterior margin variable, as it is the depth of the sulcal tongue. Dorsal valve sub-oval to sub-circular in outline, slightly convex to flat. Dorsal umbo very small and recurved on the cardinal margin. Median sulcus, when present, is faint. Ornamentation of weak growth lamellae, more evident near

the anterior margin. Ventral valve interior with dental plates slightly concave and converging near the valve floor but remaining clearly separated.

Remarks - *Transcaucasathyris araxensis* (Grunt in Ruzhentsev & Sarytcheva, 1965) is a very variable species, particularly in the outline and in the development of the ventral sulcus (Garbelli & Angiolini in Ghaderi et al., 2014). The main difference from the congeneric species is the transverse and flat dorsal valve without a median sulcus.

Occurrence - Hambast Formation, Unit 6, Abadeh section, Central Iran. Wuchiapingian.

Distribution - Wuchiapingian *Araxilevis* and *Haydenella* beds of Transcaucasia (Ruzhentsev & Sarytcheva, 1965), but its range also reaches the Changhsingian in this area, according to Shen et al. (2004); Wuchiapingian of the Ali-Bashi Mountains, North-West Iran (Ghaderi et al., 2014).

Transcaucasathyris kandevani (Fantini Sestini & Glaus, 1966)
(Pl. 5, figs 6-7)

1966 *Araxathyris kandevani* FANTINI SESTINI & GLAUS, p. 913, Pl. 65, figs 4-5.
2010 *Transcaucasathyris kandevani* (Fantini Sestini & Glaus) - ANGIOLINI & CARABELLI, p.75, Pl. 3, figs 17-21; Pl. 5, figs 1-3; text-figs 10-11.

Material - Three figured articulated shells: MPUM12268 (ABS16-3), MPUM12269 (ABS17-45), MPUM12270 (ABS25-24); six articulated shells: MPUM12271 (ABS8-68, ABS17-67), MPUM12272 (ABS22-14, ABS22-19), MPUM12273 (ABS25-8, ABS25-37).

Description - Small sized, inequally biconvex shell with a sub-pentagonal outline. Cardinal margin slightly curved, anterior commissure parasulcate. Maximum width: 7.3-11.7 mm; length: 7.6-11 mm. Ventral valve sub-pentagonal, strongly convex at the umbo. Ventral umbo short and strongly recurved on the cardinal margin. Median sulcus starting at mid-length, becoming variably deeper and wider towards the anterior margin. The development of the sulcal tongue is variable, depending on the depth of the ventral sulcus. Dorsal valve sub-oval in outline and less convex than the ventral valve. Dorsal umbo short and located beneath the ventral umbo. Median fold low and rounded. Some weak growth lamellae are concentrated near the anterior margin, particularly on the sulcal tongue. Ventral valve interior with dental plates initially parallel to each other, then dorsally

diverging and ventrally converging, forming an obtuse angle. In the most anterior section the adminicula are not visible, whereas the dental lamellae are longer and support the teeth until 1.6 mm from the umbo.

Remarks - *Transcaucasathyris kandevani* (Fantini Sestini & Glaus, 1966) differs from *T. araxensis* because of the more elongate outline, the median fold on the dorsal valve and the delayed ventral sulcus; from *T. lata* (Grunt in Ruzhentsev & Sarytcheva, 1965) because of the more elongate outline and the absence of the dorsal sulcus.

Occurrence - Hambast Formation, Unit 6, Abadeh section, Central Iran. Wuchiapingian.

Distribution - Wuchiapingian-Changhsingian of the Alborz Mountains, North Iran (Angiolini & Carabelli, 2010).

Transcaucasathyris lata (Grunt in Ruzhentsev & Sarytcheva, 1965)
(Pl. 5, figs 8-11; Fig. 12)

1878 *Spirigera protea* var. *alata* ABICH, p. 56, Pl. 9, fig. 10.
1900 *Spirigera protea* var. *alata* Abich - ARTHABER, p. 282, Pl. 22, fig. 3.
1900 *Spirigera* sp. ARTHABER, p. 282, Pl. 22, fig. 13.
1965 *Araxathyris lata* GRUNT in Ruzhetsev & Sarytcheva, p. 249, Pl. 43, fig. 5; text-fig. 45.
1986 *Araxathyris lata* Grunt in Ruzhetsev & Sarytcheva - GRUNT, Pl. 15, fig. 6.
2010 *Araxathyris lata* Grunt in Ruzhetsev & Sarytcheva - ANGIOLINI & CARABELLI, p. 80, Pl. 5, figs 12-15.
2014 *Transcaucasathyris lata* (Grunt in Ruzhetsev & Sarytcheva) - GARBELLI & ANGIOLINI in Ghaderi et al., p. 49, Pl. 3, figs 30-34; text-fig. 8.

Material - Five figured articulated shells: MPUM12274 (ABS8-40), MPUM12275 (ABS17-31), MPUM12276 (ABS22-8), MPUM12277 (ABS23-1), MPUM12279 (ABS25-50); twelve articulated shells: MPUM12278 (ABS25-47), MPUM12280 (ABS8-34, ABS8-78), MPUM12281 (ABS16-12, ABS17-13, ABS17-25, ABS17-65, ABS17-76), MPUM12282 (ABS22-7, ABS25-35, ABS25-36, ABS25-56).

Description - Small sized, sub-equally biconvex shell, slightly inflated with a transverse outline. Cardinal margin slightly curved, anterior commissure generally strongly parasulcate, with a variably developed sulcal tongue. Maximum width: 8.6-11.2 mm; length: 7.2-10.7 mm. Ventral valve convex and sub-pentagonal, with a transverse outline. Ventral umbo short and pointed, recurved on the cardinal margin. Ventral median sulcus starting at the umbo as a faint groove, becoming a narrow furrow at mid-length and wider and deeper at the anterior margin. Dorsal valve convex, sub-oval to sub-rectangular in outline. Dorsal umbo very small. Median fold very gentle and rounded, with narrow median sulcus starting from the umbo and reaching the anterior margin. Ornamentation of growth lamellae, more frequent near the anterior commissure. Ventral valve interior with clearly separated, concave dental plates reaching the valve floor.

Remarks - *Transcaucasathyris lata* is mostly similar to *T. araxensis*, from which it differs because of the more transverse outline, the strongly parasulcate anterior commissure and the narrow dorsal sulcus developed from the umbo to the anterior margin. *T. lata* differs from *T. kandevani* because of the ventral sulcus starting from the umbo.

Occurrence - Hambast Formation, Unit 6, Abadeh section, Central Iran. Wuchiapingian.

Distribution - Wuchiapingian *Oldhamina* beds of Transcaucasia (Ruzhentsev & Sarytcheva, 1965); Changhsingian Nesen Formation of the Alborz Mountains, North Iran (Angiolini & Carabelli, 2010); Wuchiapingian of the Ali-Bashi Mountains, North-West Iran (Ghaderi et al., 2014).

Transcaucasathyris spp.

(Fig. 13)

Material - One figured articulated shell: MPUM12283 (ABS17-64); sixteen articulated shells: MPUM12284 (ABS17-68), MPUM12285 (ABS7-13, ABS8-65, ABS16-8, ABS17-33, ABS17-58, ABS17-59, ABS17-63, ABS17-73, ABS17-74), MPUM12286 (ABS22-24, ABS24-1, ABS25-41, ABS25-43, ABS25-61, ABS25-71).

Description - Biconvex, small sized shell, with a sub-triangular to sub-pentagonal outline. Anterior commissure uniplicate to slightly parasulcate. Maximum width: 5.7-10 mm; length: 6.7-9.8 mm. Ventral umbo short and recurved on the cardinal margin. Ventral sulcus variable, starting from the umbo and widening near the anterior margin. Very shallow and weak dorsal sulcus in one

specimen. Ventral valve interior with straight to slightly concave dental plates, becoming slightly divergent before reaching the valve floor.

Remarks - The specimens here described do not show specific features that allow identification at the species level. The gentle fold on the dorsal valve excludes the species *T. araxensis* (Grunt in Ruzhentsev & Sarytcheva); the ventral sulcus starting from the umbo excludes the species *T. kandevani* (Fantini Sestini & Glaus, 1966); the lack of a narrow sulcus on the dorsal valve excludes the species *T. lata* (Grunt in Ruzhentsev & Sarytcheva, 1965); the slightly larger size, either longer than 7 mm, wider than 7 mm or thicker than 5 mm, excludes the species *T. minor* (Grunt in Ruzhentsev & Sarytcheva, 1965).

Occurrence - Hambast Formation, Unit 6, Abadeh section, Central Iran. Wuchiapingian.

Order SPIRIFERIDA Waagen, 1883
Superfamily RETICULARIOIDEA Waagen, 1883
Family ELYTHIDAE Frederiks, 1924
Subfamily PHRICODOTHYRIDINAE Caster, 1939

Genus *Permophricodothyris* Pavlova, 1965
Type species *Permophricodothyris ovata* Pavlova, 1965

Remarks - The genus *Permophricodothyris* Pavlova, 1965 is identified by the presence of elongated, posteriorly directed spiralia, made of several whorls, resulting in a longitudinally elongated outline.

?*Permophricodothyris* sp.
(Pl. 5, fig. 12)

Material - One figured articulated shell: MPUM12288 (ABS20-3).

Description - Medium-sized, equally biconvex shell with a sub-triangular outline. Anterior commissure parasulcate. Maximum width: 20.9 mm; length: 23 mm. Ventral valve triangular in

outline and convex. Ventral umbo large, high, and recurved on the palintrope, with straight flanks, forming a triangular outline. Dorsal valve sub-circular in outline, smaller than the ventral valve and convex. Dorsal valve is folded, with a slight rounded median fold. Dorsal umbo small, short, and pointing to the ventral palintrope. Ornamentation of very fine growth lines and fine growth lamellae.

Remarks - The lack of preserved ornamentation in the specimen under study prevents a reliable determination at the genus level. The classification of the specimen here described is based on its longitudinally elongated shape which is more compatible with spiralia pointing backwards, as in species of *Permophricodothyris*, rather than laterally, as in species of *Squamularia* Gemmellaro, 1899.

Occurrence - Hambast Formation, Unit 6, Abadeh section, Central Iran. Wuchiapingian.

Indeterminate specimens

Several specimens have been left in open nomenclature due to their poor preservation.
A single dorsal valve: MPUM12228 (ABS0-50), is identified as belonging to the family Schizophoriidae Schuchert & LeVene, 1929 because of the cardinal process resembling that present in the genera *Acosarina* Cooper & Grant, 1969 and *Orthotichia* Hall & Clarke, 1892, although it is broken. Other characters visible on this specimen are one dental socket with its ridge and fragments of the other ridge, and the ornamentation near the margin of the interior surface, made of costellae numbering 15 per 2 mm.
One hundred and forty-eight articulate shells, collectively labelled MPUM12287, have been identified as belonging to the family Athyrididae. These specimens could belong either to a species of *Araxathyris* or to a species of *Transcaucasathyris*, but the poor preservation of the umbonal region prevent the study of the dental plates arrangement, which is the only character that allows genus identification.

ACKNOWLEDGEMENTS

This project was supported by the MURST (PRIN 2017RX9XXXY, project ‘Biota resilience to global change: biomineralization of planktic and benthic calcifiers in the past, present and future’). We thank Ruben Marchesi for the photographs of the brachiopod specimens. We are grateful to

H. Zhang, Y.C. Zhang, Ma. Ghorbani, Mo. Ghorbani, and M. Ovissi for assistance during the field work.

REFERENCES

Abich H. (1878). Eine Bergkalkfauna aus der Araxesenge bei Djoulfa in Armenien. 126 pp. *Commission bei Alfred Hölder KK Hof-und Universitäts-Buchhändler*.

Agard P., Omrani J., Jolivet L. & Mouthereau F. (2005). Convergence history across Zagros (Iran): constraints from collisional and earlier deformation. *International Journal of Earth Sciences*, 94: 401-419.

Alavi M. (1994). Tectonics of the Zagros orogenic belt of Iran: New data and interpretations. *Tectonophysics*, 229: 211-238.

Albrecht J. (1924). Palaontologische und stratigraphische Ergebnisse der Forschungsreise nach Westserbien 1918. *Akademie der Wissenschaften in Wien, Mathematisch-Naturwissenschaftliche Klasse, Denkschriften*, 99: 289-307.

Allen M.B., Ghassemi M.R., Shahrabi M. & Qorashi M. (2003). Accommodation of late Cenozoic oblique shortening in the Alborz range, northern Iran. *Journal of Structural Geology*, 25: 659-672.

Amiot M., Ciry R., Fantini Sestini N., Premoli Silva I., Rossi Ronchetti C., Sartenaer P., Vandercammen A., Von Schouppé A., Zanini Buri C., Gridelli E., Müller G. & Williams L.H.J. (1965). *In* Brill E.J. (ed.). Italian expeditions to the Karakorum (K2) and Hindu Kush. *Scientific Reports, part iv palaeontology-zoology-botany*, volume 1. 431 pp. Leiden.

Angiolini L. & Carabelli L. (2010). Upper Permian brachiopods from the Nesen Formation, North Iran. *Special Papers in Palaeontology*, 84: 41-90.

Angiolini L., Carabelli L., Nicora A., Crasquin-Soleau S., Marcoux J. & Rettori R. (2007b). Brachiopods and other fossils from the Permo-Triassic boundary beds of the Antalya Nappes (SW Taurus, Turkey). *Geobios*, 40: 715-729.

Angiolini L., Crippa G., Shen S.Z., Zhang H., Zhang Y.C., Ghorbani M., Ghorbani M. & Ovissi M. (2017). Report of the Chinese, Italian, Iranian working group: The Permian-Triassic boundary sections of Abadeh revisited. *Permophiles*, 65: 24-27.

Angiolini L., Gaetani M., Muttoni G., Stephenson M.H. & Zanchi A. (2007a). Tethyan oceanic currents and climate gradients 300 my ago. *Geology*, 35: 1071-1074.

Arthaber G.V. (1900). Das jüngere paläozoicum aus der Araxes-Enge bei Djulfa. *Beiträge zur Paläontologie und Geologie Österreich-Ungarns und des Orients*, 12: 209-302.

Bagheri S. & Stampfli G.M. (2008). The Anarak, Jandaq and Posht-e-Badam metamorphic complexes in central Iran: new geological data, relationships and tectonic implications. *Tectonophysics*, 451: 123-155.

Baud A., Richoz S., Brandner R., Krystyn L., Heindel K., Mohtat T., Mohtat-Aghai P. & Horacek M. (2021). Sponge takeover from end-Permian mass extinction to Early Induan time: Records in Central Iran microbial buildups. *Frontiers in Earth Science*, 9: 586210.

Berberian M. (2014). Earthquakes and coseismic surface faulting on the Iranian Plateau. 713 pp. Elsevier.

Berberian M. & King G.C.P. (1981). Towards a paleogeography and tectonic evolution of Iran. *Canadian Journal of Earth Sciences*, 18: 210-265.

Besse J., Torcq F., Gallet Y., Ricou L.E., Krystyn L. & Saidi A. (1998). Late Permian to Late Triassic palaeomagnetic data from Iran: constraints on the migration of the Iranian block through the Tethyan Ocean and initial destruction of Pangaea. *Geophysical Journal International*, 135: 77-92.

Bittner A. (1899). Trias Brachiopoda and Lamellibranchiata. *Memoirs of the Geological Survey of India, Palaeontologia Indica, Series 15 (Himalayan Fossils)*, 3: 1-76.

Bittner A. (1901). Ueber *Pseudomonotis Telleri* und verwandte Arten der unteren Trias. *Jahrbuch der Kaiserlich-Königlichen Geologischen Reichsanstalt*, 50: 559-591.

Boucot A.J., Johnson J.G. & Staton R.D. (1964). On some atrypoid, retzioid, and athyridoid Brachiopoda. *Journal of Paleontology*, 38: 805-822.

Broglio Loriga C., Masetti D. & Neri C. (1983). La Formazione di Werfen (Scitico) delle Dolomiti Occidentali: sedimentologia e biostratigrafia. *Rivista ltaliana di Paleontologia*, 88: 501 598.

Brown T. (1845). Illustrations of the fossil conchology of Great Britain and Ireland, with descriptions and localities of all species, parts 24-28. *Maclachlan and Stuwart, Smith, Elder. Edinburgh & London*: 117-136.

Campi M.J., Shen S., Shi G.R. & Leman M.S. (2000). First record of Permianella He & Zhu, 1979 (Permianellidae; Brachiopoda) from Peninsular Malaysia. *Alcheringa*, 24: 37-43.

Campi M.J., Shi G.R. & Leman M.S. (2005). Guadalupian (Middle Permian) brachiopods from Sungai Toh, a Leptodus Shale locality in the central belt of Peninsular Malaysia. *Palaeontographica (A)*, 273: 97-160.

Caneva G. (1906). La fauna del Calcare a Bellerophon. Contributo alla conoscenza dei limiti permo-triassici. *Bollettino della Società` Geologica Italiana*, 25: 427-452.

Caster K.E. (1939). A Devonian fauna from Colombia. *Bulletins of American Paleontology*, 24: 1-218.

Chen Z.Q. & Liao Z.T. (2007). Last orthotetid brachiopods from the uppermost Permian of South China. *Journal of Paleontology*, 81: 986-997.

Chen J., Shen S.Z., Zhang Y.C., Angiolini L., Gorgij M.N., Crippa G., Wang W., Zhang H., Yuan D.X., Li X.H. & Xu Y.G. (2020). Abrupt warming in the latest Permian detected using high-resolution in situ oxygen isotopes of conodont apatite from Abadeh, central Iran. *Palaeogeography, Palaeoclimatology, Palaeoecology*, 560: 1-11.

Chen J., Yuan D.X. & Shen S.Z. (2021). Reply to the Comment of Horacek et al. (2021) on the Permian-Triassic boundary at the Abadeh section, central Iran. *Permophiles*, 71: 39-43.

Chi-Thuan T.T. (1961). Les brachiopodes permiens du Phnom-Tup (Sisophon-Cambodge). *Annales de la Faculté des Sciences, Université de Saigon*, 1961: 267-308.

Chi-Thuan T.T. (1962). Les brachiopodes permiens de Cam-lô (Province de Quang-Tri). *Annales de la Faculté des Sciences, Université de Saigon*, 1962: 485-498.

Cooper G.A. & Grant R.E. (1969). New Permian Brachiopods from West Texas. *Smithsonian Contributions to Paleobiology*, 1-20.

Cooper G.A. & Grant R.E. (1974). Permian Brachiopods of West Texas, II. *Smithsonian Contributions to Paleobiology*, 15: 233-793.

Cooper G.A. & Grant R.E. (1975). Permian Brachiopods of West Texas, III (Part II-Plates). *Smithsonian Contributions to Paleobiology*, 19: 795-1921.

Davidson T. (1881). On genera and species of spiral-bearing Brachiopoda, from specimens developed by the Rev. Norman Glass: with notes on the results obtained by Mr. George Maw from extensive washings of the Wenlock and Ludlow shales of Shropshire. *Geological Magazine*, 8: 1-13.

Davoudian A.R., Genser J., Neubauer F. & Shabanian N. (2016). $^{40}Ar/^{39}Ar$ mineral ages of eclogites from North Shahrekord in the Sanandaj-Sirjan Zone, Iran: implications for the tectonic evolution of Zagros orogen. *Gondwana Research*, 37: 216-240.

Dercourt J., Zonenshain L.P., Ricou L.E., Kazmin V.G., Le Pichon X., Knipper A.L., Grandjacquet C., Sbortshikov I.M., Geyssant J., Lepvrier C., Pechersky D.H., Boulin J., Sibuet J.C., Savostin L.A., Sorokhtin O., Westphal M., Bazhenov M.I., Laurer J.P. & Biju-Duval B. (1986). Geological evolution of the Tethys belt from the Atlantic to the Pamirs since the Lias. *Tectonophysics*, 123: 241-315.

Diener C. (1897). Himalayan fossils. The Permo-Carboniferous fauna from Chitichun, No. 1. *Palaeontologia Indica*, Series 15: 1-105.

Diener C. (1903). Permian fossils of the central Himalayas. *Palaeontologia Indica*, Series 15, 1: 1-204.

Dudás F.Ö., Yuan D.X., Shen S.Z. & Bowring S.A. (2017). A conodont-based revision of the 87Sr/86Sr seawater curve across the Permian-Triassic boundary. *Palaeogeography, Palaeoclimatology, Palaeoecology*, 470: 40-53.

Fantini Sestini N. (1965a). The geology of the Upper Djedjerud and Lar Valleys (North Iran). II. Palaeontology. On some "*Spinomarginifera*" from the Upper Permian of Mubarak-Abad. *Rivista Italiana di Paleontologia e Stratigrafia*, 71: 989-996.

Fantini Sestini N. (1965b). The geology of the Upper Djedjerud and Lar Valleys (North Iran). II. Palaeontology. Bryozoans, brachiopods and molluscs from the Ruteh Limestone (Permian). *Rivista Italiana di Paleontologia e Stratigrafia*, 71: 13-108.

Fantini Sestini N. & Glaus M. (1966). Brachiopods from the Upper Permian Nesen Formation (North Iran). *Rivista Italiana di Paleontologia e Stratigrafia*, 72: 887-930.

Feng R.L. & Jiang Z.L. (1978) Brachiopoda. *Paleontological Atlas of Southwest China, Guizhou Volume* 2: 231-305.

Frech F. (1901). Die Dyas: Lethaea geognosrica; 1. *Theil Lethaea Palaeozoica*, 2: 435-578.

Frech F. (1911). Die Dyas. *In* Richthofen F.V. (ed.). *China*, 5: 116-137.

Frederiks G.N. (1924). Paleontological studies. 2: On Upper Carboniferous spiriferids from the Urals. *Izvestyia geologicheskogo Komiteta*, 38: 295-324. [in Russian]

Gaetani M., Angiolini L., Ueno K., Nicora A., Stephenson M.H., Sciunnach D., Rettori R., Price G.D. & Sabouri J. (2009). Pennsylvanian–Early Triassic stratigraphy in the Alborz Mountains (Iran). *Geological Society, London, Special Publication*, 312: 79-128.

Gaetani M., Garzanti E. & Tintori A. (1990). Permo-Carboniferous stratigraphy in SE Zanskar and NW Lahul (NW Himalayas, India). *Eclogae Geologicae Helveticae*, 83: 143-161.

Gallet Y., Krystyn L., Besse J. & Ricou L.E. (2000). New constraints on the Upper Permian and Lower Triassic geomagnetic polarity timescale from the Abadeh section (central Iran). *Journal of Geophysical Research*, 105: 2805-2815.

Garbelli C., Angiolini L., Shen S., Crippa G., Yuan D., Bahrammanesh M., Abbasi S. & Birjandi M. (2014). Additional brachiopod findings from the Lopingian succession of the Ali Bashi Mountains, NW Iran. *Rivista Italiana di Paleontologia e Stratigrafia*, 120: 119-126.

Gemmellaro G.G. (1899). La fauna dei calcari con fusulina della Valle del fiume Sosio. *Giornale di scienze naturali ed economiche di Palermo*, 22: 95-214.

Ghaderi A., Garbelli C., Angiolini L., Ashouri A.R., Korn D., Rettori R. & Gharaie M.H.M. (2014). Faunal change near the end-Permian extinction: the brachiopods of the Ali Bashi Mountains, NW Iran. *Rivista Italiana di Paleontologia e Stratigrafia*, 120: 27-59.

Ghasemi A. & Talbot C.J. (2006). A new tectonic scenario for the Sanandaj–Sirjan Zone (Iran). *Journal of Asian Earth Sciences*, 26: 683-693.

Glaus M. (1964). Trias und Oberperm im zentralen Elburs (Persien). *Eclogae Geologicae Helveticae*, 57: 497-508.

Glennie K.W. (2000). Cretaceous tectonic evolution of Arabia's eastern plate margin: a tale of two oceans. *Society for Sedimentary Geology Special Publication*, 69: 9-20.

Gortani M. & Merla G. (1934). Fossili del Paleozoico. 323 pp. *Spedizione Italiana de Filippi nell'Himalaia*, Series 2, 5.

Grabau A.W. (1931). The Permian of Mongolia. A report on the Permian fauna of the Jisu Honguer Limestone of Mongolia and its relations to the Permian of other parts of the World. *In* Reed C.A. (ed.). Natural History of Central Asia, vol. 4. 665 pp. American Museum of Natural History, New York.

Grant R.E. (1976). Permian brachiopods from southern Thailand. *Memoir (The Paleontological Society)*: 1-269.

Gray J.E. (1840). Synopsis of the content of the British Museum, 42nd edition. 370 pp. British Museum, London.

Grunt T.A. (1986). Classification of brachiopods of the order Athyridida. *Trudy Paleontologičeskogo Instituta Akademii Nauk SSSR*, 215: 1-200.

Guex J. (1991). Biochronological correlations. 252 pp. Springer, Berlin.

Hall J. & Clarke J.M. (1892). *An introduction to the study of the genera of Palaeozoic Brachiopoda*. Natural History of New York. Palaeontology. Volume 8, Pt. 1. 394 pp. New York Geological Survey, Charles van Benthuysen & Sons, Albany.

Hassanzadeh J., Stockli D.F., Horton B.K., Axen G.J., Stockli L.D., Grove M., Schmitt A.K. & Walker J.D. (2008). U-Pb zircon geochronology of late Neoproterozoic–Early Cambrian granitoids in Iran: Implications for paleogeography, magmatism, and exhumation history of Iranian basement. *Tectonophysics*, 451: 71-96.

Hassanzadeh J. & Wernicke B.P. (2016). The Neotethyan Sanandaj-Sirjan zone of Iran as an archetype for passive margin-arc transitions. *Tectonics*, 35: 586-621.

Hauer F. von (1850). Ueber die vom Herrn Bergrath W. Fuchs in den Venetianer Alpen gesammelten Fossilien. *Denkschriften der mathematisch-naturwissenschaftliche Classe der Kaiserlichen Akademie der Wissenschaften*, 2: 1-19.

He X.L. & Zhu M.L. (1979). A new form of brachiopods and its systematic classification. *Journal of China Institute of Mining and Technology*, 4: 131-140. [in Chinese]

Hofmann R., Hautmann M. & Bucher H. (2013). A new paleoecological look at the Dinwoody Formation (Lower Triassic, western USA): Intrinsic versus extrinsic controls on ecosystem recovery after the end-Permian mass extinction. *Journal of Paleontology*, 87: 854-880.

Horacek M., Krystyn L. & Baud A. (2021). Comment to Chen et al., 2020: Abrupt warming in the latest Permian detected using high-resolution in situ oxygen isotopes of conodont apatite from Abadeh, central Iran. Importance of correct stratigraphic correlation, reporting of existing data and their scientific interpretation. *Permophiles*, 70: 33-36.

Horacek M., Richoz S., Brandner R., Krystyn L. & Spötl C. (2007). Evidence for recurrent changes in Lower Triassic oceanic circulation of the Tethys: The $\delta^{13}C$ record from marine sections in Iran. *Palaeogeography, Palaeoclimatology, Palaeoecology*, 252: 355-369.

Huang T.K. (1932). Late Permian brachiopods of southwestern China. Part 1. *Palaeontologia Sinica* (series B), 9: 1-138.

Huang T.K. (1933). Late Permian brachiopods of southwestern China. Part 1. *Palaeontologia Sinica* (series B), 9: 1-172.

Ichikawa K. (1958). Zur Taxonomie und Phylogenie der triadischen "Pteriidae" (Lamellibranch.). *Palaeontographica (A)*, 111: 131-212.

Javadi H.R., Ghassemi M.R., Shahpasandzadeh M., Guest B., Ashtiani M.E., Yassaghi A.L.I., & Kouhpeyma M. (2013). History of faulting on the Doruneh Fault System: implications for the kinematic changes of the Central Iranian Microplate. *Geological Magazine*, 150: 651-672.

Jin Y.G., Liao Z.T. & Fang B.X. (1974). Brachiopoda (Carboniferous). *In* Nanjing Institute of Geology and Palaeontology, Chinese Academy of Sciences (ed.), A Handbook of the Stratigraphy and Palaeontology inSouthwest China. Beijing: Science Press, 275-283. [in Chinese]

Jin Y.G., Ye S.L., Xu H.K. & Sun D.L. 1979. Brachiopoda. *In* Nanjing Institute of Geology and Palaeontology and Geological Institute of Qinghai Province (eds), Palaeontological Atlas of Northwestern China, Qinghai Province, Volume 1, Lower Paleozoic-Cenozoic: 60-225. [in Chinese]

Kayser E. (1883). Obercarbonische fauna von Lo-ping. *Vierter Band*: 160-208.

Kershaw S., Crasquin S., Li Y., Collin P.Y., Forel M.B., Mu X., Baud A., Wang Y., Xie S., Maurer F. & Guo L. (2012). Microbialites and global environmental change across the Permian-Triassic boundary: a synthesis. *Geobiology*, 10: 25-47.

Korte C., Kozur H.W., Joachimski M.M., Strauss H., Veizer J. & Schwark L. (2004). Carbon, sulfur, oxygen and strontium isotope records, organic geochemistry and biostratigraphy across the

Permian/Triassic boundary in Abadeh, Iran. *International Journal of Earth Sciences*, 93: 565-581.

Korte C., Pande P., Kalia P., Kozur H.W., Joachimski M.M. & Oberhänsli H. (2010). Massive volcanism at the Permian-Triassic boundary and its impact on the isotopic composition of the ocean and atmosphere. *Journal of Asian Earth Sciences*, 37: 293-311.

Kozur H.W. (1995). Some remarks to the conodonts Hindeodus and Isarcicella in the latest Permian and earliest Triassic. *Palaeoworld*, 6: 64-77.

Kozur H.W. (2004). Pelagic uppermost Permian and the PermianTriassic boundary conodonts of Iran. Part I: Taxonomy. *Hallesches Jahrbuch für Geowissenschaften B Beiheft*, 18: 39-68.

Kozur H.W. (2005). Pelagic uppermost Permian and the PermianTriassic boundary conodonts of Iran. Part II: investigated sections and evaluation of the conodont faunas. *Hallesches Jahrbuch für Geowissenschaften B Beiheft*, 19: 49-86.

Kozur H.W. (2007). Biostratigraphy and event stratigraphy in Iran around the Permian-Triassic Boundary (PTB): Implications for the causes of the PTB biotic crisis. *Global and Planetary Change*, 55: 155-176.

Kozur H.W., Leven E.J., Lozovskij V.R. & Pjatakova M.V. (1978). Rasclenenie po konodontam pogranicnych sloev permi i triasa Zakavkazja. *Bjul MOIP, otd. Geol.* 1978:15-24.

Leman M.S. (1994). The significance of Upper Permian brachiopods from Merapoh area, northwest Pahang. *Geological Society of Malaysia Bulletin*, 35: 113-121.

Leonardi P. (1960). Studio statistico-sedimentologico di alcune faune werfeniane della Valle di Fiemme nel Trentino. *Studi Trentini di Scienze Naturali*, 37: 17-29.

Liang W. (1990). Lengwu formation of Permian and its brachiopod fauna in Zhejiang Province. *People's Republic of China Ministry of Geology and Mineral Resources*, *Geological Memoirs* (series 2), 10: 1-522.

Liao Z.T. (1980). Upper Permian brachiopods from Western Guizhou. *In* Nanjing Institute of Geology and Palaeontology Chinese Academy of Sciences (ed.), Stratigraphy and Palaeontology of Upper Permian Coal-bearing Formations in Western Guizhou and Eastern Yunnan, China: 241–277. [in Chinese]

Licharew B.K. (1928). Über einige seltene und neue Brachiopoden aus dem Unterperm des nördlichen Kaukasus. *Paläontologische Zeitschrift*, 10: 258-289.

Licharew B.K. (1937). Brachiopoda of the Permian System of the USSR, Fascicule I. Permian Brachiopoda of North Caucasus. Families: Chonetidae Hall & Clarcke and Productidae Gray. 152 pp. Monografii po Paleontologii SSSR, 39, Leningrad. [in Russian]

Licharew B.K. (1939). Class Brachiopoda. *In* Licharew B.K. (Eds). *Atlas of the Leading Forms of the Fossil Faunas of the USSR*, 6: 76-121. [in Russian]

Liu L. (1964). Notes on some marine Early Triassic Lamellibranchiata from East Tsinling, southern Shangxi (Shensi). *Acta Palaeontologica Sinica*, 12: 312-324. [In Chinese with English abstract]

Liu X.C., Wang W., Shen S.Z., Gorgij M.N., Ye F.C., Zhang Y.C., Furuyama S., Kano A. & Chen X.Z. (2013). Late Guadalupian to Lopingian (Permian) carbon and strontium isotopic chemostratigraphy in the Abadeh section, central Iran. *Gondwana Research*, 24: 222-232.

Lucas S.G. & Shen S.Z. (eds) (2018). The Permian Timescale. *Geological Society, London, Special Publication*, 450: 289-320.

Mansuy H. (1913). Paléontologie de l'Annam et du Tonkin. *Mémoires du Service géologique de l'Indochine*, 2: 1-49.

Mattei M., Cifelli F., Muttoni G. & Rashid H. (2015). Post-Cimmerian (Jurassic–Cenozoic) paleogeography and vertical axis tectonic rotations of Central Iran and the Alborz Mountains. *Journal of Asian Earth Sciences*, 102: 92-101.

Mei S., Zhang K. & Wardlaw B.R. (1998). A refined succession of Changhsingian and Griesbachian neogondolellid conodonts from the Meishan section, candidate of the global stratotype section and point of the Permian–Triassic boundary. *Palaeogeography, Palaeoclimatology, Palaeoecology*, 143: 213-226.

Mei S., Henderson C.M. & Cao C. (2004). Conodont sample-population approach to defining the base of the Changhsingian Stage, Lopingian Series, Upper Permian. *Geological Society, London, Special Publication*, 230: 105-121.

Merla G. (1930). La fauna del Calcare a Bellerophon della regione dolomitica. *Memorie Istituto Geologico e Mineralogico della Università di Padova*, 9: 1-221.

Montenat C., Lapparent A.F., Lys M., Termier H., Termier G. & Vachard D. (1976). La transgression permienne et son substratum dans le Jebel Akhdar (Montagne d'Oman, Péninsule arabique). *Annales de la Société géologique du Nord*, 96: 239-258.

Muir-Wood H.M. & Cooper G.A. (1960). Morphology, classification and life habits of the Productoidea (Brachiopoda). *Memoirs Geological Society of America, 81*. 447 pp. Geological Society of America, Boulder.

Muttoni G. & Kent D.V. (2019). Adria as a promontory of Africa and its conceptual role in the Tethys twist and Pangea B to Pangea A transformation in the Permian. *Rivista Italiana di Paleontologia e Stratigrafia*, 125: 249-269.

Muttoni G., Gaetani M., Kent D.V., Sciunnach D., Angiolini L., Berra F., Garzanti E., Mattei M. & Zanchi A. (2009). Opening of the Neo-Tethys Ocean and the Pangea B to Pangea A transformation during the Permian. *GeoArabia*, 14: 17-48.

Nakazawa K. (1977). On *Claraia* of Kashmir and Iran. *Journal of the Palaeontological Society of India*, 20: 197-204.

Newell N.D. & Kummel B. (1942). Lower Eo-Triassic stratigraphy, western Wyoming and southeast Idaho. *Geological Society of America Bulletin*, 53: 937-995.

Noetling F. (1905). Untersuchungen über die Familie der Lyttoniidae Waag. Noetling. *Palaeontographica*, (1846-1933): 129-154.

Oehlert D.P. (1887). Appendice sur les brachiopods. *Manuel de Conchyliologie et de Paléontologie conchyliologique ou Histoire naturelle des Mollusques vivants et fossiles*, 4: 1189-1334.

Pacaud J.M. (2015). Catalogue des types de brachiopodes conservés dans les collections de Paléontologie du Muséum national d'Histoire naturelle de Paris. *Fossiles, hors-série*, 5: 82-98.

Pavlova E.E. (1965). Revison of the genus *Neophricodothyris* (Order Spiriferida). *Paleontologicheskii Zhurnal*, 1965: 133-137.

Posenato R. (1991). Endemic to cosmopolitan Brachiopods across the P/Tr boundary in the Southern Alps (Italy). Proceedings of Shallow Tethys 3, Sendai, 1990. Saito Ho-on Kai Special Publication, 3: 125-139.

Posenato R. (1998). The gen. Comelicania Frech, 1901 (Brachiopoda) from the Southern Alps: morphology and classification. *Rivista Italiana di Paleontologia e Stratigrafia*, 104: 43-68.

Posenato R. (2008). Global correlations of mid Early Triassic events: the Induan/Olenekian boundary in the Dolomites (Italy). *Earth-Science Reviews*, 91: 93-105.

Ramezani J. & Tucker R.D. (2003). The Saghand region, central Iran: U-Pb geochronology, petrogenesis and implications for Gondwana tectonics. *American Journal of Science*, 303: 622-665.

Ramovs A. (1958). Razvoj Zgornjega Perma v Loskih in Polhograjskih Hribih (Die Entwicklung des Oberperms in Bergland von Skofja Loka und Polhov Gradec (W. Slowenien, NW Jugoslavien). *Razprave Slovenska Akademija Znanosti in Umetnosti*, 4: 451-622.

Reed F.R.C. (1944). Brachiopoda and Mollusca from the Productus limestones of the Salt Range. *Palaeontologia Indica, new series*, 23: 1-768.

Richoz S., Krystyn L., Baud A., Brandner R., Horacek M. & Mohtat-Aghai P. (2010). Permian–Triassic boundary interval in the Middle East (Iran and N. Oman): Progressive

environmental change from detailed carbonate carbon isotope marine curve and sedimentary evolution. *Journal of Asian Earth Sciences*, 39: 236-253.

Ruzhentsev V.E. & Sarytcheva T.G. (1965). Evolution and succession of marine organisms at the Permo-Triassic boundary. *Trudy Paleontologicheskogo Instituta*, 108. 431 pp. *Akademii. Nauk SSSR, Moscow.*

Saidi A., Brunet M.F. & Ricou L.E. (1997). Continental accretion of the Iran Block to Eurasia as seen from Late Paleozoic to Early Cretaceous subsidence curves. *Geodynamica Acta*, 10: 189-208.

Sarytcheva T.G. (1964). Oldhaminid brachiopods from the Permian of Transcaucasia. *Paleontologicheskiy Zurnal*, 1964: 58-72.

Sarytcheva T.G., Licharew B.K., Sokolskaja A.N. & Orlov Y.A. (1960). Otriad Productida. 221–238. *In* Orlov Y.A. (ed.). *Osnovy Paleontologii. Mshanki Brakhiopody*. 343 pp. *Izdatel'stvo Akademii Nauk SSSR, Moscow*. [in Russian]

Sarytcheva T.G. & Sokolskaya A.N. (1959). On the classification of pseudopunctate brachiopods. In *Doklady Akademia Nauk SSSR*, 125: 181-184. [in Russian]

Schellwien E. (1900). Die Fauna der Trogkofelschicheten in den Karnischen Alpen und den Karawanken, 1 Theil: Die Brachiopoden. *Abh KK Geol Reichsanst*, 16: 1-122.

Schréter Z. (1963). Die Brachiopoden aus dem oberen Perm des Biikk-Gebirges in Nordungarn. *Geologica Hungarica, Series Palaeontologica*, 28: 79-179.

Schuchert C. (1913). Class 2. Brachiopoda. *Textbook of palaeontology*, 1(1): 355-420.

Schuchert C. & LeVene C.M. (1929). Brachiopoda (generum et genotyporum index et bibliographia). *In* J.F. Pompeckj (ed.), Fossilium Catalogus, vol. 1. Animalia, Pats 42 Junk. Berlin. 140 pp.

Şengör A.M.C. (1979). Mid-Mesozoic closure of Permo-Triassic Tethys and its implications. *Nature*, 279: 590–593.

Şengör A.M.C., Cin A., Rowley D.B. & Nie S.Y. (1993). Space-time patterns of magmatism along the Tethysides: A preliminary study. *The Journal of Geology*, 101: 51–84.

Shafaii Moghadam H. & Stern R.J. (2011). Geodynamic evolution of upper Cretaceous Zagros ophiolites: Formation of oceanic lithosphere above a nascent subduction zone. *Geological Magazine*, 148: 762–801.

Shahinfar S., Yeganeh B.Y., Arefifard S., Vachard D. & Payne J.L. (2021). Refined foraminiferal of upper Wordian, Capitanian and Wuchiapingian strata in Hambast Valley, Abadeh region (Iran), and paleobiogeographic implications. *Geological Journal*, 55: 6255-6279.

Shakerardakani F., Neubauer F., Bernroider M., Finger F., Hauzenberger C., Genser J., Waitzinger M. & Monfaredi B. (2021). Metamorphic stages in mountain belts during a Wilson cycle: A

case study in the central Sanandaj–Sirjan zone (Zagros Mountains, Iran). *Geoscience Frontiers*, 101272.

Shen S.Z., & Mei S.L. (2010). Lopingian (Late Permian) high-resolution conodont biostratigraphy in Iran with comparison to South China zonation. *Geological Journal*, 45(2-3): 135-161.

Shen S.Z. & Shi G.R. (1997). Permianella (Brachiopoda) from the Upper Permian of Transcaucasia. *Science Reports of Niigata University, Series E, Geology and Mineralogy*, 12: 19-27.

Shen S.Z. & Shi G.R. (2007). Lopingian (Late Permian) brachiopods from South China, Part 1: Orthotetida, Orthida and Rhynchonellida. *Bulletin of the Tohoku University Museum*, 6: 1-102.

Shen S.Z., He X.L. & Zhu M.L. (1992). Changhsingian brachiopods from Zhongliang Hill of Chongqing, Sichuan Province, South China. 171-196. In Gu, D. Y. (Eds). Stratigraphy and palaeontology of oil and gas bearing areas in China (3). *The Petroleum Industry Press, Beijing*, 218 pp. [In Chinese with English abstract]

Shen S.Z., Shi G.R. & Zongjie F. (2002). Permian brachiopods from the Baoshan and Simao blocks in western Yunnan, China. *Journal of Asian Earth Sciences*, 20(6): 665-682.

Shen S.Z., Grunt T.A., & Jin Y.G. (2004). A comparative study of Comelicaniidae (Brachiopoda: Athyridida) from the Lopingian (Late Permian) of South China and Transcaucasia in Azerbaijan and Iran. *Journal of Paleontology*, 78(5): 884-899.

Shen S., Gorgij M.N., Wang W., Zhang Y., Khammar H.R. & Tabatabaei S.H. (2009). Report of the field trip of the Permian stratigraphy in central and eastern Iran. *Permophiles*, 53: 2-5.

Shen S.Z., Cao C.Q., Zhang H., Bowring S.A., Henderson C.M., Payne J.L., Davydov V.I., Chen B., Yuan D.X., Zhang Y.C., Wang W. & Zheng Q.F. (2013). High-resolution $\delta 13C_{carb}$ chemostratigraphy from latest Guadalupian through earliest Triassic in South China and Iran. *Earth and Planetary Science Letters*, 375: 156-165.

Shen S.Z., Jin Y.G., Zhang Y. & Weldon E.A. (2017). Permian brachiopod genera on type species of China. *In*: Rong J.Y., Jin Y.G., Shen S.Z., Zhan R.B. (eds), *Phanerozoic Brachiopod Genera of China*. *Beijing Science Press*, 658-888.

Shen S.Z., Zhang H., Zhang Y., Yuan D.X., Chen B., He W.H., Mu L., Lin W., Wang W.Q., Chen J., Wu Q., Cao C.Q., Wang Y. & Wang X. (2019). Permian integrative stratigraphy and timescale of China. *Science China Earth Sciences*, 62(1): 154-188.

Simić V. (1933). Gornji perm u zapadnoj Srbiji. *Rasprave Geološkog Instituta Kralj*, 1/1: 1-130.

Spath L.F. (1930). The Eotriassic invertebrate fauna of east Greenland. *Meddelelser om Grönland*, 83: 1-90.

Sremac J. (1986). Middle Permian brachiopods from the Velebit Mts. (Croatia, Yugoslavia). *Palaeontologia Jugoslavica*, 35: 1-43.

Stehli F.G. (1954). Lower Leonardian Brachiopoda of the Sierra Diablo. *Bulletin of the American Museum of Natural History*, 105: 257-358.

Stepanov D.L., Golshani F. & Stöcklin J. (1969). Upper Permian and Permian-Triassic boundary in North Iran. *Geolological Survey of Iran, Report*, 12: 1–72.

Stöcklin J. (1981). A brief report on geodynamics in Iran. *Zagros Hindu Kush Himalaya Geodynamic Evolution*, 3: 70-74.

Stoyanov A.A. (1910). O novom rode brachiopoda. *Bulletin de l'Académie Impériale des Sciences de St. Pétersbourg (series 6)*, 4(11): 853–855.

Su H. & Zhou J. (2020). Timing of Arabia-Eurasia collision: Constraints from restoration of crustal-scale cross-sections. *Journal of Structural Geology*, 135: 104041.

Tadayon M., Rossetti F., Zattin M., Calzolari G., Nozaem R., Salvini F., Faccenna C. & Khodabakhshi P. (2019). The long-term evolution of the Doruneh Fault region (Central Iran): A key to underöanding the spatio-temporal tectonic evolution in the hinterland of the Zagros convergence zone. *Geological Journal*, 54(3): 1454-1479.

Takin M. (1972). Iranian geology and continental drift in the Middle East. *Nature*, 235(5334): 147-150.

Taraz H. (1969). Permo-Triassic section in central Iran. *AAPG Bulletin*, 53(3): 688-693.

Taraz H. (1974). Geology of the Surmag-Deh Bid area, Abadeh region, central Iran. *Geological Survey of Iran, Report* 37.

Taraz H., Golshani F., Nakazawa K., Shimura D., Bando Y., Ishii K.I., Maurata M., Okimura Y., Sakamura S., Nakamura K. & Tukuoka T. (1981). The Permian and the Lower Triassic Systems in Abadeh Region, Central Iran. *Memoirs of the Faculty of Science, Kyoto University, Series of Geology and Mineralogy*, 47: 62–133.

Tazawa J.I. (1987) Permian brachiopod faunas of Japan and their palaeobiogeography. *Chikyu Monthly (Gekkan Chikyu)*, 9:252-255. [in Japanese]

Tazawa J.I. (2001). Middle Permian brachiopod faunas of Japan and South Primorye, Far East Russia: their palaeobiogeographic and tectonic implications. *Geosciences Journal*, 5(1): 19-26.

Tazawa J.I. (2003). Kochiproductus and Leptodus (Brachiopoda) from the Middle Permian of the Obama area, South Kitakami Belt, northeast Japan. *Scientific Reports of Niigata University (Geology)*, 18: 25-39.

Tazawa, J.I. (2016). Middle Permian (Wordian) mixed Boreal–Tethyan brachiopod fauna from Kamiyasse–Imo, South Kitakami Belt, Japan. *Scientific Reports of Niigata University (Geology)*, 31: 7-43.

Tazawa J.I., Ono T. & Hori M. (1998). Two Permian lyttoniid brachiopods from Akasaka, central Japan. *Paleontological Research*, 2(4): 239-245.

Tazawa J.I., Kikuchi Y., Nikaido A., Adachi S. & Okumura Y. (2014). *Permian brachiopods from boulders in the Pliocene basal conglomerate of Hitachi, central Japan, and their tectonic implications. The Journal of the Geological Society of Japan,* 120(11): 377–39.

Tazawa J.I., Kikuchi Y., Nikaido A. & Fujii S. (2018). *Leptodus nobilis* (Permian Brachiopoda) from a boulder in the basal conglomerate of the Pliocene Kume Formation, Hitachi area, central Japan. *The Journal of the Geological Society of Japan*, 124(11): 913-918.

Teichert C., Kummel B. & Sweet W.C. (1973). Permian-Triassic strata, Kuh-e-Ali Bashi, Northwestern Iran. *Bulletin of the Museum of Comparative Zoology*, 145(8): 423-472.

Termier H. & Termier G. (1970). Les Productoides du Djoulfien (Permien supérieur) dans la Téthys orientale: essai sur l'agonie d'un phylum. *Société Géologique du Nord, Annales*, 90(4): 443-461.

Termier G., Termier H., De Lapparent A.F. & Marin P. (1974). Monographie du Permo-carbonifère de Wardak (Afghanistan central). *Travaux et Documents des Laboratoires de Géologie de Lyon*, 2(1): 1-78.

Verna V., Angiolini L., Baud A., Crasquin S. & Nicora A. (2011). Guadalupian brachiopods from western Taurus, Turkey. *Rivista Italiana di Paleontologia e Stratigrafia*, 117(1): 51-104.

Viaretti M., Crippa G., Shen, S. & Angiolini L. (2021). Upper Permian brachiopods from the Abadeh section, Central Iran. *Permophiles*, 71: 36-39.

Vinn O. & Rubel M. (2000). The spondylium and related structures in the Clitambonitidine brachiopods. *Journal of Paleontology*, 74(3): 439-443.

Waagen W.H. (1883). Salt Range fossils, 1 (4). Productus Limestone fossils, Brachiopoda. *Palaeontologia Indica*, (13) 1: 391-546.

Waagen W.H. (1884). Salt Range fossils, 1 (4). Productus Limestone fossils, Brachiopoda. *Palaeontologia Indica*, (13) 1: 547-728.

Wang Y. (1955). Phylum Brachiopoda. 109–171. In *Nanjing Institute of Geology and Paleontology (ed.) Index fossils of China 2. Science Press, Beijing*, 171 pp. [in Chinese]

Waterhouse J.B. & Gupta V.J. (1986). A significant new Permian athyrid brachiopod from the uppermost Gungri Formation (Kuling or Productus Shale) at Spiti, and its implications for classification and correlation. *Bulletin of the Indian Geologists' Association*, 19(1): 45-56.

Weidlich O. & Bernecker M. (2007). Differential severity of Permian–Triassic environmental changes on Tethyan shallow-water carbonate platforms. *Global and Planetary Change*, 55(1-3): 209-235.

Wendt J., Kaufmann B., Belka Z., Farsan N. & Bavandpur A.K. (2005). Devonian/Lower Carboniferous stratigraphy, facies patterns and palaeogeography of Iran Part II. Northern and central Iran. *Acta Geologica Polonica*, 55(1): 31-97.

Williams A., Carlson S.J., Brunton C.H.C., Holmer L.E. & Popov L. (1996). A supra-ordinal classification of the Brachiopoda. *Philos. Trans. R. Soc. London. Ser. B*, 351(1344): 1171-1193.

Williams S.A., Carlson S.J., Brunton C.H.C., Holmer L.E., Popov L.E., Mergl M., Laurie J.R., Basset M.G., Cocks L.R.M., Rong J.Y., Lazarev S.S., Grant R.E., Racheboeuf P.R., Jin Y.G., Wardlaw B.R., Harper D.A.T. & Wright A.D. (2000). Treatise on Invertebrate Paleontology. Part H Brachiopoda (revised): vol. 3. Linguliformea, Craniiformea, and Rhynchonelliformea (part). *Geological Society of America, Boulder and University of Kansas, Lawrence,* 424-919.

Williams A., Brunton C.H.C., Carlson S.J., Alvarez F., Blodgett R.B., Boucot A.J., Copper P., Dagys A.S., Grant R.E., Jin Y.G., MacKinnon D.I., Mancenido M.O., Owen E.F., Rong J.Y., Savage N.M. & Sun D.L. (2002). Treatise on Invertebrate Plaeontology. Part H Brachiopoda (revised): vol. 4. Rhynchonelliformea (part). *Geological Society of America, Boulder and University of Kansas, Lawrence,* 921-1688.

Xu G., & Grant R.E. (1994). Brachiopods near the Permian-Triassic boundary in south China. *Smithsonian Contributions to Paleobiology*, 76: 1-68.

Yang D. (1984). Systematic description of palaeontology: Brachiopoda. *In* Yichang Institute of Geology and Mineral Resources, ed., Biostratigraphy of the Yangtze Gorge area, vol. i. Geology Publishing House, Beijing, 203-239. [in Chinese]

Yin H.F. (1985). Bivalves near the Permian-Triassic boundary in South China *Journal of Paleontology,* 59(3): 572-600.

Zanchetta S., Berra F., Zanchi A., Bergomi M., Caridroit M., Nicora A. & Heidarzadeh G. (2013). The record of the Late Palaeozoic active margin of the Palaeotethys in NE Iran: constraints on the Cimmerian orogeny. *Gondwana Research*, 24(3-4): 1237-1266.

Zanchetta S., Malaspina N., Zanchi A., Benciolini L., Martin S., Javadi H.R., & Kouhpeyma M. (2018). Contrasting subduction–exhumation paths in the blueschists of the Anarak Metamorphic Complex (Central Iran). *Geological Magazine*, 155(2): 316-334.

Zanchi A., Berra F., Mattei M., Ghassemi M.R. & Sabouri J. (2006). Inversion tectonics in central Alborz, Iran. *Journal of Structural Geology*, 28(11): 2023-2037.

Zanchi A., Zanchetta S., Garzanti E., Balini M., Berra F., Mattei M. & Muttoni G. (2009a). The Cimmerian evolution of the Nakhlak–Anarak area, Central Iran, and its bearing for the reconstruction of the history of the Eurasian margin. *Geological Society, London, Special Publication*, 312(1): 261-286.

Zanchi A., Zanchetta S., Berra F., Mattei M., Garzanti E., Molyneux S., Nawab A. & Sabouri J. (2009b). The Eo-Cimmerian (Late? Triassic) orogeny in North Iran. In: Brunet, M.-F., Wilmsen, M. & Granath, J. W. (Eds) *South Caspian to Central Iran Basins*. *Geological Society, London, Special Publication*, 312(1): 31-55.

Zanchi A., Malaspina N., Zanchetta S., Berra F., Benciolini L., Bergomi M., Cavallo A., Javadi H.R. & Kouhpeyma M. (2015). The Cimmerian accretionary wedge of Anarak, Central Iran. *Journal of Asian Earth Sciences*, 102: 45-72.

Zanchi A., Zanchetta S., Balini M. & Ghassemi M.R. (2016). Oblique convergence during the Cimmerian collision: evidence from the Triassic Aghdarband Basin, NE Iran. *Gondwana Research*, 38: 149-170.

Zeng Y., He X.L. & Zhu M.L. (1995). *Permian Brachiopods and Community Succession in the Huayin Mountains, Sichuan*. China University of Mineralogy Press, Xuzhou, 187 pp. [in Chinese with English abstract]

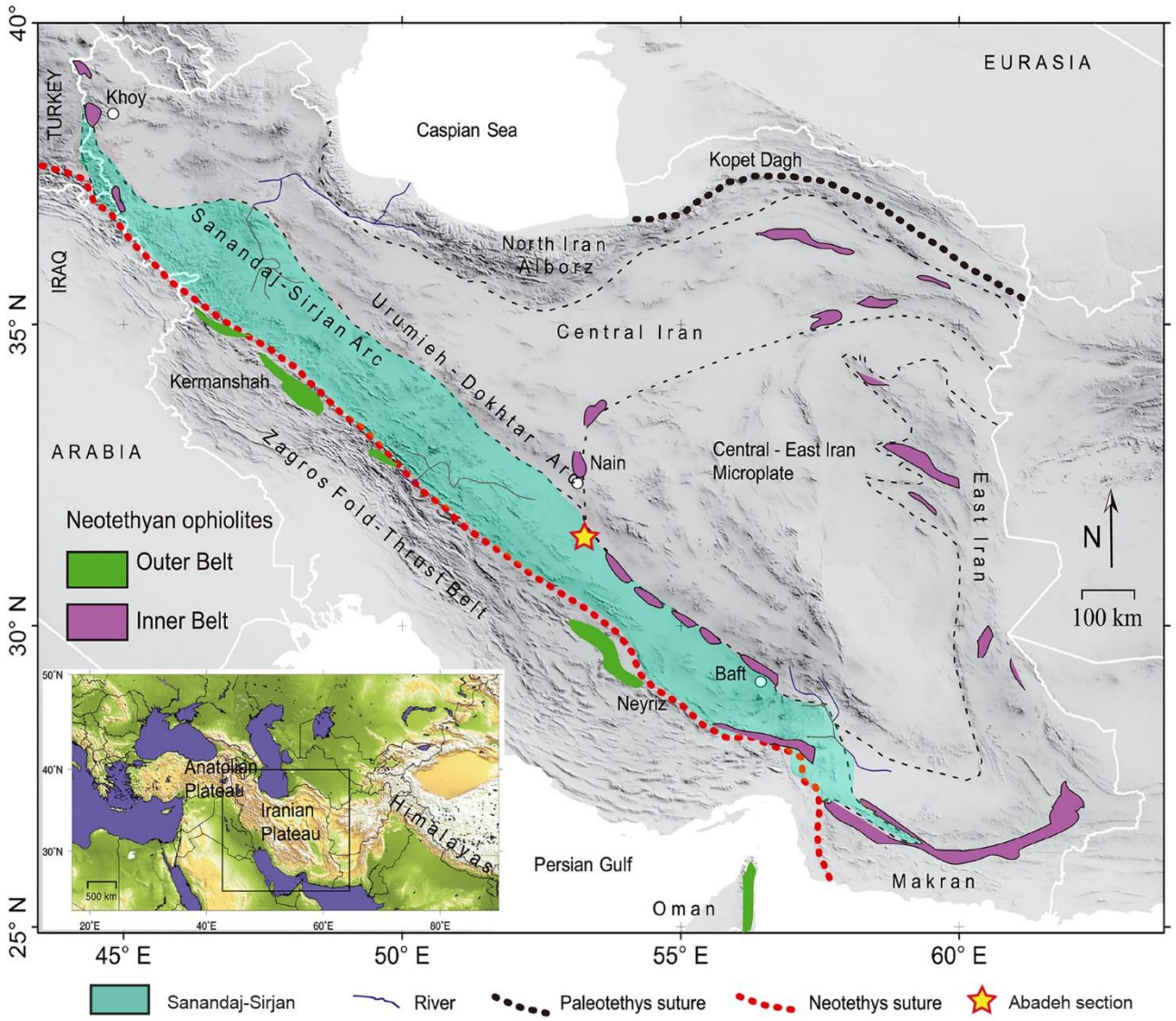

Fig. 1 - Distribution of the Neotethyan ophiolite belts in Iran. The Inner Belt is also called “Coloured Mélange”. Modified from Hassanzadeh & Wernicke (2016).

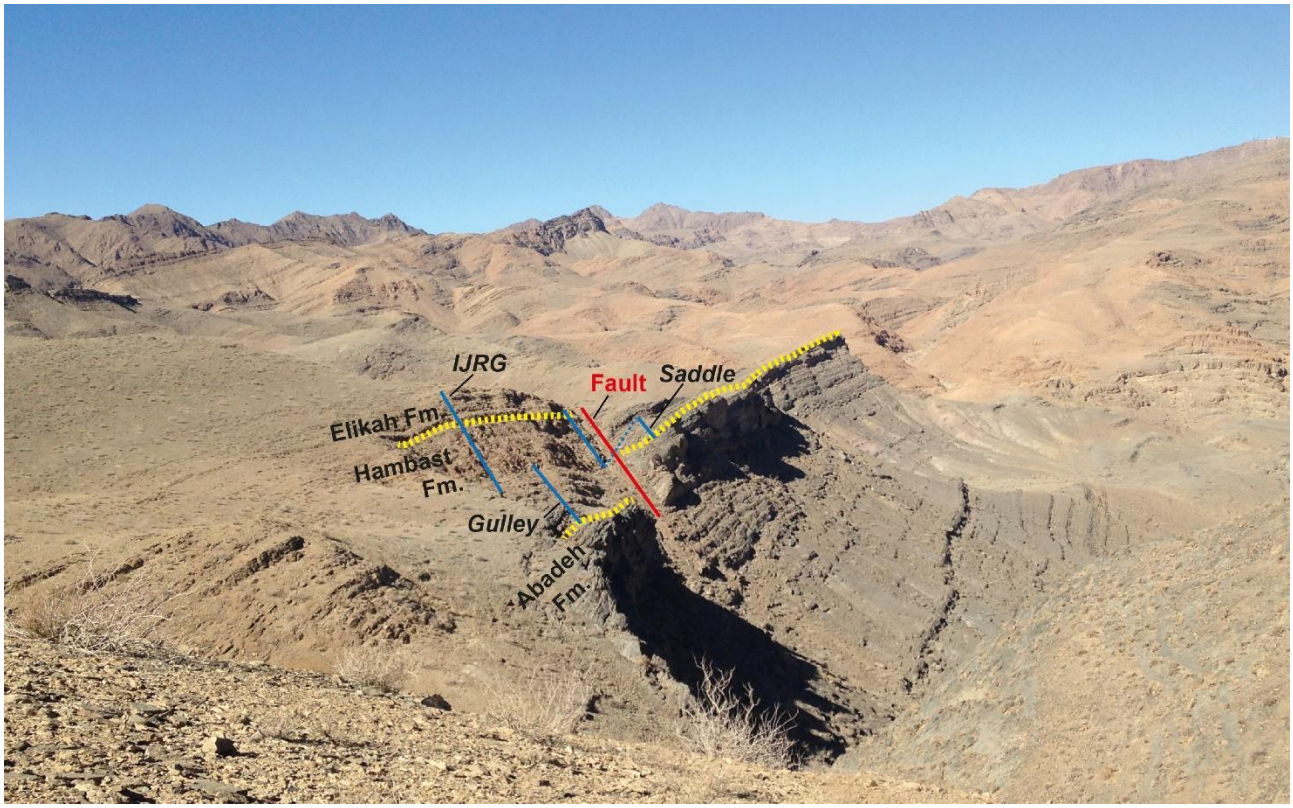

Fig. 2 - Position of the two measured logs at Abadeh.

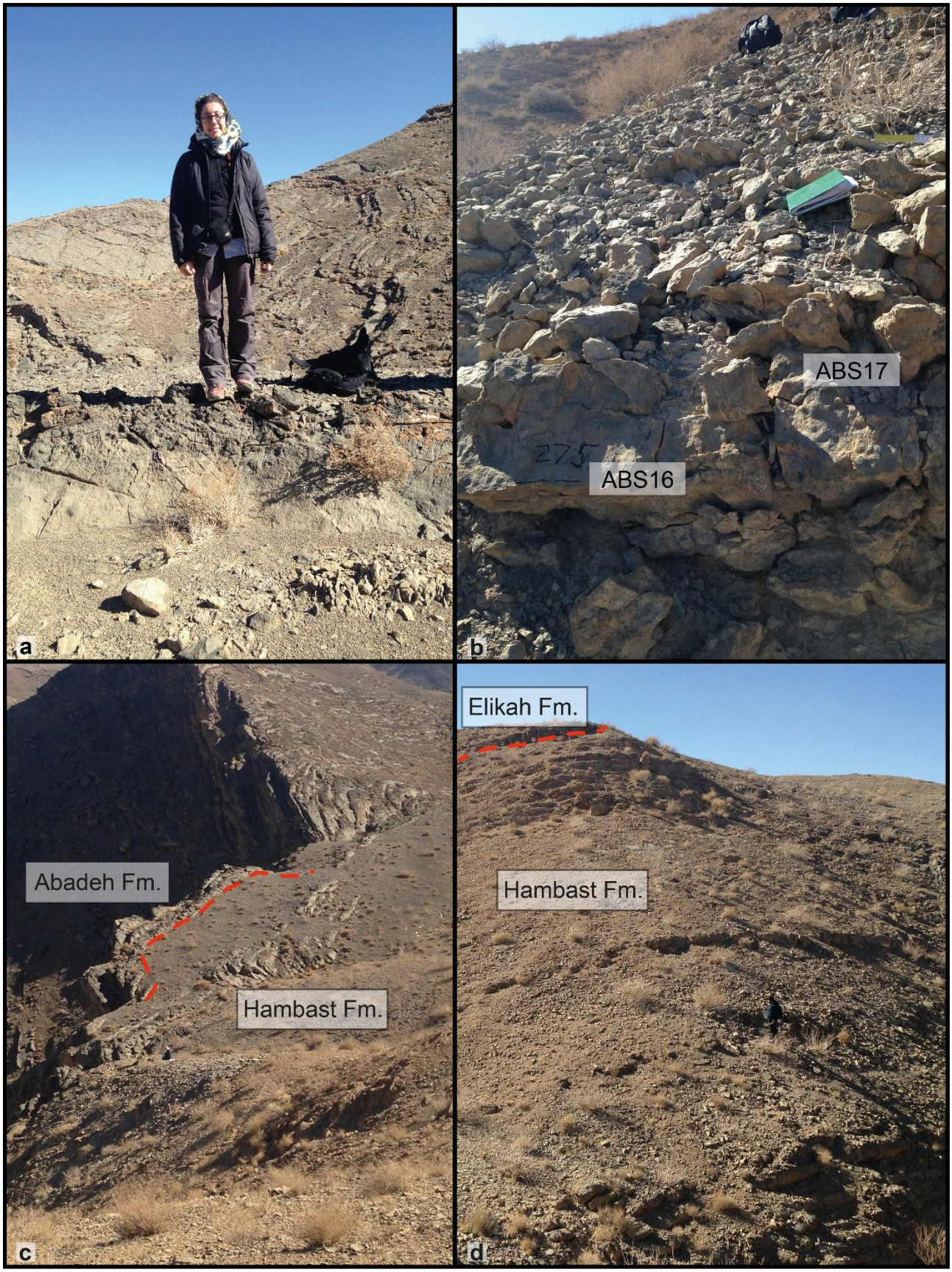

Fig. 3 - a) Dr. Gaia Crippa standing above the top of the Abadeh Formation. b) Grey limestones, position of samples ABS 16 and ABS 17. c) Gulley section, poorly outcropping and covered by scree. d) Saddle section.

Fig. 4 - a) Thin section from bed ABS 27 showing bioclasts consisting mainly of brachiopods and an ammonoid. Scale bar is 1.5 mm. b) Boundary Clay. c) Fan-like structures in the microbialites. d) Succession of nodular limestones, claystones and microbialites at the passage between the Paratirolites Limestone and the Elikah Formation.

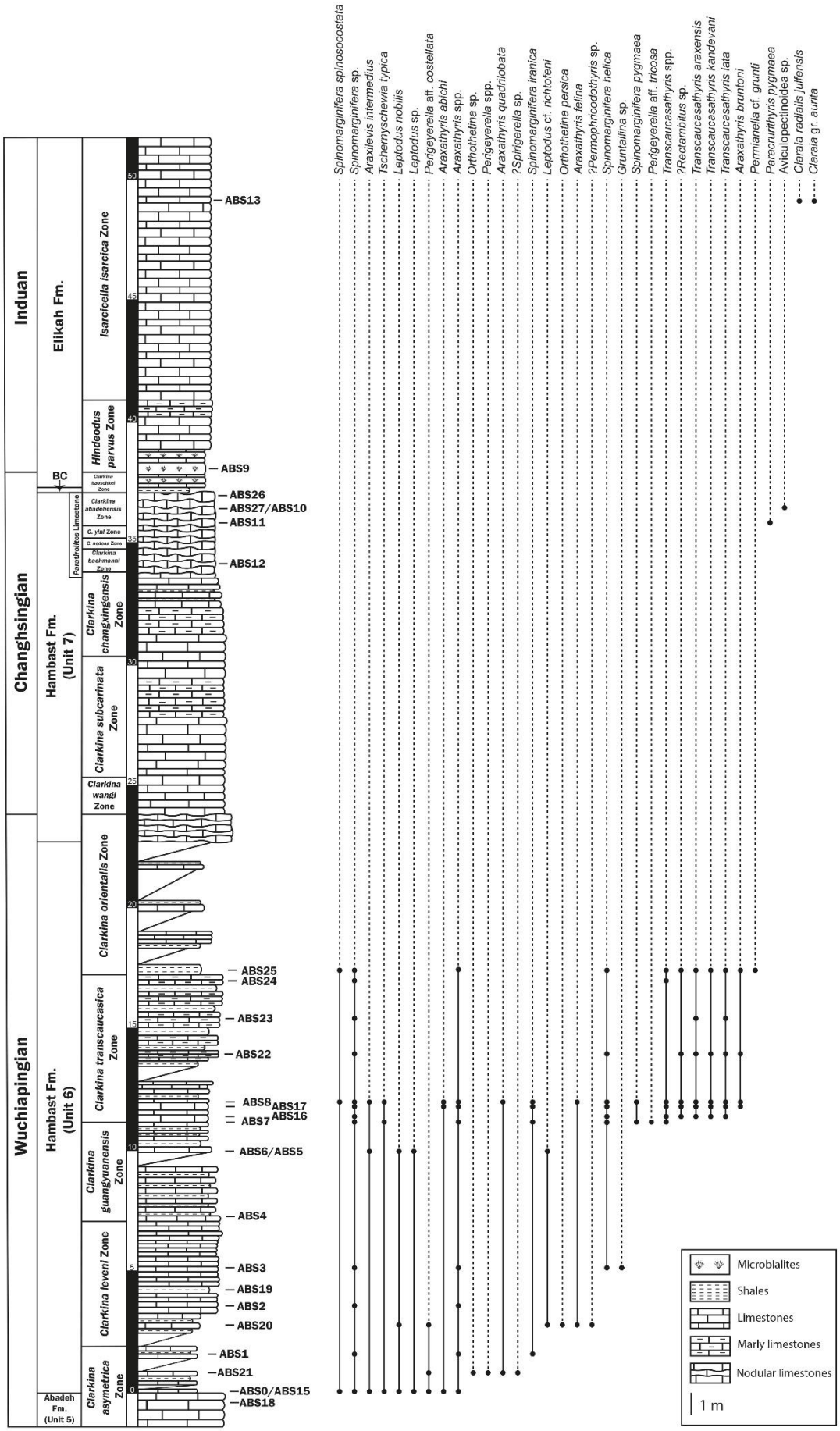

Fig. 5 - Composite stratigraphic section at Abadeh.

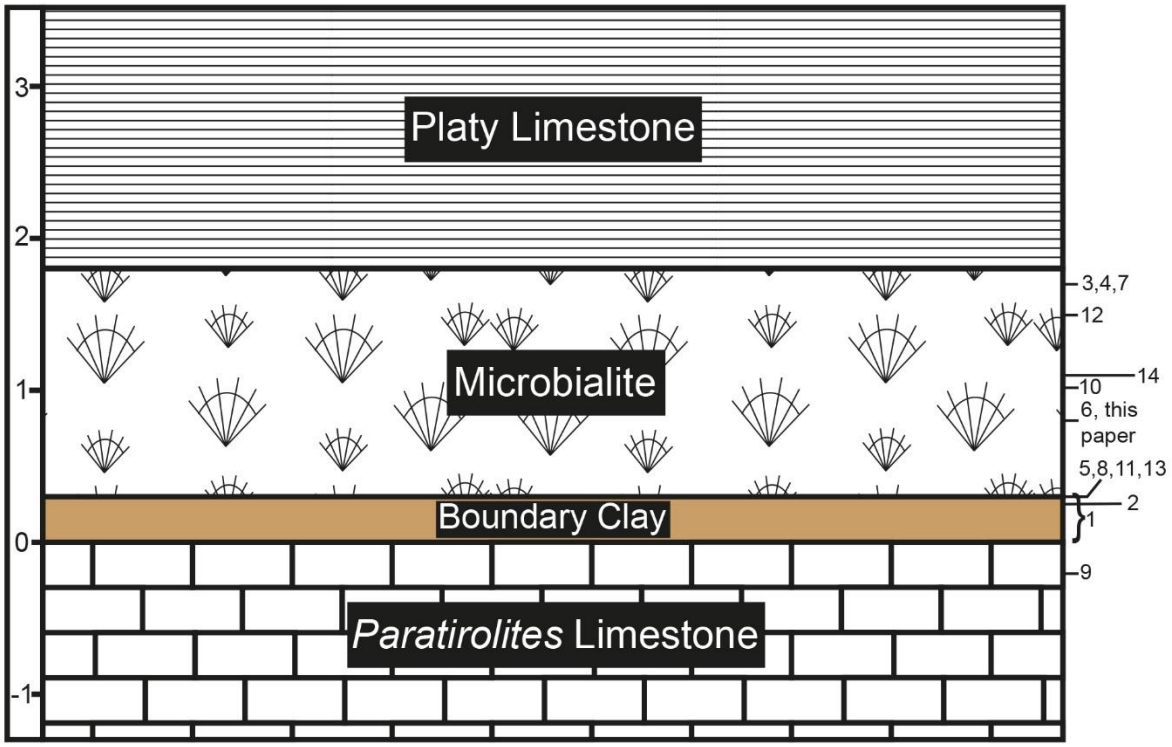

Fig. 6 - Graphic scheme showing the different positions of the PTB at Abadeh published by the authors cited in the text. The numbers refer to the different papers as in Tab. 3.

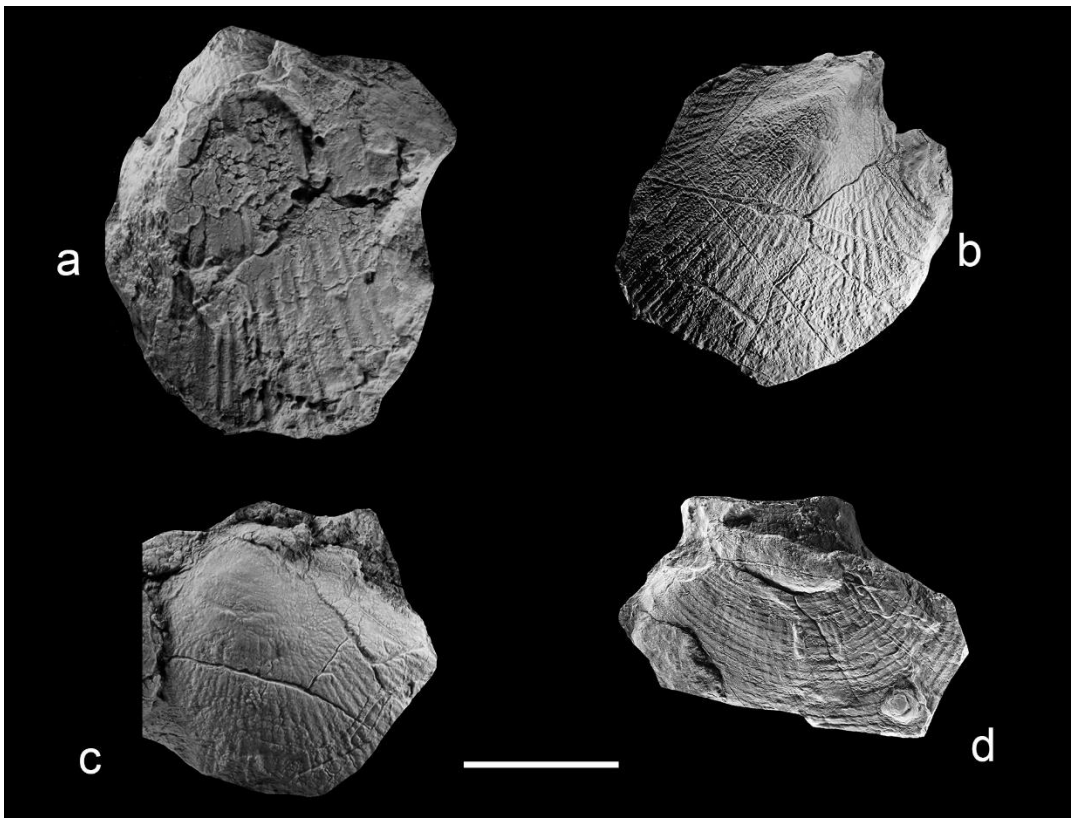

Fig. 7 - Bivalves from the Abadeh section. a) Aviculopectinoidea sp. b-c) *Claraia radialis julfensis* Nakazawa. d) *Claraia* gr. *aurita* (Hauer). Scale bar corresponds to 2 cm.

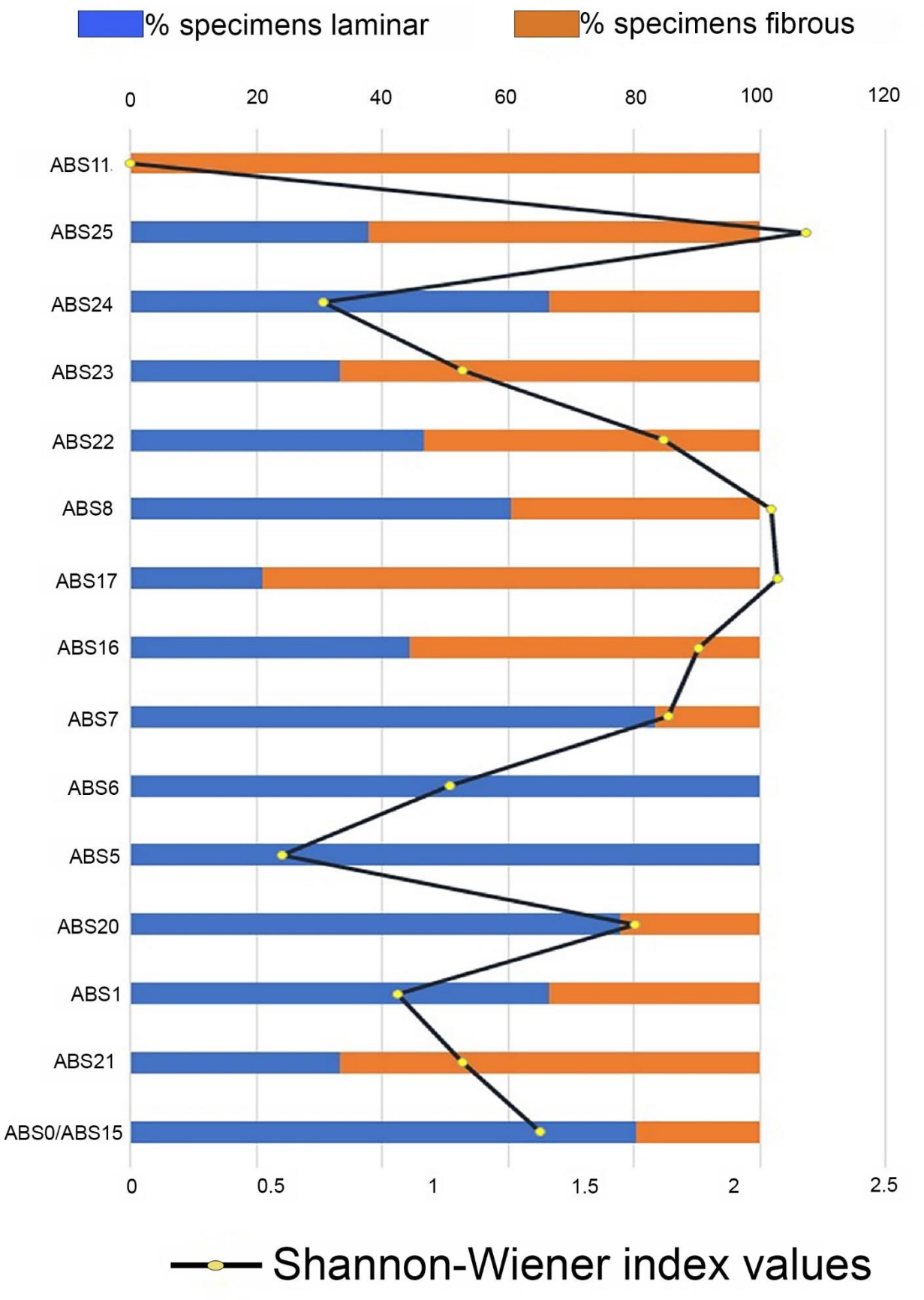

Fig. 8 - Graph showing the alternation in prevalence of laminar vs fibrous shell microstructural type.

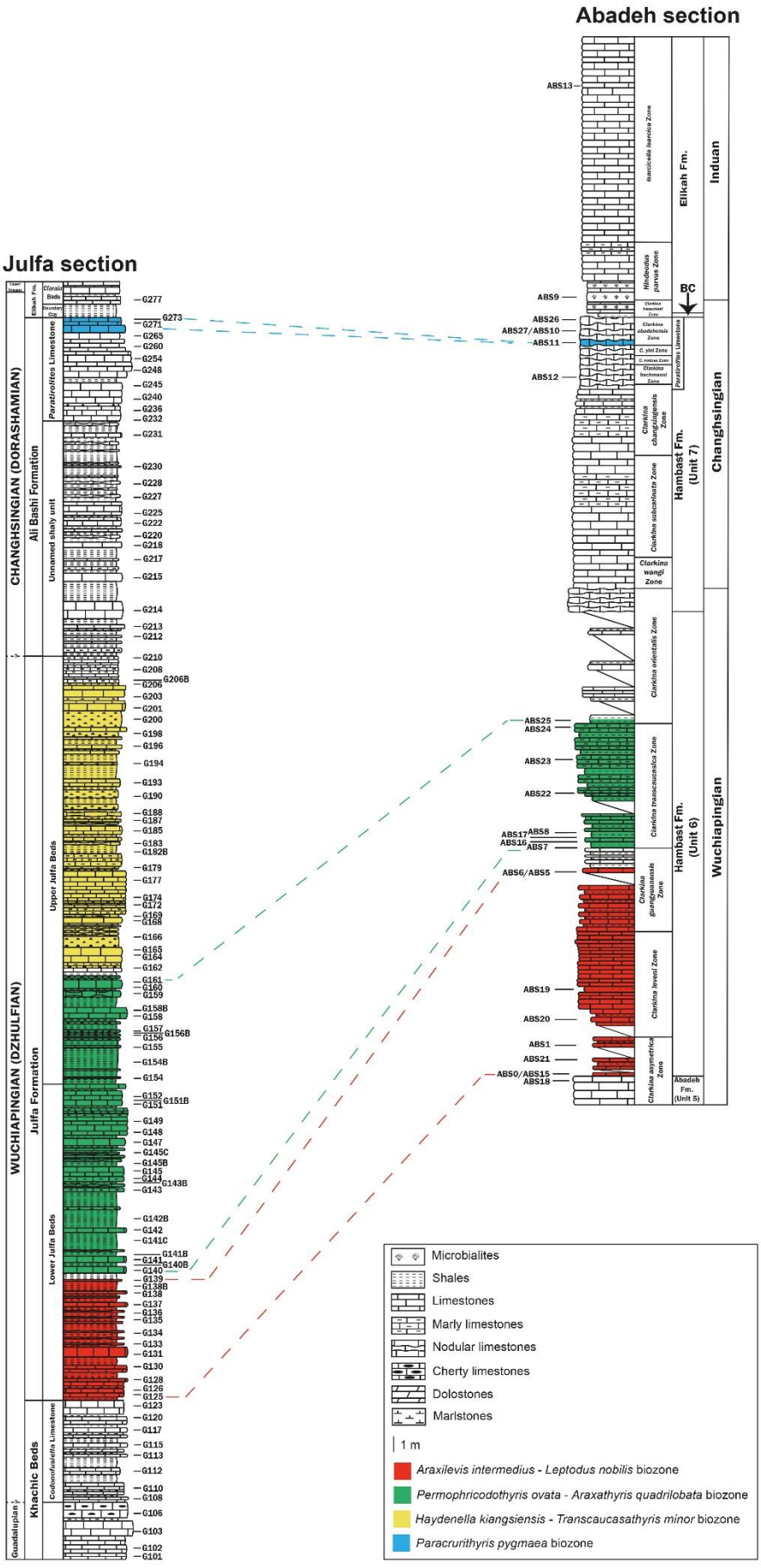

Fig. 9 - Correlation of Julfa and Abadeh sections.

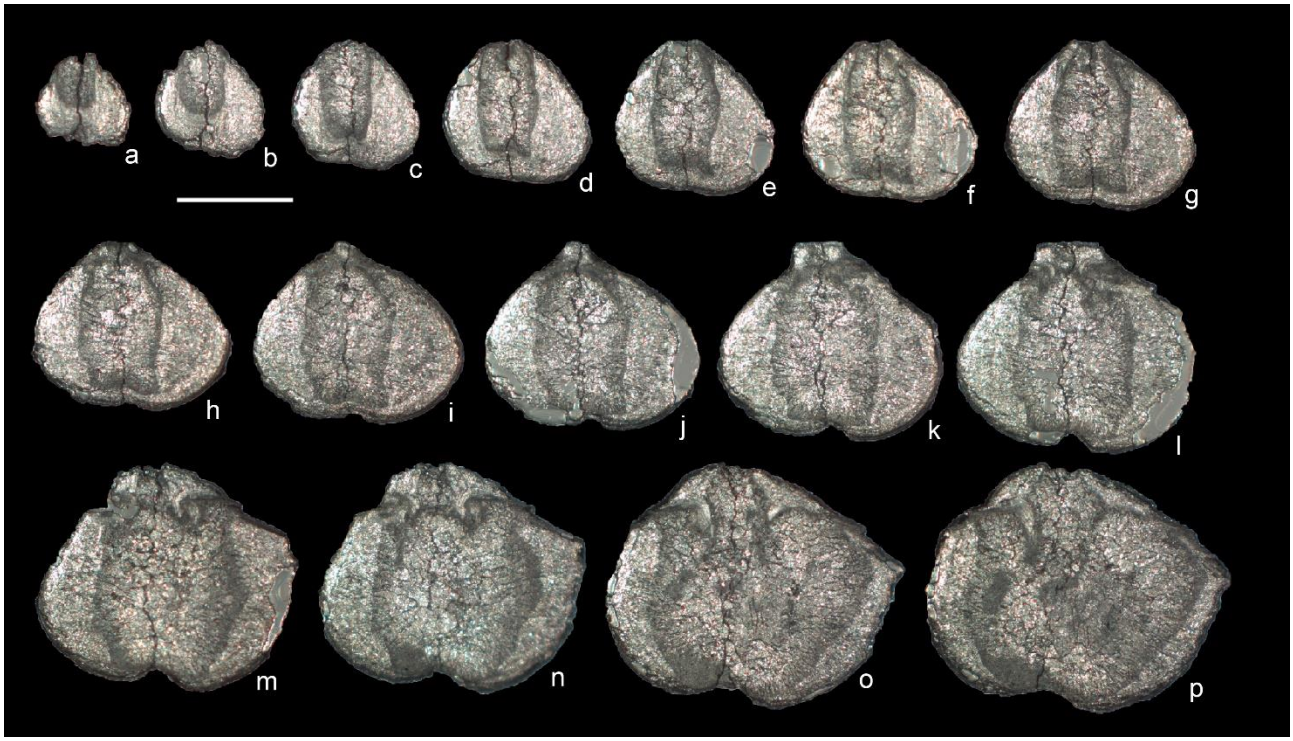

Fig. 10 - *Araxathyris abichi*, serial sections of the specimen MPUM12230. Distance from the umbo: a) 0.1 mm, b) 0.2 mm, c) 0.3 mm, d) 0.4 mm, e) 0.5 mm, f) 0.6 mm, g) 0.7 mm, h) 0.8 mm, i) 0.9 mm, j) 1 mm, k) 1.1 mm, l) 1.2 mm, m) 1.3 mm, n) 1.4 mm, o) 1.7 mm, p) 1.8 mm. Scale bar corresponds to 2 mm.

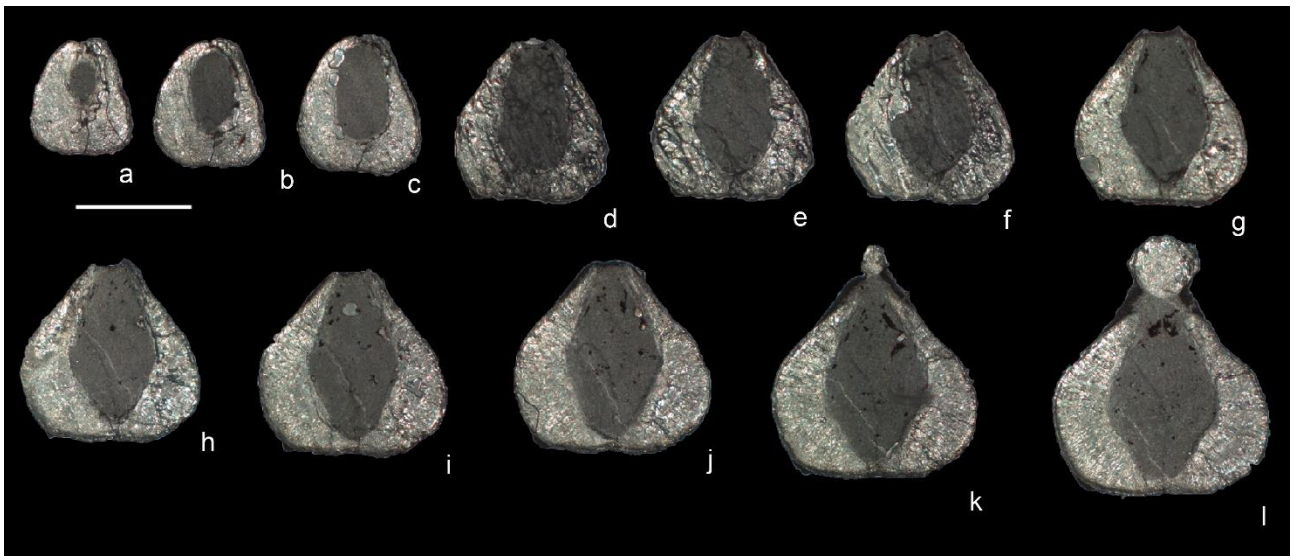

Fig. 11 - *Araxathyris* sp., serial sections of the specimen MPUM12245. Distance from the umbo: a) 0.1 mm, b) 0.2 mm, c) 0.3 mm, d) 0.4 mm, e) 0.6 mm, f) 0.7 mm, g) 0.8 mm, h) 0.9 mm, i) 1 mm, j) 1.1 mm, k) 1.2 mm, l) 1.3 mm. Scale bar corresponds to 2 mm.

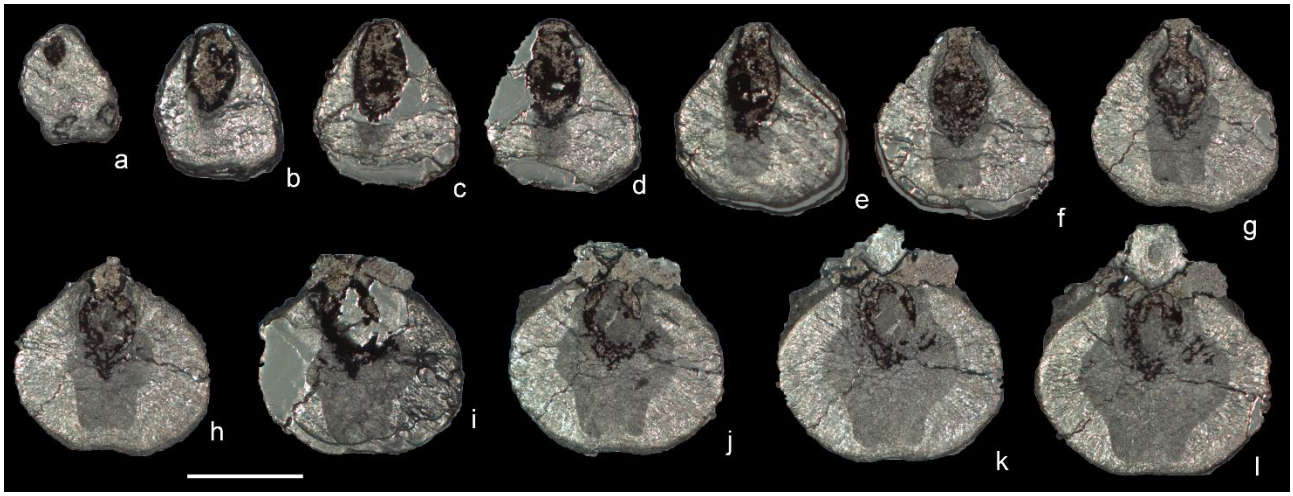

Fig. 12 - *Transcaucasathyris lata*, serial sections of the specimen MPUM12279. Distance from the umbo: a) 0.6 mm, b) 1 mm, c) 1.2 mm, d) 1.3 mm, e) 1.4 mm, f) 1.6 mm, g) 1.7 mm, h) 1.8 mm, i) 1.9 mm, j) 2 mm, k) 2.1 mm, l) 2.2 mm. Scale bar corresponds to 2 mm.

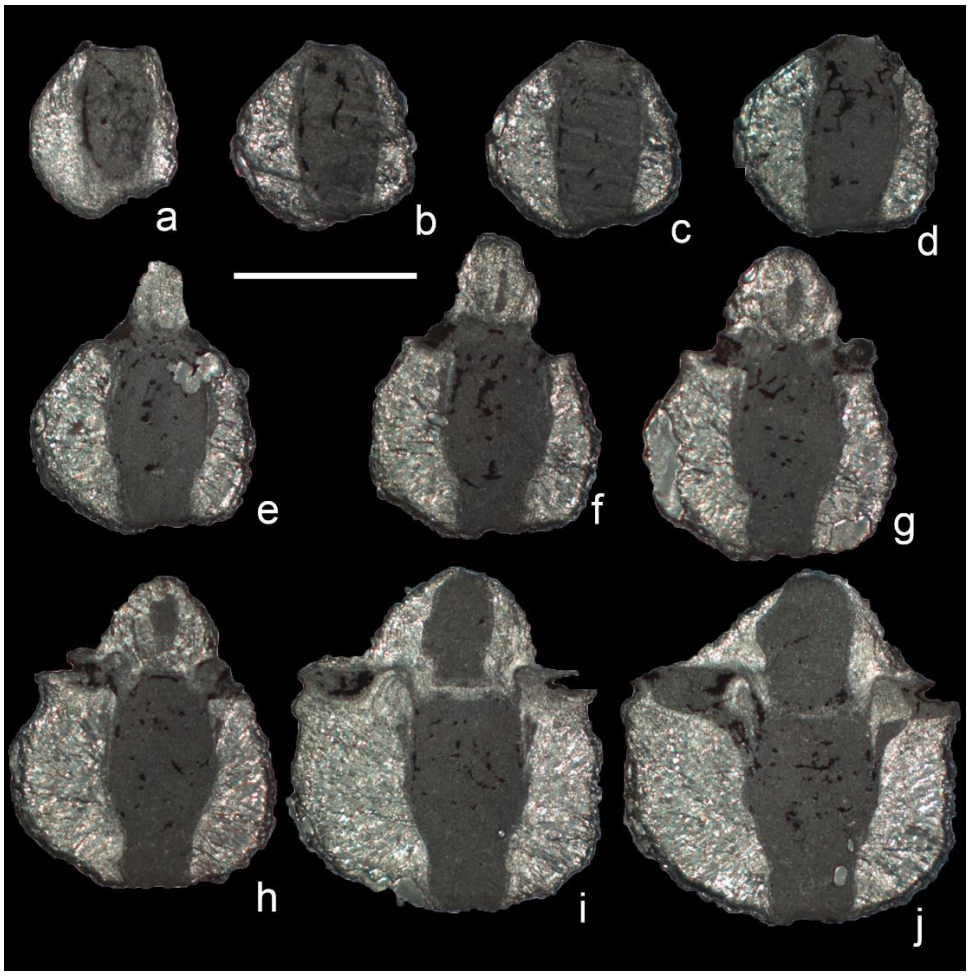

Fig. 13 - *Transcaucasathyris* sp., serial sections of the specimen MPUM12283. Distance from the umbo: a) 0.3 mm, b) 0.5 mm, c) 0.6 mm, d) 0.7 mm, e) 0.8 mm, f) 0.9 mm, g) 1 mm, h) 1.1 mm, i) 1.3 mm, j) 1.4 mm. Scale bar corresponds to 2 mm.

Formation	Lithology	Beds
Hambast Formation (Unit 7)	Grey to pinkish nodular marly limestones (not sampled)	
Hambast Formation (Unit 6)	430 cm covered on shales and limestones	
	40 cm amalgamated light grey limestones in 7-15 cm thick beds	
	160 cm covered on shales	
	320 cm dark grey marly limestones (wackestones) in 10-15 cm-thick beds, with shale interbeds less thick than the limestones	ABS22, ABS23, ABS24
	280 cm covered on shales and limestones	
	90 cm grey limestones (packstones) in 7-25 cm-thick beds, thinning upward	ABS16, ABS17
	530 cm covered on shales with thin limestone beds. At the top very thin (3-5 cm-thick) nodular limestones	ABS4
	250 cm grey limestones (packstones) in 7-30 cm-thick beds with thin shale interbeds	ABS2, ABS3, ABS20
	250 cm covered on shales	ABS0, ABS1, ABS21
Top Abadeh Formation	Not sampled	
	Base of the section at 30°53’43.2’’N - 53°12’17.5’’E	

Tab. 1 - The Gulley section. Beds have been measured and sampled from the base of the Hambast Formation.

Formation	Lithology	Beds
Elikah Formation	15 m of platy bioturbated limestones with bivalves	ABS13
	120 cm microbialites with fan-like structures intercalated to marlstones	ABS9
	30 cm grey limestones	
Boundary Clay	30 cm red claystones passing to yellowish claystones; no reaction to HCl	
Hambast Formation (Unit 7)	3 cm grey limestones	ABS26
	570 cm of pink nodular limestones in 3-8 cm-thick beds. Occasional occurrence of brachiopod bioclasts and bivalves	ABS10, ABS11, ABS12, ABS27
	Part of Hambast Formation missing and lower part of section measured slightly to the east on the other side of the fault	
Hambast Formation (Unit 6)	Fault	
	60 cm limestones in 10-15 cm-thick beds, with shale interbeds	ABS25
	50 cm two bioclastic limestone beds (10 and 40 cm-thick respectively) with calcite vein	
	450 cm covered	
	230 cm grey limestones in 7-25 cm-thick beds, with shale interbeds as thick as the beds, occasionally thicker, rich in brachiopods	ABS5, ABS6, ABS7, ABS8
	150 cm covered	
	270 cm prominent dark limestones in 15-30 cm-thick beds, with thicker shale interbeds (up to 13 cm thick) than the interval below; Rare chert at the top	
	310 cm prominent grey limestones in 7-30 cm-thick beds, with thin shale interbeds	ABS19

	300 cm partially covered black limestones in 7-15 cm-thick beds, alternating with shales of similar thickness	ABS15
Abadeh Formation	30 cm black marly limestones (packstones) with calcite veins, fetid	ABS18
	> 200 cm black limestones (packstones) in 15-50 cm-thick beds, with calcite veins, very thin interbeds	
	Base of the section at 30°53’46.2’’N - 53°12’15.3’’E	

Tab. 2 - The Saddle section. Beds have been measured and sampled from the top of the Abadeh Formation.

Authors	*PTB Position*
Taraz et al. (1981)	Shales, no further indication (1)
Gallet et al. (2000)	Upper 10 cm of the “Transition bed” (2)
Korte et al. (2004)	1.4 m above the base of the Elikah Formation (3)
Kozur (2007)	1.4 m above the base of the Elikah Formation (4)
Horacek et al. (2007)	30 cm above the boundary shale (5)
Shen & Mei (2010)	80 cm above the top of *Paratirolites* Limestone (6)
Korte et al. (2010)	1.4 m above the base of the Elikah Formation (7)
Richoz et al. (2010)	25 cm above the base of the Elikah Formation (8)
Liu et al. (2013)	0.5 m below the base of the main microbialite bed (9)
Shen et al. (2013)	1 m above the top of *Paratirolites* Limestone (10)
Dudás et al. (2017)	Base of the microbialites (11)
Chen et al. (2020)	1.5 m above the top of *Paratirolites* Limestone (12)
Horacek et al. (2021)	Top of the Boundary Clay (13)
Chen et al. (2021)	0.8 m above the top of “boundary clay” (14)

Tab. 3 - Different Permian-Triassic Boundary (PTB) positions proposed for the Abadeh section. Note the different levels of reference taken by the different authors to locate the boundary and the different terminology adopted. Bracketed numbers refer to Fig. 6.

Bed	Margalef Index	Shannon-Wiener Index	% specimens laminar microstructure	% specimens fibrous microstructure	n° taxa laminar microstructure	n° taxa fibrous microstructure
ABS11	/	0	0	100	0	1
ABS25	2.9	2.24	37.9	62.1	4	7
ABS24	0.9	0.64	66.6	33.3	1	1
ABS23	1.8	1.10	33.3	66.6	1	2
ABS22	2.2	1.76	46.6	53.4	2	5
ABS8	4.1	2.12	60.4	39.6	7	10
ABS17	2.6	2.14	20.9	79.1	3	8
ABS16	2.7	1.88	44.4	55.5	2	5
ABS7	2.8	1.78	83.3	16.7	6	2
ABS6	0.9	1.06	100	0	3	0
ABS5	0.3	0.50	100	0	2	0
ABS20	2.2	1.67	77.7	22.3	4	2
ABS1	0.8	0.88	66.6	33.3	2	1
ABS21	1.8	1.10	33.3	66.6	1	2
ABS0-ABS15	2.1	1.35	80.4	19.6	6	3

Tab. 4 - Biodiversity indices and percentages of shell microstructural types bed by bed.

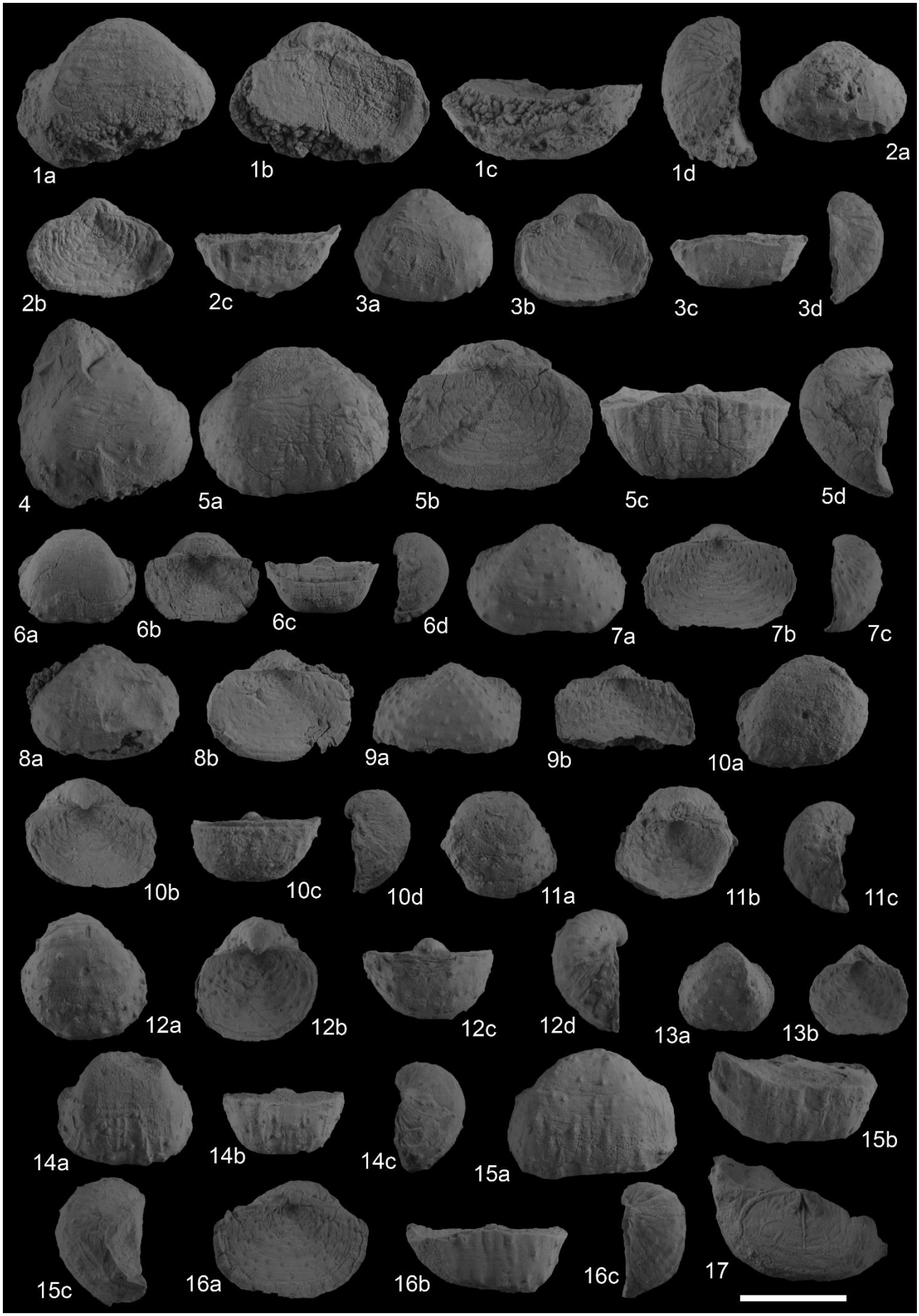
1a
1b
1c
1d
2a
2b
2c
3a
3b
3c
3d
4
5a
5b
5c
5d
6a
6b
6c
6d
7a
7b
7c
8a
8b
9a
9b
10a
10b
10c
10d
11a
11b
11c
12a
12b
12c
12d
13a
13b
14a
14b
14c
15a
15b
15c
16a
16b
16c
17

EXPLANATION OF PLATE 1

Lopingian brachiopods from the Hambast Fm. Scale bar is 1 cm.

Figs 1-5 - *Spinomarginifera helica.*

1 - MPUM12170 (ABS3-1) in ventral (a), dorsal (b), anterior (c) and lateral (d) views; x2.

2 - MPUM12171 (ABS16-18) in ventral (a), dorsal (b) and anterior (c) views; x2.

3 - MPUM12172 (ABS17-70) in ventral (a), dorsal (b), anterior (c) and lateral (d) views; x2.

4 - MPUM12173 (ABS22-1) in ventral view; x2.

5 - MPUM12174 (ABS25-4) in ventral (a), dorsal (b), anterior (c) and lateral (d) views; x2.

Figs 6-9 - *Spinomarginifera iranica.*

6 - MPUM12177 (ABS8-37) in ventral (a), dorsal (b), anterior (c) and lateral (d) views; x2.

7 - MPUM12178 (ABS17-43) in ventral (a), dorsal (b) and lateral (c) views; x2.

8 - MPUM12179 (ABS17-46) in ventral (a) and dorsal (b) views; x2.

9 - MPUM12180 (ABS17-61) in ventral (a) and dorsal (b) views; x2.

Figs 10-13 - *Spinomarginifera pygmaea.*

10 - MPUM12185 (ABS7-7), in ventral (a), dorsal (b), anterior (c), and lateral (d) views; X2.

11 - MPUM12186 (ABS8-27), in ventral (a), dorsal (b), and lateral (c) views; X2.

12 – MPUM12187 (ABS8-29), in ventral (a), dorsal (b), anterior (c), and lateral (d) views; X2.

13 - MPUM12188 (ABS8-39), in ventral (a) and dorsal (b) views; X2.

Figs 14-16 - *Spinomarginifera spinosocostata.*

14 - MPUM12190 (ABS8-24) in ventral (a), dorsal (b) and lateral (c) views; x2.

15 - MPUM12191 (ABS25-5) in ventral (a), dorsal (b) and lateral (c) views; x2.

16 - MPUM12192 (ABS25-10) in dorsal (a), anterior (b) and lateral (c) views; x2.

Fig. 17 - *Spinomarginifera* sp. MPUM 12195(ABS16-1) in dorsal view; x2.

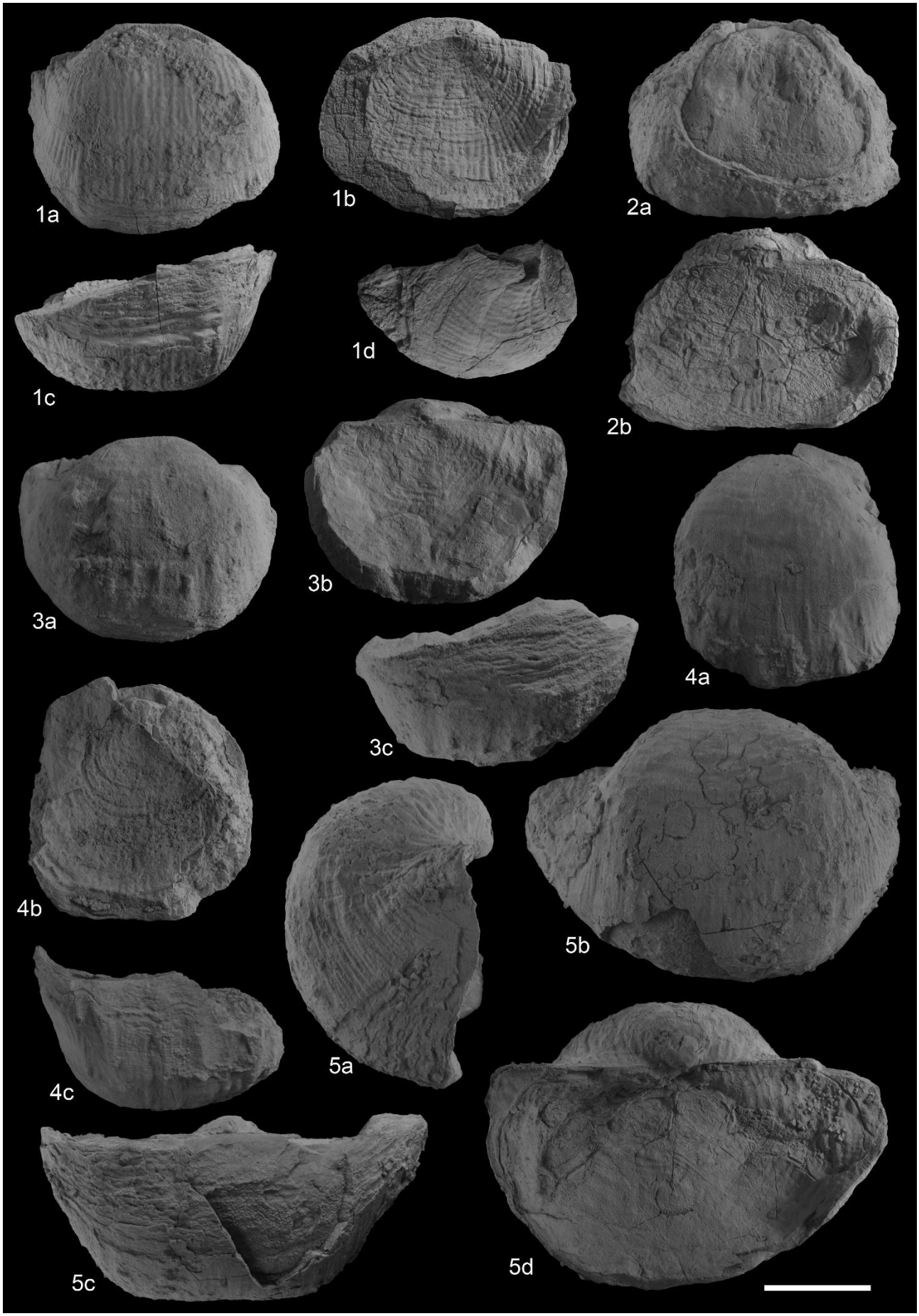
1a
1b
2a
1c
1d
2b
3a
3b
4a
3c
4b
5b
5a
4c
5c
5d

EXPLANATION OF PLATE 2

Lopingian brachiopods from the Hambast Fm. Scale bar is 2 cm.

Figs 1-5 - *Araxilevis intermedius.*

1 - MPUM12197 (ABS0-1) in ventral (a), dorsal (b), anterior (c) and lateral (d) views; x1.

2 - MPUM12198 (ABS0-25) in ventral (a) and dorsal (b) views; x1.

3 - MPUM12199 (ABS0-28) in ventral (a), dorsal (b) and anterior (c) views; x1.

4 - MPUM12200 (ABS5-12) in ventral (a), dorsal (b) and anterior (c) views; x1.

5 - MPUM12201 (ABS5-14) in lateral (a), ventral (b), anterior (c) and dorsal (d) views; x1.

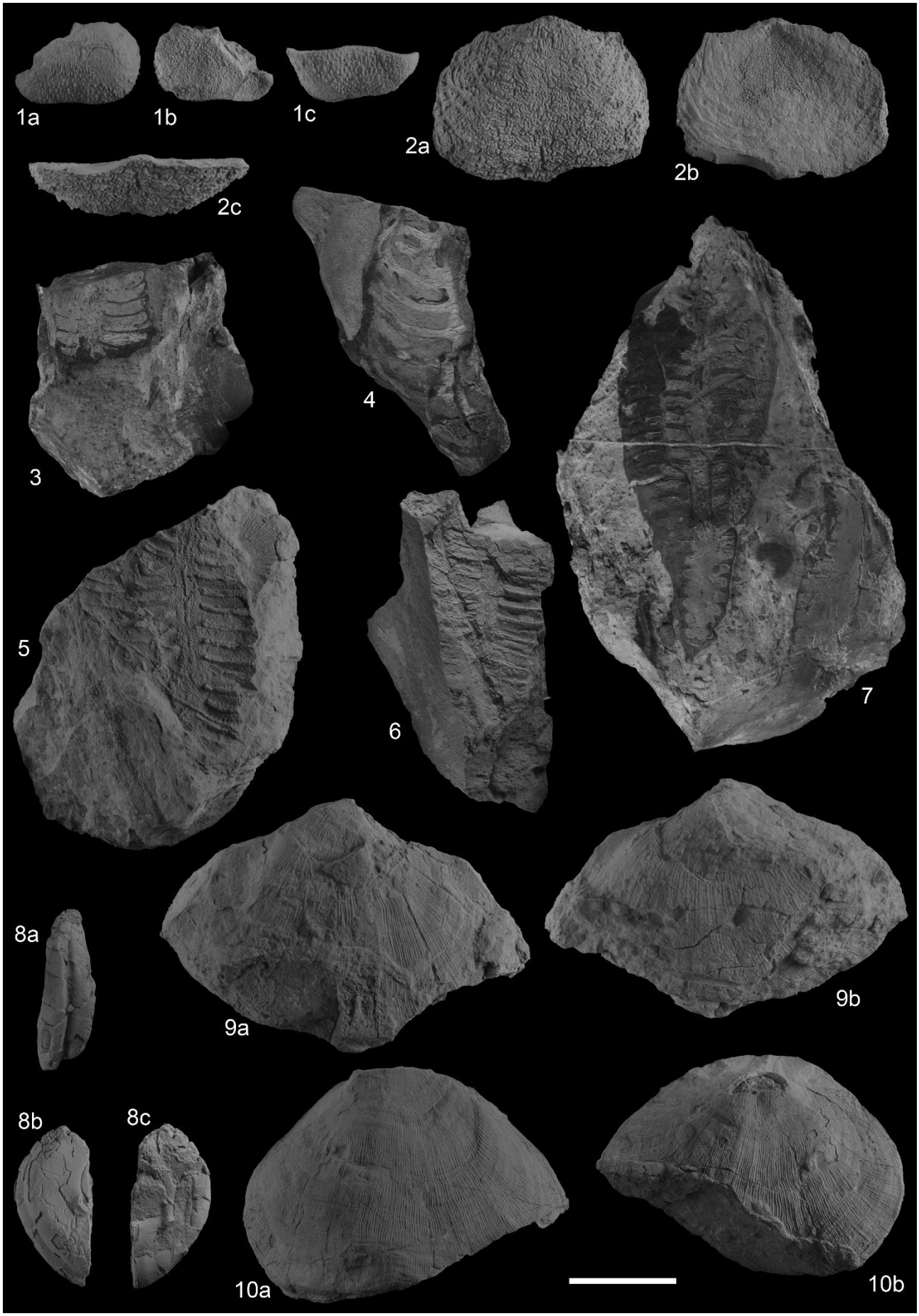
1a
1b
1c
2a
2b
2c
3
4
5
6
7
8a
8b
8c
9a
9b
10a
10b

EXPLANATION OF PLATE 3

Lopingian brachiopods from the Hambast Fm. Scale bar is 2 cm.

Figs 1-2 - *Tschernyschewia typica*.

1 - MPUM12208 (ABS7-1) in ventral (a), dorsal (b) and anterior (c) views; x1.

2 - MPUM12209 (ABS8-8), ventral (a), dorsal (b)and anterior (c) views; X1.

Figs 3-4 - *Leptodus* cf. *richtofeni*.

3 - MPUM12211 (ABS20-7); x1.

4 - MPUM12212 (ABS100-2); x1.

Figs 5-7 - *Leptodus nobilis.*

5 - MPUM12214 (ABS6-6); x1.

6 - MPUM12215 (ABS20-8); x1.

7 - MPUM12216 (ABS15-1b); x1.

Fig. 8 - *Permianella* cf. *grunti*. MPUM12219 (ABS25-1) in ventral (a), right lateral (b) and left lateral (c) views; x1.

Fig. 9 - *Orthothetina persica.* MPUM12220 (ABS20-2) in ventral (a) and dorsal (b) views; x1.

Fig. 10 - *Perigeyerella* aff. *costellata*. MPUM12222 (ABS20-1) in ventral (a) and dorsal (b) views; x1.

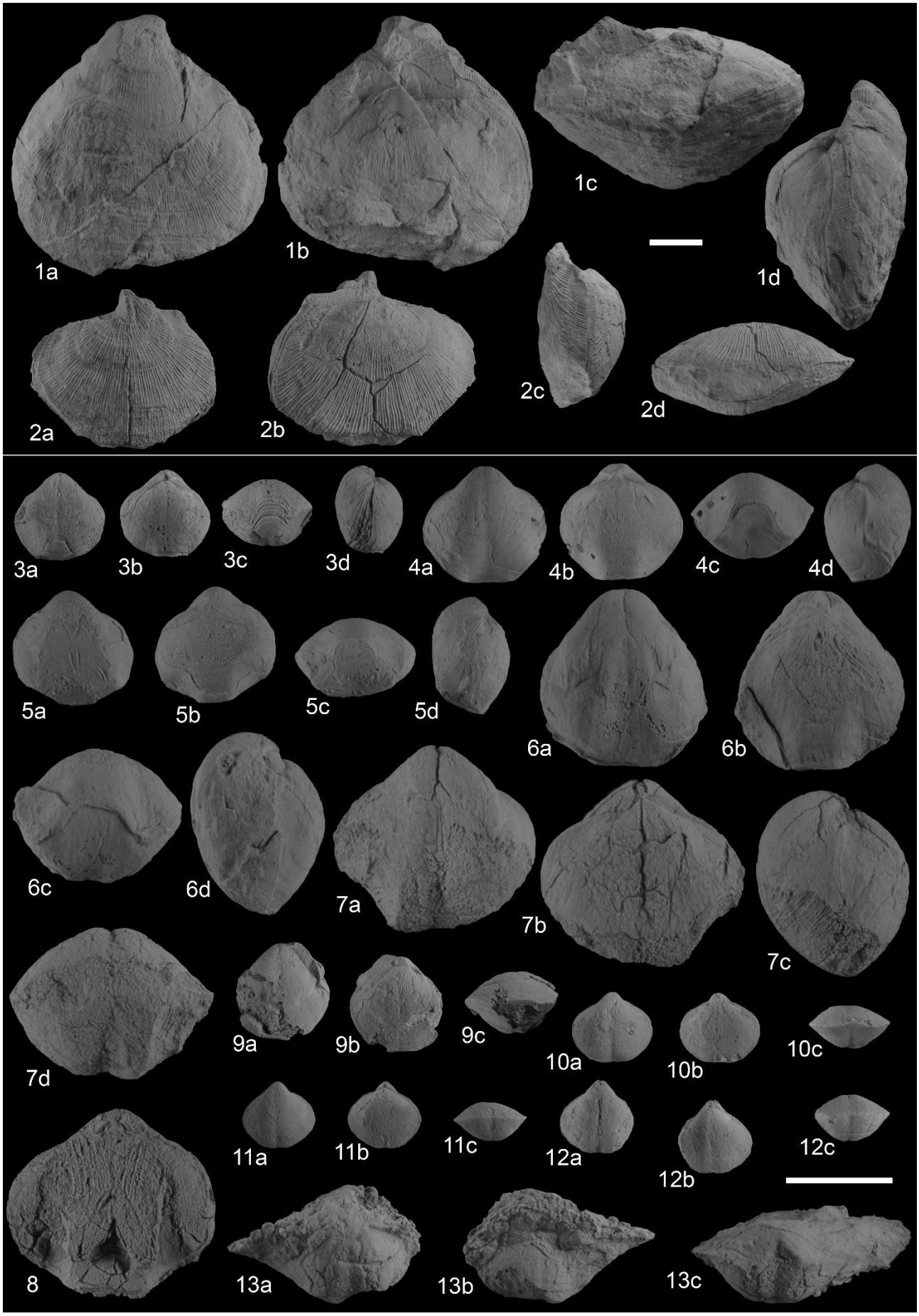
1a
1b
1c
1d
2a
2b
2c
2d
3a
3b
3c
3d
4a
4b
4c
4d
5a
5b
5c
5d
6a
6b
6c
6d
7a
7b
7c
7d
8
9a
9b
9c
10a
10b
10c
11a
11b
11c
12a
12b
12c
13a
13b
13c

EXPLANATION OF PLATE 4

Lopingian brachiopods from the Hambast Fm. Scale bar is 1 cm.

Fig. 1 - *Perigeyerella* aff. *costellata.* MPUM12223 (ABS21-10) in ventral (a), dorsal (b), anterior (c) and lateral (d) views; x1.

Fig. 2 - *Perigeyerella* aff. *tricosa*. MPUM12225 (ABS7-2) in ventral (a), dorsal (b), lateral (c) and anterior (d) views; x 1.

Fig. 3 - *Araxathyris abichi.* MPUM12229 (ABS8-53) in ventral (a), dorsal (b), anterior (c) and lateral (d) views; x2.

Figs 4-5 - *Araxathyris bruntoni.*

4 - MPUM12232 (ABS17-9) in ventral (a), dorsal (b), anterior (c) and lateral (d) views; x2.

5 - MPUM12233 (ABS25-40) in ventral (a), dorsal (b), anterior (c) and lateral (d) views, x2.

Fig. 6 - *Araxathyris felina.* MPUM12238 (ABS8-3) in ventral (a), dorsal (b), anterior (c) and lateral (d) views; x2.

Figs 7-8 - *Araxathyris quadrilobata*.

7 - MPUM12240 (ABS8-1) in ventral (a), dorsal (b), lateral (c) and anterior (d) views; x2.

8 - MPUM12241 (ABS21-4) in dorsal view; x2.

Figs 9-12 - ?*Rectambitus* sp.

9 - MPUM12248 (ABS16-2) in ventral (a), dorsal (b) and anterior (c) views; x2.

10 - MPUM12249 (ABS17-15) in ventral (a), dorsal (b) and anterior (c) views; x2.

11 - MPUM12250 (ABS17-18) in ventral (a), dorsal (b) and anterior (c) views; x2.

12 - MPUM12251 (ABS17-40) in ventral (a), dorsal (b) and anterior (c) views; x2.

Fig. 13 - *Gruntallina* sp. MPUM12258 (ABS3-4) in ventral (a), dorsal (b) and anterior (c) views; x2.

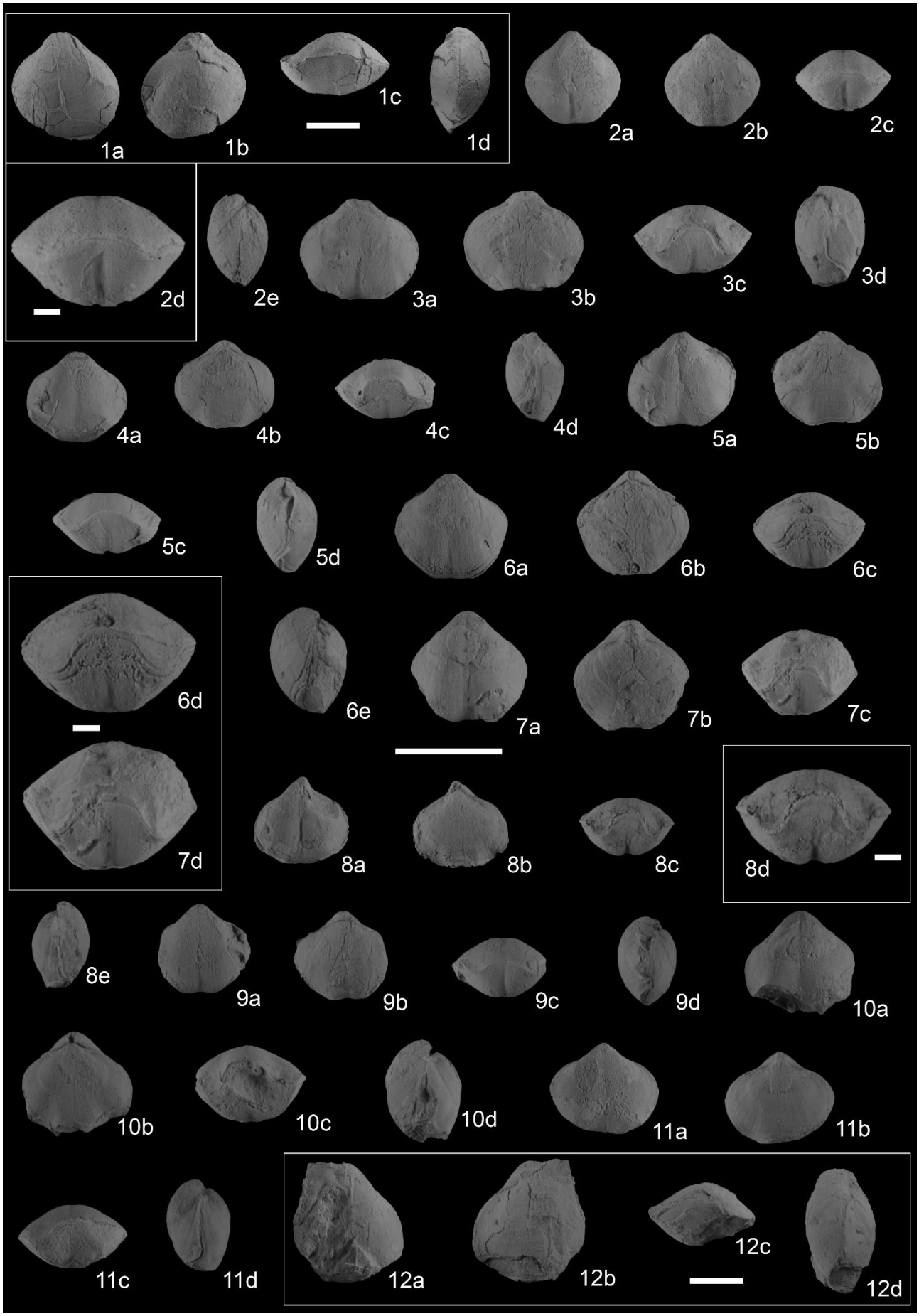
1a
1b
1c
1d
2a
2b
2c
2d
2e
3a
3b
3c
3d
4a
4b
4c
4d
5a
5b
5c
5d
6a
6b
6c
6d
6e
7a
7b
7c
7d
8a
8b
8c
8d
8e
9a
9b
9c
9d
10a
10b
10c
10d
11a
11b
11c
11d
12a
12b
12c
12d

EXPLANATION OF PLATE 5

Lopingian brachiopods from the Hambast Fm. Scale bar is 1 cm.

Fig. 1 - ?*Spirigerella* sp. MPUM12259 (ABS21-7) in ventral (a), dorsal (b), anterior (c) and lateral (d) views; x1.

Figs 2-5 - *Transcaucasathyris araxensis*.

2 - MPUM12260 (ABS16-6) in ventral (a), dorsal (b), anterior (c, d) and lateral (3) views; x2 (a-c, e) and x4 (d).

3 - MPUM12261 (ABS17-37) in ventral (a), dorsal (b), anterior (c) and lateral (d) views; x2.

4 - MPUM12262 (ABS17-51) in ventral (a), dorsal (b), anterior (c) and lateral (d) views; x2.

5 - MPUM12263 (ABS17-71) in ventral (a), dorsal (b), anterior (c) and lateral (d) views; x2.

Figs 6-7 - *Transcaucasathyris kandevani.*

6 - MPUM12268 (ABS16-3) in ventral (a), dorsal (b), anterior (c, d) and lateral (e) views; x2 (a-c, e) and x4 (d).

7 - MPUM12269 (ABS17-45) in ventral (a), dorsal (b), and anterior (c, d) views; x2 (a-c) and x4 (d).

Figures 8-11 - *Transcaucasathyris lata.*

8 - MPUM12274 (ABS8-40) in ventral (a), dorsal (b), anterior (c, d) and lateral (e) views; x2 (a-c, e) and x 4 (d).

9 - MPUM12275 (ABS17-31) in ventral (a), dorsal (b), anterior (c) and lateral (d) views; x2.

10 - MPUM12276 (ABS22-8) in ventral (a), dorsal (b), anterior (c) and lateral (d) views; x2.

11 - MPUM12277 (ABS23-1) in ventral (a), dorsal (b), anterior (c) and lateral (d) views; x2.

Fig. 12 - ?*Permophricodothyris* sp. MPUM12288 (ABS20-3) in ventral (a), dorsal (b), anterior (c) and lateral (d) views; x1.

Supplementary Table 1 - Range chart of the brachiopods from the Abadeh section.

Supplementary Table 2 - PAST outputs from the Unitary Associations method applied to correlate the Abadeh and Julfa sections. a) Correlation table. b) UA Sorted Graph. c) UA Reproducibility Graph. d) Reproducibility Graph.